

NON-POLAR AND AFFINITY MONOLITHIC STATIONARY PHASES  
FOR BIOPOLYMER SEPARATIONS BY CAPILLARY  
ELECTROCHROMATOGRAPHY AND NANO-  
LIQUID CHROMATOGRAPHY

By

FRED MARTIN OKANDA

Bachelor of Science in Chemistry

Moi University

Eldoret, Kenya

1999

Submitted to the Faculty of the Graduate College of the  
Oklahoma State University in partial fulfillment  
of the requirements for the degree of  
DOCTOR OF PHILOSOPHY

December, 2006

NON-POLAR AND AFFINITY MONOLITHIC STATIONARY PHASES  
FOR BIOPOLYMER SEPARATIONS BY CAPILLARY  
ELECTROCHROMATOGRAPHY AND NANO-  
LIQUID CHROMATOGRAPHY

Dissertation Approved:

Dr. Ziad El Rassi

---

Thesis Advisor

Dr. Darrell Berlin

---

Dr. Richard Bunce

---

Dr. LeGrande Slaughter

---

Dr. Earl Mitchell

---

Dr. Gordon Emslie

---

Dean of the Graduate College

## ACKNOWLEDGEMENTS

My profound and sincere appreciation goes to my research advisor, Dr. Ziad El Rassi, whose advice, guidance, sincerity and devotion to his work and students have made this work possible. Being his student is an unforgettable experience that taught me with hard work anything is possible. Although my time under his tutelage is coming to an end, I will always be indebted to him and very grateful that I had the opportunity to work as his student and for that I say, *Erokamano*-Thank you.

I would also like to express my cordial thanks to my committee members, Dr. Darrell Berlin, Dr. Richard Bunce, Dr. LeGrande Slaughter and Dr. Earl Michell for their support and valuable suggestions. I would like to extend my thanks to the Chemistry Department at OSU, the administrative staff (Cheryl, Caroline, Cindy and Bob) and the OSU community at large. Thanks also go to Dr. El Rassi's research group members, for their friendship and sharing the ups and downs of research together. I would also like to thank my friends in Stillwater for their encouragement and I wish to add that I value and appreciate their friendship deeply.

Many thanks also go to my sisters Diana, Irene, Linda, Millicent and brother, Paul for their encouragement, patience and confidence in me, even though I was so far from home. Special thanks to my Mom for all that she has done for me and the great advice that she kept on giving me all the time. To all members of my family for their unconditional love and support which was dearly needed and was provided constantly

without request that eased the stressful graduate life. Thank you all and I will always love you and be there for you.

Last but not least, I want to dedicate this dissertation to my parents, my Dad Michael and Mom Clarice, who never for once doubted my ability to achieve the goals I set to myself. Dad, even though you are not there, the foundation of your love and support have always motivated me to go through even the most difficult times in life. I'm proud and honored to be your son. This dissertation is specially for you and you will be forever remembered in my heart.

## TABLE OF CONTENTS

CHAPTER	Page
CHAPTER I.....	1
BACKGROUND, RATIONALE AND SCOPE OF THE STUDY.....	1
Introduction and Scope of the Investigation.....	1
Historical Background: The Development of CEC.....	3
Instrumentation.....	4
General Aspects of Instrumentation.....	4
Sample Introduction.....	6
Detection.....	6
Column Technologies.....	8
Packed Columns.....	8
Open Tubular Columns.....	9
Monolithic (Fritless) Columns.....	10
Background and Progress Made in Organic Polymer Monoliths.....	11
Acrylamide-Based Monoliths.....	13
Polystyrene-Based Monolithic Capillary Columns.....	14
Methacrylate Ester-Based Monolithic Columns.....	15
Overview of Progress Made in Affinity CEC and Affinity Nano-LC.....	17
Affinity Nano-LC.....	18
Affinity Capillary Electrochromatography.....	21
Some Basic Principles of Capillary Electrochromatography.....	24
Theory of Electroosmotic Flow.....	24
Flow in Packed Columns.....	28
Retention Factor in CEC.....	29
Neutral solutes.....	29
Charged solutes.....	30
Selectivity Factor.....	31
Separation Efficiency.....	31
Resolution.....	32
Band Broadening.....	33
Rationale of the Investigation.....	36
Conclusions.....	38
References.....	39

CHAPTER II.....	47
PREPARATION OF NEUTRAL STEARYL-ACRYLATE MONOLITHS AND THEIR EVALUATION IN CAPILLARY ELECTROCHROMATOGRAPHY OF NEUTRAL AND CHARGED SMALL SPECIES AS WELL AS PEPTIDES AND PROTEINS .....	47
Introduction.....	47
Experimental .....	50
Instrumentation .....	50
Reagents and Materials .....	51
Column Pretreatment .....	51
<i>In situ</i> Polymerization.....	52
Results and Discussion .....	53
Choice of Monomers and Porogens .....	53
Characterization of the Optimal Neutral Monolith.....	55
EOF .....	55
Retention of Homologous Series .....	58
Migration and Retention of Charged Solutes – Ion-Pair CEC.....	61
Peptides and Proteins .....	65
Conclusions.....	67
References.....	68
 CHAPTER III .....	 69
POLYMETHACRYLATE MONOLITHS WITH IMMOBILIZED LECTINS FOR GLYCOPROTEIN SEPARATION BY AFFINITY CAPILLARY ELECTROCHROMATOGRAPHY AND AFFINITY NANO-LIQUID CHROMATOGRAPHY IN EITHER A SINGLE COLUMN OR COLUMNS COUPLED IN SERIES .....	      69
Introduction.....	69
Experimental .....	72
Instrumentation .....	72
Reagents and Materials .....	72
Column Pretreatment .....	73
<i>In situ</i> Polymerization.....	74
Immobilization of Lectins.....	75
Results and Discussion .....	75
Evaluation of EOF and Pressure Driven Flow of the Various Monoliths .....	76
Lectin Affinity Nano-LC and CEC with Single Lectin Monolithic Columns.....	79
Nano-LC and CEC with LCA Monoliths .....	79
Nano-LC and CEC with WGA Monoliths.....	86
Nano-LC and CEC with Coupled Lectin Affinity Monolithic Columns.....	91
Nano-LC with LCA-monolith →WGA-Monolith Coupled in Series .....	91
CEC with LCA-monolith ⇔WGA-Monolith Coupled in Series .....	91
Conclusions.....	97

References.....	98
CHAPTER IV .....	103
PEPTIDE MAPPING BY REVERSED-PHASE CAPILLARY ELECTROCHROMATOGRAPHY USING A NEUTRAL MONOLITHIC STATIONARY PHASE .....	103
Introduction.....	103
Experimental .....	105
Instrumentation .....	105
Reagents and Materials .....	105
Column Pretreatment .....	105
<i>In situ</i> Polymerization .....	106
Sample Preparation .....	106
Results and Discussion .....	107
CEC Peptide Mapping of Proteins.....	107
Case of Myoglobin.....	107
Case of Cytochrome C.....	117
CEC Peptide Mapping of Glycoproteins .....	120
Case of AGP .....	120
Case of Ribonuclease B .....	127
Case of Ovalbumin .....	130
Case of Transferrin .....	133
Conclusions.....	137
References.....	138
CHAPTER V .....	141
GLYCOPEPTIDES SEPARATION BY SINGLE AND TANDEM LECTIN AFFINITY MONOLITHIC CAPILLARY COLUMNS AND BY SERIAL LECTIN AFFINITY NANO LIQUID CHROMATOGRAPHY AND REVERSE-PHASE CAPILLARY ELECTROCHROMATOGRAPHY .....	141
Introduction.....	141
Experimental .....	144
Instrumentation .....	144
Reagents and Materials.....	145
Column Pretreatment .....	145
<i>In situ</i> Polymerization.....	146
<i>In situ</i> Polymerization for GMA Monolith.....	146
<i>In situ</i> Polymerization for PEDAS Monolith.....	146
Immobilization of Lectins.....	146
Sample Preparation .....	147

Serial Use of Lectin Column and C17 Column for Selective Capturing of Glycopeptides and Their Subsequent Separation by RP-CEC .....	147
Results and Discussion .....	148
Single Lectin Columns.....	148
Tandem Lectin Columns.....	157
Serial Selective Capturing of Glycopeptides by Immobilized Lectins and Their Subsequent Separation by RP-CEC .....	159
Conclusions.....	171
References.....	172



## LIST OF TABLES

TABLE	Page
CHAPTER II	
1. Dimensionless retention parameters of Dns-AA in the presence and absence of TBAB in the mobile phase.....	62
CHAPTER IV	
1. Amino acid names, three and one-letter standard abbreviations. ....	108
2. Amino acid sequence and tryptic fragments of myoglobin as well as the net charge and L/W ratio of the various peptide fragments .....	109
3. Amino acid sequence and tryptic fragments of cytochrome C as well as the net charge and L/W ratio of the various peptide fragments.....	118
4. Amino acid sequence and tryptic peptide fragments of AGP as well as the net charge and L/W ratio of the various peptide fragments. ....	121
5. Amino acid sequence or fragment of ribonuclease B as well as the net charge and L/W ratio of the various peptide fragments. ....	128
6. Amino acid sequence or fragment of ovalbumin B as well as the net charge and L/W ratio of the various peptide fragments. ....	131
7. Amino acid sequence or fragment of transferrin as well as the net charge and L/W ratio of the various peptide fragments. ....	134
CHAPTER V	
1. Structures of known N-glycans derived from human IgG at different degree of sialylation.....	150
2. Structures of known N-glycans derived from human AGP at varying degree of sialylation.....	155
3. Structures of known N-glycans derived from ovalbumin.....	162

4. Structures of known sialylated N-glycans derived from human transferrin. ....	166
--	-----

## LIST OF FIGURES

FIGURE	Page
CHAPTER I	
1. Schematic representation of a manual instrument used in CE/CEC.....	5
2. Illustration (a) of the electric double layer at solid-liquid interface as well as the generation and direction of EOF, and (b) Stern-Gouy-Chapman model depicting potential gradient with respect to distance from the charged surface. ....	26
3. Comparison of mobile phase flow profiles and their effect on column efficiency, i.e. band broadening and resulting peak shape. (a) Laminar flow profile observed in pressure or pump-driven methods. (b) Plug/flat flow profile observed in electrically driven methods.....	27
4. Illustration of the plate height contribution for each van-Deemter term and the resulting observed curve. ....	35
CHAPTER II	
1. Structure of pentaerythritol diacrylate monostearate (PEDAS) used in the preparation of the neutral monolith.....	49
2. Plot of the apparent EOF velocity versus the pH of the mobile phase. ....	56
3. Effect of percent ACN (v/v) in the mobile phase on the apparent EOF velocity of the M-1 monolithic column. ....	58
4. Plots of log $k'$ for alkyl benzene homologous series versus percent ACN (v/v) in the mobile phase .....	59
5. Plots of the retention factor $k'$ of alkyl benzene homologous series obtained on the M-1 monolithic column versus the pH of the mobile phase at 60% (v/v) ACN. ...	60
6. Electrochromatogram of some peptides.....	65
7. Electrochromatogram of some proteins .....	66

### CHAPTER III

1. Specificity of WGA and LCA toward <i>N</i> -glycans. ....	71
2. Chromatogram of lipoxidase in the presence of non-glycosylated proteins, e.g., $\alpha$ -lactalbumin, myoglobin and $\beta$ Lac B, using LCA-monolith based on the positive AP1 monolithic column. ....	80
3. Chromatogram of human transferrin (HT) in the presence of non-glycosylated proteins, e.g., $\alpha$ -lactalbumin, trypsin inhibitor (TI) and carbonic anhydrase (CA), using LCA immobilized on a neutral monolithic column. ....	81
4. Electrochromatogram of lipoxidase and AGP obtained on an LCA-monolith based on the positive AP1 monolithic column by a three-step process.. ....	84
5. Electrochromatogram of lipoxidase, AGP and avidin, using LCA immobilized on a neutral monolithic column. ....	85
6. Chromatogram of fetuin in the presence of non-glycosylated $\alpha$ -lactalbumin, using WGA immobilized on a positive monolithic column of the AP1 type. ....	87
7. Chromatogram of AGP in the presence of ovalbumin, using WGA immobilized on a neutral monolithic column.. ....	88
8. Electrochromatogram of glucose oxidase (GO), fetuin and HT in the presence of non-glycosylated TI, obtained on WGA immobilized on a neutral monolithic column by a three-steps process. ....	90
9. Chromatogram of AGP, lipoxidase, avidin and fetuin, obtained on coupled lectin columns in the order LCA $\rightarrow$ WGA where the lectins were immobilized on a neutral monolith. ....	92
10. Electrochromatogram of AGP, HT, collagen, $\kappa$ -casein, avidin and fetuin, obtained on coupled lectin columns in the order WGA $\rightarrow$ LCA where the lectins were immobilized on a neutral monolith. ....	93
11. Electrochromatogram of AGP glycoforms, obtained on coupled lectin columns in the order LCA $\rightarrow$ WGA where the lectins were immobilized on a neutral monolith. ....	95

## CHAPTER IV

1. Electrochromatogram of the tryptic digest of myoglobin.....	112
2. Electrochromatogram of the tryptic digest of myoglobin.....	115
3. Electrochromatogram of the tryptic digest of cytochrome C.....	119
4. Electrochromatogram of the tryptic digest of AGP.. .....	122
5. Electrochromatogram of the tryptic digest of AGP .....	125
6. Electrochromatogram of the tryptic digest of AGP. ....	126
7. Electrochromatogram of the tryptic digest of ribonuclease B.. ..	129
8. Electrochromatogram of the tryptic digest of ovalbumin. ....	132
9. Electrochromatogram of the tryptic digest of transferrin. ....	136

## CHAPTER V

1. Structures exhibiting strong binding and requiring 0.1 M galactose for elution. Specificity of RCA towards N-glycans.....	143
2. Chromatogram of IgG glycopeptides and peptides, using an LCA monolithic column.....	149
3. Electrochromatogram of IgG glycopeptides and peptides obtained on and LCA monolithic column. ....	152
4. Electrochromatogram of AGP glycopeptides and peptides obtained on and LCA monolithic column g.....	154
5. Electrochromatogram of AGP glycopeptides and peptides obtained on and WGA monolithic column. ....	156
6. Electrochromatogram of AGP glycopeptides and peptides obtained on and WGA→LCA monolithic column... ..	158
7. Chromatogram of AGP glycopeptides and peptides obtained on and RCA→WGA→LCA monolithic column . ....	160

8. Different glycopeptides of ovalbumin on different lectin columns. (a) RCA reactive (b) LCA reactive and (c) WGA reactive..... 165
9. Different glycopeptides of transferrin on different lectin columns. (a) RCA reactive (b) LCA reactive and (c) WGA reactive..... 168
10. Different glycopeptides of AGP on different lectin columns. (a) RCA reactive (b) LCA reactive and (c) WGA reactive. .... 170

## LIST OF SYMBOLS AND ABBREVIATIONS

$\alpha$	Selectivity factor
$\varphi$	conductivity
$\Delta p$	pressure drop over the column
$\varepsilon$	dielectric constant
$\varepsilon'$	porosity of the stationary phase
$\varepsilon_0$	permittivity of the vacuum
$\zeta$	zeta potential
$\zeta_p$	zeta potential on a stationary particle
$\mu_{ep}$	electrophoretic mobility
$\mu_{eo}$	electroosmotic mobility
$u_{ep}$	electrophoretic velocity
$u_{eo}$	electroosmotic velocity
$\sigma_t$	standard deviation of the peak in unit time
$\sigma_L$	standard deviation of the peak in unit length
$\sigma^2$	peak variance
$d_p$	particle size of the stationary phase
$E$	electric field strength
$I$	ionic strength of the medium

$k'$	chromatographic retention factor
$k^*$	retention factor of a charged solute in CEC
$k_c^*$	Peak locator
$k_e^*$	velocity factor of a charged solute in CEC
$L$	total length of the separation capillary
$l$	length of separation capillary from the inlet to the detection point
$N$	number of theoretical plates
$R_s$	resolution
$t_o$	migration time of a neutral solute
$t_m$	migration time of retained solute
$w_b$	peak width at the base
$w_h$	peak width at half height
$w_i$	peak width at the point of inflection
ACN	acetonitrile
AETA	[2-(acryloyloxy)ethyl]trimethylammonium methyl sulfate
AIBN	2,2'-azobisisobutyronitrile
BMA	butyl methacrylate
CE	capillary electrophoresis
CEC	capillary electrochromatography
CZE	capillary zone electrophoresis
DAD	diode array detector
Dns-AA	dansyl amino acids
DETA	diethylenetriamine



EDA	ethylenediamine
EDMA	ethylene glycol dimethacrylate
EG	ethylene glycol
EMA	ethyl methacrylate
EOF	electroosmotic flow
GC	gas chromatography
GMA	glycidol methacrylate
HPLC	high performance liquid chromatography
LAC	lectin affinity chromatography
LC	liquid chromatography
LCA	<i>lens culinaris</i> agglutinin
MAETA	[2-(methacryloyloxy)ethyl]trimethylammonium chloride
MMA	methylmethacrylate
Nano-LC	nano-liquid chromatography
PEDAS	pentaerythritol diacrylate monostearate
RCA	<i>ricinus communis</i> agglutinin
RP-CEC	reversed-phase capillary electrochromatography
SEM	scanning electron microscope
TBAB	tetrabutylammonium bromide
TETA	triethylenetetramine tetrahydrochloride
TFA	trifluoroacetic acid
WGA	wheat germ agglutinin

## CHAPTER I

### BACKGROUND, RATIONALE AND SCOPE OF THE STUDY

#### Introduction and Scope of the Investigation

Capillary electrochromatography (CEC) is a technique that combines the separation principles of both high performance liquid chromatography (HPLC) and capillary zone electrophoresis (CZE). This hybrid technique has been gaining interest due to its easy manipulation of retention and selectivity, the relatively high sample loading capacity, selective electromigration and the high separation efficiency [1-9]. CEC involves the application of an electrical field across a fused-silica capillary column possessing a chromatographic stationary phase, that is, either a particle packed column or a monolithic polymeric column. Separation in CEC is based on a dual mechanism whereby neutral analytes are separated according to their chromatographic partitioning between stationary (which also drives the electroosmotic flow, EOF) and mobile phases, while charged solutes experience an additional separation factor based on their differential electrophoretic migration. While the use of columns containing a solid stationary phase and a separation mechanism based on specific interactions of solutes with this stationary phase is a feature of HPLC, the capillary column format and the application of electrical field is characteristic of CZE.

Pumping liquid through a column by exerting pressure at one end leads to a parabolic flow profile observed with HPLC pressure gradient methods. On the other hand, in CEC, the EOF is formed across the entire column and results in a pressureless flow with an almost flat or plug flow profile leading to higher separation efficiencies. The disadvantage of high backpressures in HPLC due to small diameter particles is also eliminated by the EOF flat profile, not to mention the miniaturization that has allowed the decreased consumption of reagents and analysis of small sample volumes.

The scope of this dissertation encompasses the development, characterization and applications of novel organic polymer monolithic stationary phases for use in CEC and nano-liquid chromatography (nano-LC) which is a miniaturized version of normal LC and the small diameter goes hand in hand for use with CEC. The development of neutral monoliths with high separation efficiency and its application to separate different analytes, e.g. peptides and proteins, has been shown. Also covered is the development of affinity capillary electrochromatography and affinity nano-LC for the separation of glycoproteins and glycopeptides.

The aim of this first chapter is to provide an overview of the fundamental aspects of CEC along with its basic principles or modes of operation. This chapter will also feature a brief historical introduction, overview of instrumentation including performance parameters and an in-depth discussion of different column technologies. In addition, the dissertation contains four other chapters.

Chapter II is concerned with the development of a neutral, nonpolar monolithic capillary column having a relatively strong EOF yet free of electrostatic interactions with charged solutes for the reversed-phase capillary electrochromatography (RP-CEC) of

neutral and charged species including peptides and proteins. In Chapter III, microcolumn separation schemes involving monolithic capillary columns with immobilized lectins, and relevant to nanoglycomics and nanoproteomics were introduced. Positive and neutral monoliths were designed to achieve lectin affinity chromatography (LAC) by nano-LC and CEC. Chapter IV describes in detail the applications of the neutral monolithic stationary phase column in the reversed-phase peptide mapping of various proteins by CEC. Lastly, Chapter V further investigates or reports the glycopeptide isolation and separation by lectin affinity CEC and RP-CEC using the neutral monolith. In order to familiarize the reader with the basic concepts and principles of CEC, various fundamental terms and/equations including instrumentation are described in the following sections.

#### Historical Background: The Development of CEC

The application of a direct current electric field to generate a flow and hence separation was first introduced by Arne Tiselius, a Swedish scientist for the separation of horse serum globulins into three fractions in the year 1937 [10, 11]. Strain in 1939, using both electrophoretic and chromatographic forces separated various dyes by adsorption chromatography on alumina column [12]. In the early 1950s, Mould and Synge attempted to use EOF to separate polysaccharides on a collodion membrane [13, 14].

The application of an electrical field to generate a flow across a chromatographic column was first proposed by Pretorius et al. 32 years ago [15]. Using a 1 mm glass tube packed with a stationary phase 75-125  $\mu\text{m}$  mean particle diameter, they showed that EOF was an alternative to pressure for driving mobile phases. They showed that column efficiency could be significantly increased in an electro-driven separation system

compared to traditional pressure-driven flow chromatography. However, due to poor heat dissipation in columns with large internal diameters, only weak electrical fields could be used, resulting in slow EOF and significantly slow analysis. Jorgenson and Lukacs demonstrated the concept of electrochromatography in the early 1980s using 170  $\mu\text{m}$  capillary columns packed with 10  $\mu\text{m}$  octadecyl-silica particles [16, 17]. The small internal diameter of the column enabled rapid dissipation of the joule heat formed at high applied voltages and efficient separations were achieved. Knox and co-workers demonstrated the use of CEC as a separation technique when they separated a mixture of aromatic hydrocarbons using capillaries packed with C18-coated silica particles of 3-5 and 1.5  $\mu\text{m}$  mean particle diameter [18-20]. The major revival of CEC occurred in the 1990s as a result of the need for new miniaturized separation methods with vastly enhanced efficiency and peak capacity [21, 22].

## Instrumentation

### General Aspects of Instrumentation

A CEC instrument can either be manual or automated. The manual instrument can be a home-made one as illustrated in the schematic in Fig. 1. The automated one is a modification of the manual version in which there is a sample tray for injection of sample and run that are automated including the ability to apply gas pressure. The separation column is composed of a fused-silica capillary, which is coated with a polyimide coating on the outside for durability. The capillary contains some type of packing material or

monolith as the stationary phase. The polyimide coating is stripped at the detection point to facilitate light transmittance from the detector.

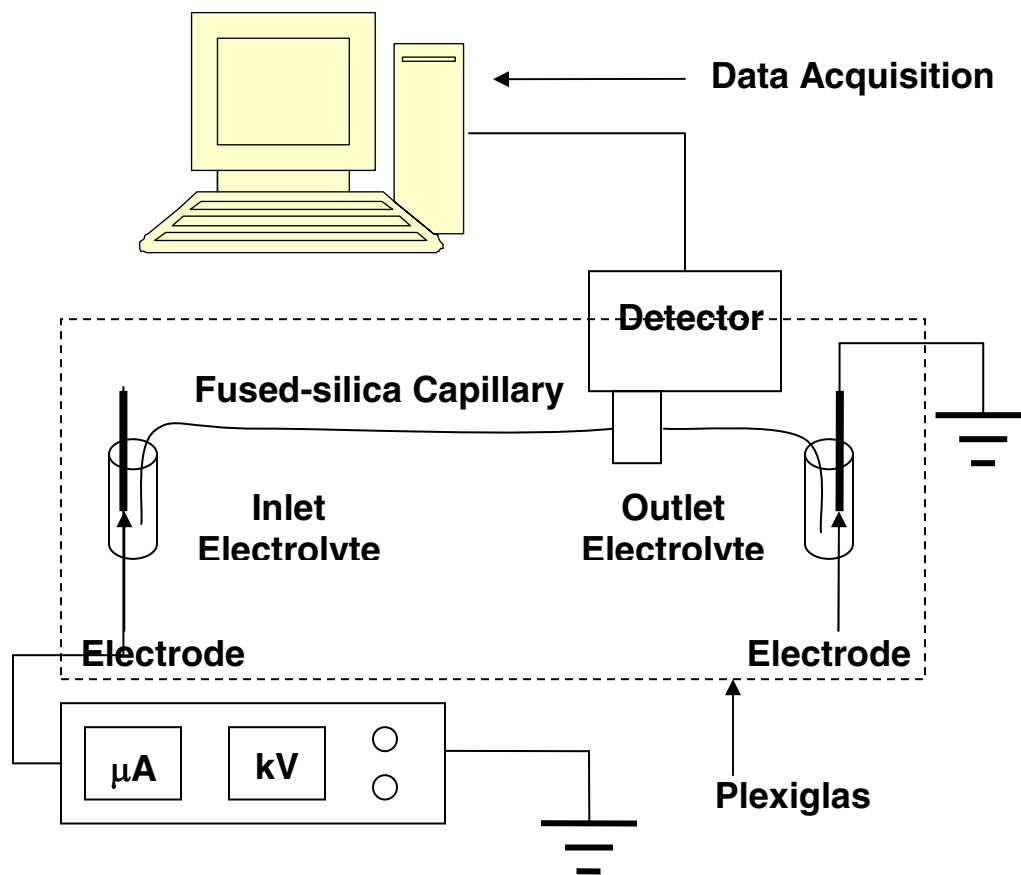


**Figure 1.** Schematic representation of a manual instrument used in CE/CEC.

Each end of the capillary is immersed into the mobile phase electrolyte reservoirs. Two platinum electrodes are also immersed into the two reservoirs with one electrode connected to a high direct current voltage power supply, and the other to earth/ground. The voltage is provided by a power supply that is capable of introducing electrical potentials of up to 30 kV. Detection is made either on-column as in the case of fluorescence and UV-Vis or off-column like in mass spectrometry. The detector output is connected to a data acquisition device in which the software displays or integrates the

data. The high voltage connections, the capillary column and the reservoirs are all enclosed in a plexiglass box equipped with a safety cutoff switch for safety reasons. Automated and modern instruments are equipped with auto samplers, temperature and pressure controls for both the inlet and outlet vials.

### Sample Introduction

There are two methods of introducing sample into the capillary namely, hydrodynamic or electrokinetic injection. The former involves the application of external pressure within the sample vial, in which the capillary inlet is immersed. In this case therefore, the viscosity of the sample matrix and the applied pressure are of importance, since there is a possibility of extremely high backpressure resulting from the separation beds or monolith of low porosity. For electrokinetic injection mode, the sample matrix is introduced by means of EOF. Since the buffer will move in to the capillary, the sample will also move into the capillary. However the amount of sample introduced will be dependent on the relative charge or conductivity of the analyte and running buffer, hence careful selection of the conditions is necessary.

### Detection

For the detection of analytes in CEC, UV and fluorescence are the most commonly used. Many analytes absorb in the UV range and if not they can be derivatized with chromophores that allow their detection. While UV detection is used in CEC, the sensitivity is generally poor due to the scattering of light arising from the

curved surface of the capillary and the short optical path length in the range of 50-100  $\mu\text{m}$  [23]. In CEC on-column detection is usually performed in the unpacked portion just after the stationary phase and to address the sensitivity of detection a number of approaches have been employed by different groups. Ross et al. incorporated a high sensitivity detection cell design to increase the optical path length [24]. The effective optical path length of 1.2 mm for a 100  $\mu\text{m}$  I.D. capillary by using a detection cell that is perpendicular to the capillary and aligned to the beam path. This concept increased the sensitivity 10 fold and was implemented later by Agilent Technologies [25].

Another kind of detection for CEC, which is more sensitive than UV is the fluorescence detection. Dadoo et al. reported sub-attomole detection for polycyclic aromatic hydrocarbons, although fluorescence is limited to a number of analytes without the use of derivatization [26]. Modern trends involving the use of online detection or coupling to a mass spectrometer (MS) for even more sensitive CEC detection have been used. Given the nano flow rate and high compatibility of CEC with the ionization techniques of MS especially electrospray ionization (ESI), where sensitivity does not depend on the size of the detection cells or path length, ESI-MS has gained increased importance and interest.[27] Another reason for this is the increase in information provided like characterization of complex matrices. A number of papers have been published recently dealing with CEC-MS analysis including microfluidic device [28], peptides [29-32], glycans mixtures [33], drug enantiomers [34] and steroids [35]. The hyphenation of small volume separations to information rich detection offers the promise of unmatched analytical information on the components of complex mixtures. NMR provides information about molecular structure and the instrumental aspects of the



capabilities of CEC-NMR analysis of drug metabolites [36, 37] and pharmaceuticals [38] have been shown.

### Column Technologies

Despite significant progress in the fabrication of columns for CEC, there is still room for further improvements of the technology. Several research groups seeking new microseparation methods with enhanced efficiencies, peak capacities and selectivities have expanded rapidly and the number of published papers has grown exponentially [39]. To meet the unique requirements arising from the combined separation powers of chromatographic retention and electric field, different column technologies and stationary phases have to be designed for the CEC separations of the various analytes. At present, there are three major categories which include packed, open tubular (OT) and monolithic columns.

Packed Columns. The use of packed columns for CEC has already been demonstrated in numerous reports [5, 40-42]. The preparation of these columns includes the packing of small diameter particles into capillaries and the fabrication of retaining frits or incorporating internal or external tapers/restrictors within the capillary. Both of these steps require considerable experimental skills and experience in order to obtain stable columns with repeatable properties. Although packing is currently a well-established technique for the production of CEC columns, repeatability, fragility, different resistivities and bubble formation are major drawbacks [43].

To support EOF the majority of applications involve the use of uncapped silica-based materials or segmented capillaries [44, 45] and mixed mode stationary phases [46, 47]. Various methods are used to pack capillaries for CEC. Pressure packing is the most common and this is done at elevated pressures greater than 5000 psi, by connecting the capillary to the slurry reservoir and to a high pressure pump [48]. Others have used pseudoelectropacking, that is using the inherent charges fixed on the packing material, a high electric field and hydrodynamic flow to pack the column [49] while some used supercritical CO<sub>2</sub> as the transporting medium [50] and centripetal force by placing the slurry at the center of the rotating packing apparatus [51].

Open Tubular Columns. Open tubular CEC (OT-CEC) have stationary phases coated onto the walls of fused-silica capillaries (ca. 10 μm I.D.) and their fabrication is relatively simple [52, 53]. The slow rate of diffusion of the mobile phase and narrow channels enhances the interaction of analytes with immobilized ligands leading to high separation efficiencies [54]. For the fabrication an etching process to the inner wall is done to increase surface area prior to ligand attachment [55].

Generally, there are four major groups of stationary phases used for OT-CEC and these include chemically bonded, physically or dynamically adsorbed, organic-polymer based and sol-gel coated [56]. Chemically bonded phases are prepared by bonding of an organic moiety to the etched surface of a capillary using the silanization or hydrosilanization processes [57], and electrostatic interactions are used to adsorb the desired stationary phase ligands such as proteins to the silica surface [58]. Physically adsorbed stationary phases involve stronger interactions in comparison to dynamically

adsorbed ligands, whereby the addition of an adsorbing agent to the mobile phase is necessary [59]. The organic polymer based and the sol-gel involve the polymerization of organic polymers [60] and inorganic alkoxides [61, 62]. These processes are similar to the methods used for the generation of monolithic columns, with the only difference being that the process is limited to the coating of the walls with a porous layer as opposed to a continuous bed that occupies the entire volume of the capillary.

Monolithic (Fritless) Columns. Monolithic columns are continuous macroporous material (rods) fabricated *in-situ* by polymerization of monomers. Their unique properties including their high permeability (i.e., back pressures are three times lower than that of packed columns) and absence of retaining frits have attracted considerable attention. Perhaps the most appealing aspect of monoliths is the ease of their preparation directly within the confines of a capillary or a microfluidic chip that avoids the problems encountered both with packing and frit formation. The porous monolith is covalently attached or anchored to the capillary wall, which increases the robustness of the column [63, 64]. Furthermore, columns of virtually any length and shape are easily accessible and the control that can be exerted over the preparation process facilitates optimization of the porous properties of the monolith, and consequently the chromatographic performance of the entire system.

Monolithic columns have been an area of intensive research and are classified into two major categories: (i) The rigid organic polymer-based monoliths usually prepared by vinyl polymerization, and these include acrylamide-based, acrylate- or methacrylate-based, and styrene-based polymers [65, 66], and (ii) The silica-based monoliths,

prepared using sol-gel technology, used to create a continuous sol-gel network throughout the column formed by the gelation of a sol solution within the capillary [67, 68]. Different applications using monolithic columns have been reported namely the analysis of environmental pollutants [69], pharmaceuticals [7, 70], chiral [71, 72] and biomolecules separations [73-76]. In the present dissertation attention is paid on the development of organic polymer-based monoliths, hence the next section provides an overview on monolithic columns as it pertains to the significant progress made in this area.

### Background and Progress Made in Organic Polymer Monoliths

Despite significant progress in the fabrication of efficient monolithic stationary phases and columns, there is still room for further improvements of the technology in terms of morphology, column efficiency, retention properties and selectivity [43]. This section will provide the reader with a summary of the work by numerous national and international research groups.

The organic polymer-based monolithic columns are made by a single step polymerization of an organic monomer in the presence of a cross-linker, initiator and porogenic mixture of solvents [66, 77, 78]. The composition of the polymerization mixture controls the morphology of the polymer monoliths [79, 80]. Polymerization is usually initiated either by UV light or thermal treatment of a free radical, and it proceeds until the polymer reaches a threshold of insolubility in the porogenic solvent, at which point the polymer precipitates and cross-links with other precipitated macroporous globules producing a three-dimensional organic network.

Adjusting the thermodynamic properties of the porogen by using different solvents allows the pore size to be varied over a wide range, as demonstrated by scanning electron micrographs (SEM) [81]. Changes in the thermodynamic quality of the porogenic solvent directly affect the point at which the phase separation occurs during the polymerization process. The time elapsed before the onset of phase separation controls the size of the basic structural units of the monolith, that is, the microglobules, and consequently the pore size [82]. In a solvent with low polarity, phase separation is delayed due to increased solubility of the polymer that is formed in the polymerization mixture. At the time of phase separation, the system contains more polymer that precipitates in the form of numerous nuclei, which are allowed to grow for only a limited period of time before all the monomers are exhausted. As a result, a monolith with small microglobules and small pores is formed. In contrast, if a porogen with a higher polarity is used, phase separation occurs at an early stage of the polymerization, leading to the formation of a limited number of nuclei. Polymer chains continue to form in the solution phase but these chains tend to be captured by the already precipitated nuclei, which therefore grow to a large size, and consequently, the pores represented by voids between these large microglobules are also much larger.

A variety of monomers can be employed to fabricate the final monolith, being both charged and hydrophilic, to generate an EOF, or uncharged and hydrophobic, to allow reversed-phase interactions. The cross-linker concentration can also be adjusted to vary the degree of cross-linking which influences the overall porosity.

Despite the success of the use of purely aqueous polymerization systems, the poor solubility of a number of monomers in water, such as those used for the preparation of

monolithic capillaries for reversed-phase CEC (RP-CEC), led to the development of polymerization systems containing various organic solvents. In contrast to the “fixed” solubilizing properties of water, the wealth of organic solvents possessing polarities ranging from highly nonpolar to extremely polar allows the formulation of mixtures with solvating capabilities that may be tailored over a broad range. An additional feature of organic solvents is their ability to control the porous properties of the monoliths as explained above.

#### Acrylamide-Based Monoliths

Palm and Novotny simplified the incorporation of highly hydrophobic ligands into acrylamide-based matrices [83]. Rather than forming a dispersion by sonication, mixtures of aqueous buffer and *N*-methylformamide were used to prepare homogenous polymerization solutions containing acrylamide, methylene bisacrylamide, acrylic acid and C4, C6 or C12 alkyl acrylate, with the overall concentration of the monomers in solution kept constant. Column efficiencies were more than 200,000 plates/m for phenyl ketones and carbohydrates. Xie et al. [84] prepared porous poly(acrylamide-co-butyl methacrylate-co-*N,N'*-methylenebisacrylamide) monolithic column for hydrophobic interaction chromatography of proteins. Zhang and El Rassi demonstrated the dual role that may be played by the charged groups incorporated primarily to support EOF on the CEC separation of some neutral, moderately polar compounds [85]. The columns exhibited excellent performance with separation efficiencies of over 400,000 plates/m achieved for herbicides and carbamate insecticides. Plieva et al. prepared a supermacroporous monolithic polyacrylamide-based columns by radical polymerization

with functional co-monomer, allyl glycidyl ether and crosslinker *N,N'*-methylene-bis-acrylamide directly in glass columns of 10mm ID [86]. A novel synthetic route to amphiphilic acrylamide-based monolithic stationary phases for CEC employing water-sol cyclodextrins as solubilizing agents have been explored [87]. The impact of the incorporated alkylene groups in the acrylamide-based macroporous polymer on retention was studied with neutral solutes by CEC in the normal phase elution mode and in the reversed-phase elution mode. Hoegger and Freitag [88] studied the influence of the cross-linker concentration, the porogen and the solvent type as well as type and concentration of the three functional, interactive monomers on the morphology and the chromatographic properties of the acrylamide-based hydrophilic monoliths.

#### Polystyrene-Based Monolithic Capillary Columns

The monomers usually used to prepare the polystyrene (PS) monolithic rod are styrene and 4-(chloromethyl) styrene and the cross linker is frequently divinylbenzene (DVB). Since the styrene monomer is hydrophobic, the poly(styrene-co-divinylbenzene) monolithic rod can be directly used in reversed-phase chromatography [89-91].

Horvath and co-workers first reported the preparation of polystyrene-based porous rigid monolithic capillary columns for CEC by polymerizing mixtures of chloromethylstyrene and divinylbenzene in the presence of various porogenic solvents such as methanol, ethanol, propanol, toluene and formamide [92]. The capillary columns were then used for the reversed phase separation of basic and acidic peptides, three angiotensins and insulin with over 200,000 plate/m. Horvath's research group further reported the preparation of a porous monolith for CEC of proteins and peptides by

copolymerizing chloromethylstyrene and ethylene dimethacrylate in the presence of propanol and formamide [93]. Xiong et al. also reported the preparation of monolithic CEC columns by polymerizing mixtures of styrene with divinylbenzene and methacrylic acid in the presence of toluene as the porogenic solvent [94]. Using these monoliths, separation of phenols, chlorobenzenes, anilines, alkybenzenes and some isomeric phenylenediamines was achieved in less than 4.5 min.

Recently, Jin et al. expanded on this concept to demonstrate the excellent separations of a diverse series of neutral and ionic samples like basic pharmaceuticals [95]. Mixtures of styrene, divinylbenzene and methacrylic acid were polymerized in the presence of toluene and isooctane as the porogenic solvents. Aoki et al. also used glycerol dimethacrylate (GDMA) as monomer and monodisperse saturated polystyrene solution in chlorobenzene as porogen [96]. These monoliths were prepared *in situ* in test tubes with saturated PS having a variety of molecular weights from 50,000 to 3,840,000 and their morphology was compared to that of poly-GDMA with the poor porogenic solvent toluene. According to the scanning electron microscope (SEM) observation, the structure of poly-GDMA monolith prepared *in situ* with toluene showed a typical agglomerated structure, whereas for PS was transformed from aggregated globule to three dimensional continuous skeletal structure with its increase, implying it delays dynamically the phase separation of polymer mixture, and hence afford a better separation efficiency.

#### Methacrylate Ester-Based Monolithic Columns

In addition to acrylamide and styrene-based monoliths, extensive work has been done regarding the materials development and optimization of monolithic CEC



capillaries prepared from methacrylate ester monomers. In the preparation, poly-(glycidyl methacrylate-co-ethylene dimethacrylate) is the most frequently used support which affords the reactive epoxide groups for easy derivatization. Svec and Frechet [97, 98] introduced the amino group by reaction with diethyleneamine for weak anion exchange chromatography.

Peters et al. prepared thermally responsive polymer monoliths for temperature controlled hydrophobic interaction chromatography by a two step grafting procedure [99]. Jiri et al. studied the factors affecting the porosity of methacrylate-ester based monolithic columns by varying the proportions of butyl methacrylate and EDMA monomers and of 1,4 butanediol and 1-propanol as the porogenic solvent in the polymerization mixtures [100]. Methacrylate-ester based monoliths containing quaternary ammonium groups were prepared, and their retention behavior was found to be similar to that of columns packed with C18 modified silica particles, using polyaromatic hydrocarbons [64]. Huang et al. separated eight benzophenones and food preservatives then studied the effects of composition and pH of mobile phase, porogenic solvent ratio and 2-acrylamido-2-methyl-1-propane sulfonic acid (AMPS) content on their separation [101, 102]. Recently, much effort have been made to develop high efficiency separation of techniques for determination of microorganisms [9]. Fast identification, characterization and monitoring of microorganisms or living cells without isolation of pure culture are very important in clinical diagnosis, analysis in food industry and quality control of several processes [103, 104]. Recently, Okanda and El Rassi [105] developed a neutral, non-polar C17-monolithic capillary column having a relatively strong EOF yet free of electrostatic interactions with charged solutes allowing for the first

time the rapid and efficient separations of proteins and peptides at neutral pH. This development is discussed in details in chapter II.

The above summary shows that the area of column technology for CEC is still an active topic of research in the aim of providing high performance columns for solving a wide range of separation problems in the life sciences. This dissertation has contributed to further developing monolithic column technology especially designed for RP-CEC (Chapter II).

#### Overview of Progress Made in Affinity CEC and Affinity Nano-LC

Another principal objective of this dissertation was also to develop monoliths with surface bound bioactive ligands (namely immobilized lectins) for biospecific (affinity) CEC and affinity nano-LC (Chapters III and V). Affinity interactions are complementary to general type of interactions, e.g., RP-CEC, since both modes of electrochromatography can work in concert to solve difficult bio-separation problems. Thus, an overview of previous work done in this area is in order.

Monoliths have also been used for biospecific interaction (affinity) based separations performed in microchannels, e.g., capillaries and microchips, using either a pressure driven flow (i.e., nano LC) or electro-driven flow (i.e., CEC). The separation microchannels are either packed with the affinity stationary phases or their walls are chemically bonded with affinity ligands.

## Affinity Nano-LC

In this section, affinity capturing performed on microchips and in capillaries is referred to as “affinity Nano-LC”. The affinity stationary phase is either bonded to the walls of the separation channel (i.e. open tubular affinity chromatography) or bonded to the packing confined in the separation channel.

The miniaturization of chemical analysis systems, which is referred to as “lab-on-a-chip”, has gained tremendous interest recently due to its potential for automating sample preparation and analysis just to mention a few. A bead based affinity chromatography system, based on photolytic elution was integrated into a glass-silicon microchip to purify specific proteins [106]. In this investigation, the affinity-based beads consisted of photo-cleavable ligands, such as biotin and an RNA aptamer. Yue et al. [107] introduced an integrated microchip with protein digestion and immobilized metal affinity chromatography (IMAC) for phosphopeptide enrichment and utilized  $\beta$ -casein to evaluate their integrated microchip coupled with MS detection. In a more recent investigation, an integrated glass microdevice for proteomics, which directly couples proteolysis with an affinity selection, was introduced [108].

Monolithic capillary columns with surface-immobilized mannan for affinity-based nano-LC and CEC have been reported recently [109]. Two kinds of polymethacrylate monoliths were prepared, namely poly(glycidyl methacrylate-*co*-ethylene dimethacrylate) (GMA-EDMA) and poly(glycidyl methacrylate-*co*-ethylene dimethacrylate-*co*-trimethyl ammonium chloride) (GMA-EDMA-MAETA) to yield neutral and cationic macroporous polymers, respectively. Both types of monoliths with immobilized mannan exhibited strong affinity toward mannose-binding proteins such as

the plant lectins concanavalin A (Con A) and *Lens culinaris* agglutinin (LCA), and a mammalian lectin (e.g., rabbit serum mannose-binding protein). The same monoliths just described (i.e., GMA-EDMA and GMA-EDMA-MAETA) were also used with surface bound lectins for performing lectin affinity chromatography (LAC) [110]. In this study, two lectins including concanavalin A (Con A) and wheat germ agglutinin (WGA) were immobilized onto the monolithic capillary columns. Both types of monoliths with immobilized lectins exhibited strong affinity toward particular glycoproteins and their oligosaccharide chains (i.e., glycans) having sugar sequences recognizable by the lectin. To further demonstrate the effectiveness of LAC, microcolumn separation schemes involving the coupling of lectin capillary columns in series (i.e., tandem columns) for enhanced separation of glycoproteins and their glycoforms were reported recently [111], see chapter III. In this report, the tandem monolithic capillary columns consisted of immobilized LCA and WGA, which generated one peak for each lectin column, i.e., two peaks for the two-lectin columns.

Usually, GMA-based monoliths for affinity chromatography are typically prepared using EDMA as the crosslinking monomer. In an interesting contribution, trimethylpropane trimethacrylate (TRIM) was used as the crosslinking monomer instead of EDMA [112]. The GMA-TRIM monoliths proved to be mechanically more stable than the GMA-EDMA monolith. Besanger *et al.* [113] reported recently on the application of protein doped monolithic silica columns for immobilized enzyme reactor chromatography, which allowed screening of enzyme inhibitors present in mixtures using MS detection. A biotinylated-DNA aptamer that binds adenosine and analogues was immobilized by reaction with streptavidin, which had been covalently attached to porous

chromatographic supports, e.g., 20  $\mu\text{m}$  polystyrene porous particles or 5  $\mu\text{m}$  porous (500 Å) glass beads [114]. Aptamer microparticles have also been packed into fused silica capillaries to yield aptamer-based affinity chromatography columns [115, 116]. It was demonstrated that the aptamer affinity column could selectively retain and separate cyclic adenosine monophosphate (cyclic-AMP), nicotinamide adenine dinucleotide ( $\text{NAD}^+$ ), AMP, adenosine diphosphate (ADP), adenosine triphosphate (ATP) and adenosine, even in complex mixture such as tissue extracts. Affinity nano-LC involving the use of protein G affinity capillary column was demonstrated in noncompetitive immunoassays with laser induced fluorescence detection [116]. Fluorescein isothiocyanate labeled bovine serum albumin (BSA) was used as the tracer to determine monoclonal anti-BSA in pM level.

Although some significant progress have been made in the area of affinity nano-LC, the exploitation of the full potentials of the technique is yet to come. This will require the demonstration of a wider range of immobilized affinity ligands in solving a number of significant separation problems in the life sciences. It should be mentioned that in view of the above description of recent literature, capillary-based affinity nano-LC has been applied to a wider range of affinity-based separations than chip-based affinity nano-LC. This is due in major part to the availability of capillary technology and instrumentation to an increasing number of research and applied laboratories whereas the microfabrication technology is only accessible to a limited number of researchers. However, capillary-based systems that integrate various chromatographic and other events in multidimensional formats are still lacking. The development of such integrated systems are anticipated in the near future, as the nano-valve technology will certainly

make more progress. Despite this technical deficiency, this dissertation has attempted multidimensional separation schemes involving serial lectin affinity nano-LC and RP-CEC of glycopeptides (see Chapter V).

### Affinity Capillary Electrochromatography

In this section, the overview covers investigations dealing with affinity-based electrokinetic separations that were performed in micro-channels containing immobilized affinity ligands in chips and capillaries. An integrated, electroosmotically driven, microfabricated system was recently developed for proteomic analysis by combining trypsin digestion, affinity selection and a reversed phase separation on microchips [117]. The affinity selection step consisted of copper(II) – immobilized metal affinity chromatography [117], which allowed the enrichment of histidine-containing peptides prior to their reversed-phase separation by electrochromatography. Trypsin digestion and Cu(II)-IMAC were performed on particle-based microchannels with a microfabricated frit whereas reversed-phase separations were achieved on a column of collocated monolithic support structures. The microchip technology was also extended to include lectin affinity electrochromatography [118]. Affinity capture on a microchip was also exploited in the rapid determination of concentrations of inflammatory cytokines in the cerebrospinal fluid of patients with head trauma [119]. The selective isolation of the reactive cytokines was achieved by immunoaffinity capture using a panel of six immobilized antibodies directly attached to the injection port of the microchip.

Microcolumn separation schemes involving monolithic capillary columns with immobilized mannan [109] and lectins [111] have been reported. An on-line affinity

selection method using a polymeric support for the retention of histidine-containing peptides and their subsequent separation by CZE was recently described [120]. Also, single stranded oligonucleotides (aptamers) with affinity toward target molecules have been used as stationary phases in affinity CEC [121, 122]. In one instance, a novel aptameric stationary phase for the CEC separation of proteins has been reported [123]. The affinity ligands which consisted of DNA aptamers that form a 4-plane, G-quartet conformation were covalently attached to a capillary surface for open tubular CEC (OTCEC) separation of bovine  $\beta$ -lactoglobulin variants A and B, which vary by 2 of their 162 amino acid residues. Affinity stationary phase were also utilized in concentrators/microreactors prior to capillary electrophoretic separations. In this regards, immunoaffinity based concentrators/microreactors have been developed for many tasks. In one instance, the analyte concentrator was positioned at approximately 10 cm from the inlet of the capillary [124]. This was accomplished by immobilizing the affinity ligands, which were Fab fragments (Fab is the antibody fragment that binds to the antigen), to controlled-pore glass silica, and the resulting immunosorbent was packed into a fused silica capillary between two frit structures. This analyte concentrator was then connected to two separation capillaries by a Teflon sleeve, which was glued to the capillaries by an epoxy resin. The tandem IACEC-CE just described was coupled to mass spectrometry and was demonstrated in the direct and rapid determination of immunoreactive gonadotropin-releasing hormone in serum and urine [124], clinical disease-state marker proteins in human serum [125], used to enhance detection limits [126], analysis of recombinant cytokines in human body fluids [127] and the analysis of intracellular regulatory proteins [128]. A second kind of tandem IACEC – CE involved a four-part

cross – shaped or cruciform configuration for improved on-line solid – phase microextraction prior to CE separation [129]. This cruciform design includes a large-bore tube to transport sample and washing buffers and a small-bore fused-silica capillary for separation of analytes. At the intersection of the transport and separation tubes, a small cavity was fabricated, and is called the analyte concentrator – microreactor. The cavity contains four porous walls or semipermeable membranes (one for each inlet and outlet of the tubes), which permit the confinement of beads or suitable microstructures to which affinity ligands (e.g., antibodies) can be immobilized. This on-line concentration set up was tested with controlled porosity glass beads having immobilized Fab' fragment derived from IgG antibody. The high specificity polyclonal antibodies were individually raised against the acidic nonsteroidal anti-inflammatory drugs ibuprofen and naproxen, and the neuropeptides angiotensin II and neurotensin [129], also in the determination of neurotensin, met-enkephalin and cholecystokinin sulfate in a urine specimen [130]. More details about IACEC – CE can be found in two recent reviews by Guzman and Phillips [131] and Guzman *et al* [132].

Based on the above overview of the published literature, microchip affinity electrochromatography is still in the development stage as its counter part microchip affinity chromatography. This is partly due to the fact that micro-fabrication technology is only accessible to a limited number of research laboratories. Furthermore, although capillary-based affinity electrochromatography has made more progress than microchip affinity electrochromatography, both approaches have not yet found a wide acceptance in the bioanalytical arena, as they still require further development.



This dissertation has addressed this lacking by introducing novel monolithic capillary columns for affinity CEC, and has shown not only the capability of affinity CEC in the selective isolation and concentration of specific analytes, but also its additional advantage over nano-LC in that it allows the separation of captured analytes by virtue of differences in charge-to-mass ratio under the influence of the applied electric field [111]. In affinity nano-LC the captured analytes are usually eluted as a single band upon the application of the eluting mobile phase.

## Some Basic Principles of Capillary Electrochromatography

### Theory of Electroosmotic Flow

The EOF is a consequence of the charges on the solid surface of the packing or monolith as well as the inner wall of the capillary column. For instance, silanol groups at the surface of the silica begin to ionize at  $\text{pH} > 3.5$  and also the solid packing or monoliths with charged moieties can ionize to support the EOF.

When a charged surface comes in contact with an electrolyte solution, an electrical double layer forms thus producing a potential gradient. To balance this charge, counter-ions in solution will begin to accumulate near the charged surface while co-ions are repelled as shown in figure 2a. At the solid (packing, monolith or silica)-liquid interface, due to electrostatic forces, the cations (counter-ions in solution) are tightly bound leading to a compact region or stern-layer, which is immobile. Thermal motion causes some of these ions in the compact region to diffuse further into the solution to form the diffuse region (Gouy-Chapman layer) of the electric double layer. A potential

gradient is established that decreases linearly in the compact region and exponentially in the diffuse region as shown in figure 2b, where  $\psi_o$  and  $\psi_d$  represent the electrical potentials at the solid-solution interface and compact-diffuse region interface. The potential value at the plane of shear (a slipping plane) that is, where bulk solution flows tangentially to the surface is known as the zeta potential ( $\zeta$ ).

The thickness of the electric double layer ( $\delta$ ) is the distance between the compact-diffuse region interface and the point where the potential is equal to  $0.37\psi_d$ , and is given by:

$$\delta = \frac{1}{\kappa} = \left( \frac{\epsilon_o \epsilon_r RT}{2cF^2} \right)^{\frac{1}{2}} \quad (1)$$

where  $\epsilon_o$  is the permeability in vacuum,  $\epsilon_r$  is the dielectric constant of the eluent, R is the universal gas constant, T is the absolute temperature, c is the molar concentration, and F is the Faraday constant. When an electric field is applied, the hydrated counter-ions in the diffuse region migrate towards the opposite electrode (cathode), dragging the bulk solution with it causing the EOF. Because of the frictional forces among the solvent molecules, the bulk liquid moves with the counter-ions in the diffuse layer when an electric field is applied across the capillary [133]. The direction of the EOF is influenced by the sign of the zeta potential whereby, negatively charged surfaces have a negative zeta potential exhibiting a cathodal EOF and vice versa.

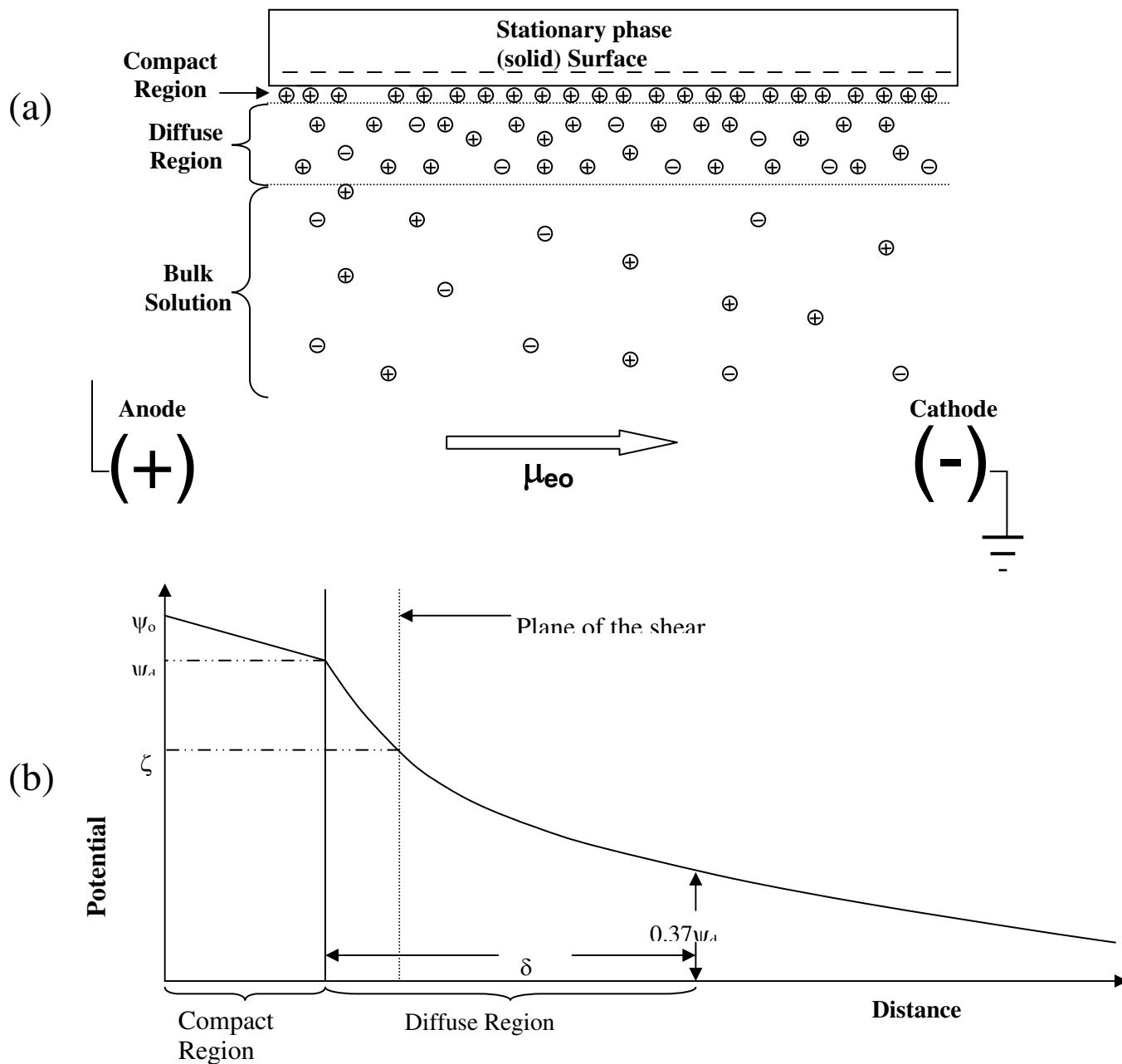


**Figure 2.** Illustration (a) of the electric double layer at solid-liquid interface as well as the generation and direction of EOF, and (b) Stern-Gouy-Chapman model depicting potential gradient with respect to distance from the charged surface.

This generates a plug or flat-flow profile leading to superior or better separation efficiencies unlike that observed with pressure driven flow which exhibit a parabolic flow, leading to band broadening hence low separation efficiencies as shown in Fig. 3.

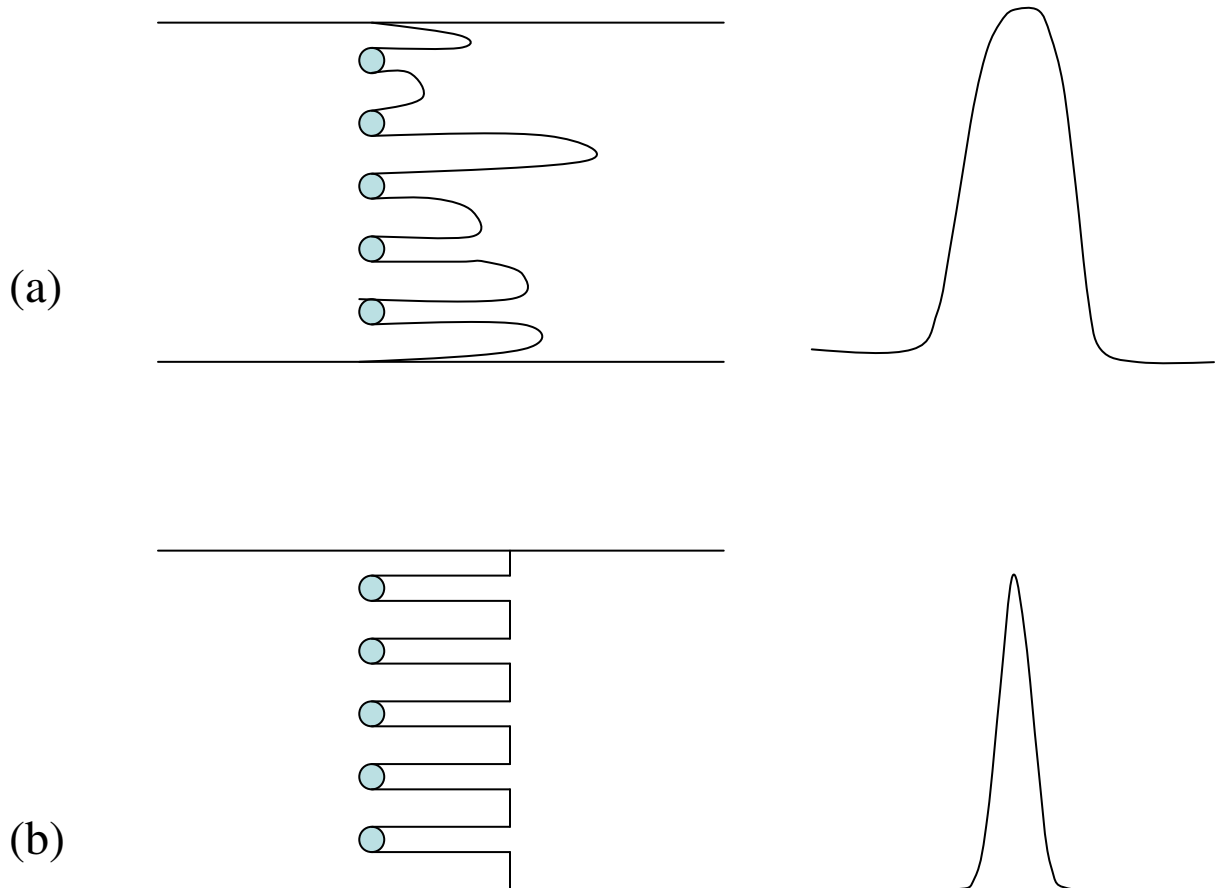


**Figure 3.** Comparison of mobile phase flow profiles and their effect on column efficiency, i.e. band broadening and resulting peak shape. (a) Laminar flow profile observed in pressure or pump-driven methods. (b) Plug/flat flow profile observed in electrically driven methods.

The magnitude of the EOF is dictated by the surface charge densities and the pH of the mobile phase as it affects the ionization of the charged groups on the packing surface and/or the adsorption of the ions from the mobile phase to the solid surface.

### Flow in Packed Columns

The electroosmotic velocity ( $u_{eo}$ ) in packed columns using non conducting porous and non-porous packing particles is given by an expression similar to Smoluchowski's equation [134, 135] and based on Overbeek's suggestion that equation 2 below describes the average EOF generated [136]:

$$u_{eo} = -\frac{\varepsilon\varepsilon_o\zeta_p E}{\eta} \left( \frac{\varphi_{packed}}{\varphi_{open}} \right) \quad (2)$$

Where  $\varepsilon$  is the dielectric constant of the medium,  $\varepsilon_o$  is the permittivity of the vacuum,  $\zeta_p$  is the zeta potential at the surface of the packing material,  $E$  is the electric field strength,  $\eta$  is the viscosity of the bulk solution, and  $\varphi_{packed}$  and  $\varphi_{open}$  are the conductivities of a completely packed column and an open tube, both filled with the electrolyte solution, respectively. The conductivity ratio ( $\varphi_{packed}/\varphi_{open}$ ) is introduced to the equation for application to the packing particles in the capillary. Packed capillaries exhibit lower conductance than a corresponding open capillary, and this ratio can be estimated using the current generated upon the application of an electric field under the same electrolyte solution in packed and empty capillaries.

Equation 2 does not include the size of the particles of the packing material, which seems that a submicron particle size could be used in CEC. However, the particle

size of the packing material has a predicted limit of 0.5  $\mu\text{m}$  in CEC [137]. Overlapping of the electric double layer and thus dramatic decrease in the magnitude of the EOF can occur when the particle size falls within 40 times that of the thickness of the electric double layer [133, 138].

For pressure driven flow, the average velocity ( $v'$ ) in packed columns can be expressed using the Kozeny-Carman equation [139]:

$$v' = \frac{\varepsilon'^2 d_p^2 \Delta p}{180(1-\varepsilon')^2 \eta L} \quad (3)$$

Where  $\varepsilon'$  is the porosity,  $d_p$  is the particle diameter of the stationary phase and  $\Delta p$  is the pressure drop over the length of the column,  $L$ . In pressure driven flow, the particle size is represented in the flow equation, and decreasing particle size would have a two-fold effect on the velocity since column porosity would decrease upon the decrease in particle size of the packing material. This effect on the average flow velocity must be compensated by an increase in applied pressure.

### Retention Factor in CEC

Neutral solutes. Just like in regular HPLC the retention factor for a neutral solute in CEC is similar and is expressed as:

$$k' = \frac{t_m - t_0}{t_0} \quad (4)$$

Where  $k'$  is the dimensionless retention factor,  $t_m$  is the retention or migration time of the retained species and  $t_0$  is the retention time of an inert neutral EOF tracer. To accurately determine the column dead volume, the tracer selected must not interact with the

stationary phase. The components of a sample mixture are separated due to the difference in partition between the stationary and the mobile phase. The higher the degree of partitioning or interaction with the stationary phase, the higher the  $k'$  values which can range from 0 to  $\infty$ , depending on the analyte.

Charged solutes. Upon application of an electric field, the retention of charged solutes in CEC is due to both their electrophoretic mobility and chromatographic partitioning. Under these circumstances,  $k'$  as defined in equation 4 does not represent the chromatographic partitioning as for neutral solutes, rather it is used as a peak locator. An insightful characterization of the migration of a charged solute was introduced by Rathore and Horvath [134, 140]. The retention factor ( $k^*$ ) is used to evaluate the migration of charged solutes in CEC and  $k^*$  is defined as:

$$k^* = \frac{t_m(1 + k_e^*) - t_o}{t_o} \quad (5)$$

Where the velocity factor  $k_e^*$ , describes the contribution of electrophoretic mobility to the separation of a charged species in CEC and is given by:

$$k_e^* = \frac{u_{ep}}{u_{eo}} \quad (6)$$

Where,  $u_{eo}$  is the interstitial electroosmotic velocity of the mobile phase in the CEC column and  $u_{ep}$  is the electrophoretic velocity of the charged solutes. For neutral solutes  $k_e^*$  is zero and equation 5 is condensed back to equation 4 which describes  $k'$  as found in chromatography.  $u_{ep}$  for charged species can be calculated by running the solutes in CZE mode using the same experimental parameters as in CEC. This dissertation will discuss in-depth in chapter II the retention parameters  $k^*$  and  $k_e^*$  of charged solutes in CEC.

### Selectivity Factor

Selectivity factor ( $\alpha$ ) is defined as the measurement of separation of two distinct solute peaks, and is calculated by the ratio of retention factors of the specified solutes:

$$\alpha = \frac{k_2'}{k_1'} \quad (7)$$

where,  $k_2'$  is always greater than  $k_1'$ . Thus,  $1 \leq \alpha \leq \infty$  is a measure of the discriminative power of the chromatographic system. For CEC of charged solutes, we invoke the substitution of  $k'$  for  $k_c^*$  as will be shown in the next chapter.

### Separation Efficiency

In chromatography, the separation efficiency is used to measure the extent of band broadening for eluted peaks. The height equivalent to a theoretical plate  $H$  is used as a measure of efficiency and is defined as the ratio of peak variance ( $\sigma_L^2$ ) in unit length to the column effective length ( $l$ ).

$$H = \frac{\sigma_L^2}{l} \quad (8)$$

The number of theoretical plates per column ( $N$ ) is a dimensionless value defined as  $N = l/H$  and is used for expressing separation efficiency. Often,  $N$  is divided by the effective length of the column ( $l$ ) to give a better indication of the degree of band broadening per unit length and is given in units of plates per meter. By substituting  $H$  from equation 8 and using migration time  $t_m$ , obtained from the chromatogram instead of column effective length,  $N$  is expressed as:



$$N = \frac{l^2}{\sigma_L^2} = \left( \frac{t_m}{\sigma_t} \right)^2 \quad (9)$$

The peak standard deviation  $\sigma_t$  is also easily obtained from the electrochromatogram. The CEC peaks are usually approximated as Gaussian distributions, and peak variance can be calculated from the peak width at base ( $w_b$ ), half height ( $w_h$ ) or at the inflection point ( $w_i$ ) and are equal to  $4\sigma$ ,  $2.354\sigma$  and  $2\sigma$ , respectively. The inflection point is located at 0.607 of peak height. Thus substitution for  $\sigma$  yields:

$$N = 4 \left( \frac{t_m}{w_i} \right)^2 = 5.54 \left( \frac{t_m}{w_h} \right)^2 = 16 \left( \frac{t_m}{w_b} \right)^2 \quad (10)$$

### Resolution

Resolution ( $R_s$ ) measures the extent of separation between 2 adjacent peaks. It is calculated from the electrochromatogram by the ratio of the difference between the migration times of the 2 adjacent peaks ( $\Delta t_m$ ) to the average bandwidth of both peaks at base ( $w = 4 \overline{\sigma_t}$ ) as follows:

$$R_s = \frac{\Delta t_m}{4 \overline{\sigma_t}} \quad (11)$$

where  $\overline{\sigma_t}$  is the mean standard deviation of the two peaks. Resolution is a function of the selectivity, retention factor and efficiency as can be seen in equation 12:

$$R_s = \left( \frac{\alpha - 1}{\alpha} \right) \left( \frac{k_2'}{1 + k_2'} \right) \left( \frac{\sqrt{N}}{4} \right) \quad (12)$$

where  $k_2'$  is the retention factor of the more retained peak of the two adjacent peaks. Therefore, we need optimal conditions of the three parameters  $N$ ,  $\alpha$  and  $k'$  to achieve high resolution and promote maximum separation. For CEC of charged solutes  $k_c^*$  reflects  $k'$ .

### Band Broadening

To fully understand the superior separation efficiency of CEC, it is worthwhile to explore the factors that contribute to band broadening. The basic measure of band broadening is the variance of a Gaussian peak. Statistical theory has it that, the variance of a complex random process equals the sum of the variances generated by the individual processes, provided that they are independent, i.e., the processes are not coupled. Therefore, for an electrochromatographic peak, the observed variance,  $\sigma^2$ , may be expressed as:

$$\sigma^2 = \sigma_{\text{joule}}^2 + \sigma_{\text{inj}}^2 + \sigma_{\text{det}}^2 + \sigma_{\text{conn}}^2 + \sigma_{\text{col}}^2 \quad (13)$$

where  $\sigma_{\text{joule}}^2$ ,  $\sigma_{\text{inj}}^2$ ,  $\sigma_{\text{det}}^2$ ,  $\sigma_{\text{conn}}^2$  and  $\sigma_{\text{col}}^2$  are the variance associated with the band broadening due to Joule heat, injection, detection, connections and column, respectively.

Since the plate height  $H$  is proportional to the peak variance (see equation 8).  $H$  is therefore expected to obey the same additivity rule as the variance. Thus, the plate height of a chromatographic peak is expressed as the sum of increments arising from the process that contribute independently to band broadening as follows:

$$H_{\text{obs}} = H_{\text{joule}} + H_{\text{inj}} + H_{\text{det}} + H_{\text{conn}} + H_{\text{col}} \quad (14)$$

Where the contributions of Joule heating ( $H_{\text{joule}}$ ), sample injection ( $H_{\text{inj}}$ ), detection ( $H_{\text{det}}$ ), column connections ( $H_{\text{conn}}$ ) and column itself ( $H_{\text{col}}$ ) are additive. The first four terms of

equations 13 and 14 are associated with the extra-column band broadening processes and can be minimized. Indeed, column connections are not a major factor in CEC, however, plate height contribution resulting from heat generated by the passage of current, or Joule heat ( $H_{\text{joule}}$ ) is a major extra-column contributor to the observed band broadening. Also, detection is usually performed on column and sample injection is made directly as a thin plug at the inlet end of the column. Non-uniform temperature gradients and in turn local changes in viscosity are caused by joule heating which leads to band broadening. However the effect of  $H_{\text{joule}}$  can be minimized in most applications by using supporting electrolytes in the mobile phase with low conductivity (e.g. low ionic strength and low ionic mobility). Also, narrow bore capillaries for efficient heat dissipation and field strengths of 1000 v/cm or less, with control of column temperature. Band broadening between pressure and electro driven conditions have been studied and it has been reported that plate height contributions from  $H_{\text{joule}}$ ,  $H_{\text{inj}}$  and  $H_{\text{det}}$  were all negligible compared to  $H_{\text{col}}$  and hence the observed plate height is determined by the passage of the sample through the column [141]. For LC techniques, factors affecting  $H_{\text{col}}$  include: flow maldistribution ( $H_f$ ), longitudinal molecular diffusion ( $H_{\text{md}}$ ) and mass transfer resistance in the pore ( $H_p$ ). Dropping the negligible terms equation 14 changes to:

$$H_{\text{obs}} = H_f + H_{\text{md}} + H_p \quad (15)$$

When we substitute the corresponding parameters that define these plate height contributions into equation 15 we obtain the van Deemter equation, which is usually represented in a simplified manner by summing up the constants (A, B and C) for the given set of conditions and relating each plate height contributor in terms of mobile phase velocity:

$$H = A + \frac{B}{u} + Cu \quad (16)$$

Figure 4 illustrates a typical Van Deemter plot and the relative plate height contributions of each term in the van Deemter equation as a function of mobile phase velocity. The optimum flow velocity ( $u_{opt}$ ) produces the minimum plate height ( $H_{min}$ ). Longitudinal molecular diffusion term ( $B/u$ ) is dependent on the nature of the solute, and increasing mobile phase velocity can minimize this term. The mass transfer resistance in the pores ( $Cu$ ) increases with increasing mobile phase velocity. This diffusional mass transfer resistance is decreased in CEC due to the generated EOF within the flow through pores, which increases kinetics associated with the mass transfer [141].

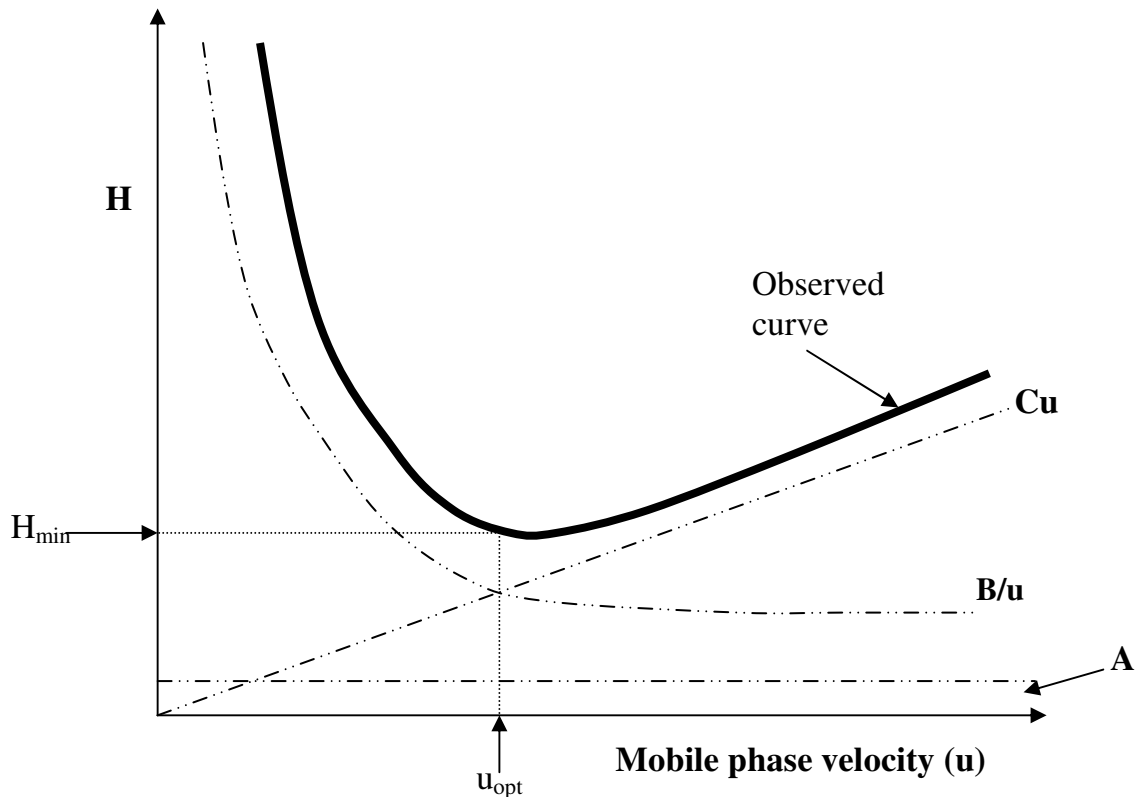


**Figure 4.** Illustration of the plate height contribution for each van-Deemter term and the resulting observed curve.

The greatest gain in CEC separation efficiency results from decreasing the maldistribution of flow (the A term) observed in pressure driven flow in packed columns, which is also known as “eddy diffusion” [139]. The “A” term becomes negligible in determining the overall separation efficiency because of plug flow profile in CEC. Hence, the overall higher separation efficiency in CEC compared to pressure-driven LC is attributed to reducing the broadening effects in both the A and C terms of the van Deemter equation. The end result being reduced band broadening effects, and separation efficiencies that are 5-10 times better than those for pressure-driven mode and the same conditions.

#### Rationale of the Investigation

As featured above, CEC is in fact an important microseparation technique. Although significant advances have been made, many aspects of CEC, and principally column technology (i.e., the heart of the separation process), still requires further development to realize the full potentials of the technique.

The broad objective of this research entails an integrated approach to furthering the advancement of CEC by providing (i) improved design of stationary phase for use in reversed-phase CEC for the separation of complex biomolecules (e.g., peptides, glycopeptides and proteins just to mention a few), (ii) ensuring a relatively strong EOF without the presence of fixed charges on the stationary phase surface but still achieve fast analysis and good chromatographic selectivity and (iii) the development of biospecific (affinity) interactions in microcolumns, e.g., affinity CEC and affinity nano-LC for the selective isolation and separation of minute amounts of biopolymers.

The major problem encountered in CEC of biopolymers with the presence of fixed charges on the stationary phase surface, which are meant to support EOF, has been the pronounced electrostatic interaction of macromolecules with the negatively or positively charged surfaces, thus resulting in mixed mode retention mechanism, which complicates the optimization of the separation conditions. Furthermore, the presence of electrostatic interactions in addition to nonpolar retention often gives rise to band broadening and low recovery of the separated analytes. To provide a solution to this problem we have developed and evaluated a neutral C17-monolithic stationary phase devoid of fixed charges but still having a relatively strong EOF for CEC (Chapter II). This monolith proved effective in RP-CEC and allowed high separation efficiencies of different biopolymers, including proteins, peptides and glycoconjugates. Studies involving the detailed characterization of this monolith and its robustness are the subject of Chapters II, IV and V for a wide range of biological species.

On another front, we have developed specially designed monoliths for affinity CEC and affinity nano-LC based on poly(glycidylmethacrylate) polymers with immobilized lectins for affinity separation of glycopeptides and glycoproteins. Chapters III and V describe single and tandem lectin monolithic capillary columns in CEC and nano-LC separations of glycoproteins and glycopeptides. Finally, Chapter V introduces the serial use of lectin affinity nano-LC and RP-CEC for the sequential capturing and separation of glycopeptides. In these novel serial schemes, the glycopeptides are first captured on a given lectin column by nano-LC, and then transferred to a C17 monolithic capillary column for further separation by RP-CEC.

The overall investigation described in this dissertation has contributed to enlarging the scope of CEC by demonstrating its capabilities in areas that were not exploited previously. Also, the novel stationary phases developed within the framework of this investigation will not only facilitate the solution of many important analytical separation problems in the life sciences, but will also contribute to new concepts that will open the way to increasing the utility of the technique in the future.

### Conclusions

This chapter has provided the reader with an introduction to the instrumentation and column technology used in CEC as well as an overview of the various separation principles of CEC. Furthermore, this chapter has summarized and discussed the advances made in the various kinds of polymer-based monolithic columns including those bearing affinity ligands on their surface. Also, a summary of the rationale of the study was given as the last part of this chapter.

## References

- (1) Pyell, U. *Anal. Bioanal. Chem.* **2003**, 375, 20-22.
- (2) Patel, K., Jerkovich, A., Link, J., Jorgenson, J. *Anal. Chem.* **2004**, 76, 5777-5786.
- (3) Mistry, K., Krull, I., Grinberg, N. *J. Sep. Sci.* **2002**, 25, 935-958.
- (4) Miksik, I., Deyl, Z. *J. Chromatogr. Lib.* **2003**, 67, 623-658.
- (5) Lynen, F.; Buica, A., de Villiers, A., Crouch, A., Sandra, P. *J. Sep. Sci.* **2005**, 28, 1539-1549.
- (6) Jiskra, J., Claessens, H., Cramers, C. *J. Sep. Sci.* **2003**, 26, 1305-1330.
- (7) Eeltink, S., Rozing, G., Kok, W. *Electrophoresis* **2003**, 24, 3935-3961.
- (8) Bedair, M., El Rassi, Z. *Electrophoresis* **2004**, 25, 4110-4119.
- (9) Klodzinska, E., Moravcova, D., Jandera, P., Buszewski, B. *J. Chromatogr.A* **2006**, 1109, 51-59.
- (10) Tiselius, A. *Biochem. J.* **1937**, 31, 313-317.
- (11) Tiselius, A. *Biochem. J.* **1937**, 31, 1464-1477.
- (12) Strain, H. *J. Am. Chem. Soc.* **1939**, 61, 1292-1293.
- (13) Mould, D., Synge, R. *Analyst.* **1952**, 77, 964-970.
- (14) Mould, D., Synge, R. *Biochem. J.* **1954**, 58, 571-585.
- (15) Pretorius, V., Hopkins, B., Schieke, J. *J. Chromatogr.* **1974**, 99, 23-30.
- (16) Jorgenson, J., DeArman, L. *J. Chromatogr.* **1981**, 218, 209-216.
- (17) Jorgenson, J., Lukacs, K. *Anal. Chem.* **1981**, 53, 1298-1302.
- (18) Knox, J., Grant, I. *Chromatographia* **1987**, 24, 135-143.
- (19) Knox, J. *Chromatographia* **1988**, 26, 329-337.
- (20) Knox, J., Grant, I. *Chromatographia* **1991**, 32, 317-328.



- (21) Smith, N., Evans, M. *Chromatographia* **1994**, 38, 649-657.
- (22) Rathore, A., Horvath, C. *Anal. Chem.* **1998**, 70, 3069-3077.
- (23) Dittmann, M., Rozing, G., Ross, G.; Adam, T., Unger, K. *J. Cap. Electrophoresis* **1997**, 4, 201-212.
- (24) Ross, G., Kaltenbach, P., Heiger, D. *Today's Chemist Work* **1997**, 6, 31-36.
- (25) Heiger, D., Kaltenbach, P., Sievert, H. *Electrophoresis* **1994**, 15, 1234-1247.
- (26) Dadoo, R., Yan, C., Zare, R., Anex, D., Rakestraw, D., Hux, G. *LC-GC* **1997**, 15, 630-632, 634-635.
- (27) Klampfl, C. *J. Chromatogr., A* **2004**, 1044, 131-144.
- (28) Lazar, L., Li, L., Yang, Y., Karger, B. *Electrophoresis* **2003**, 24, 3655-3662.
- (29) Ivanov, A., Horvath, C., Karger, B. *Electrophoresis* **2003**, 24, 3663-3673.
- (30) Gucek, M., Gaspari, M., Walhagen, K., Vreeken, R., Verheij, E., Van der Greef, J. *Rapid Commun. Mass Spec.* **2000**, 14, 1448-1454.
- (31) Gaspari, M., Gucek, M., Walhagen, K., Vreeken, R., Verheij, E., Tjaden, U., Van der Greef, J. *J. Microcolumn Sep.* **2001**, 13, 243-249.
- (32) Walhagen, K., Gaspari, M., Tjaden, U., Rozing, G., Van der Greef, J. *Rapid Commun. Mass Spectrom.* **2001**, 15, 878-883.
- (33) Que, A., Mechref, Y., Huang, Y., Taraszka, J., Clemmer, D., Novotny, M. *Anal. Chem.* **2003**, 75, 1684-1690.
- (34) Von Brocke, A., Wistuba, D., Gfrorer, P., Stahl, M., Schurig, V., Bayer, E. *Electrophoresis* **2002**, 23, 2963-2972.
- (35) Que, A., Palm, A., Baker, A., Novotny, M. *J. Chromatogr., A* **2000**, 887, 379-391.

- (36) Schewitz, J., Gfroerer, P., Pusecker, K., Tseng, L., Albert, K., Bayer, E., Wilson, I., Bailey, N., Scarfe, G., Nicholson, J., Lindon, J. *Analyst* **1998**, *123*, 2835-2837.
- (37) Pusecker, K., Schewitz, J., Gfroerer, P., Tseng, L., Albert, K., Bayer, E. *Anal. Chem.* **1998**, *70*, 3280-3285.
- (38) Gfroerer, P., Schewitz, J., Pusecker, K., Tseng, L., Albert, K., Bayer, E. *Electrophoresis* **1999**, *20*, 3-8.
- (39) Svec, F. *J. Sep. Sci.* **2004**, *27*, 1255-1272.
- (40) Maloney, T., Colon, L. *J. Sep. Sci.* **2002**, *25*, 1215-1225.
- (41) Patel, K., Jerkovich, A., Link, J., Jorgenson, J. *Anal. Chem.* **2004**, *76*, 5777-5786.
- (42) Vanhoenacker, G., Van den Bosch, T., Rozing, G., Sandra, P. *Electrophoresis* **2001**, *22*, 4064-4103.
- (43) Eeltink, S., Rozing, G., Schoenmakers, P., Kok, W. *J. Sep. Sci.* **2004**, *27*, 1431-1440.
- (44) Yang, C., El Rassi, Z. *Electrophoresis* **1998**, *19*, 2061-2067.
- (45) Yang, C., El Rassi, Z. *Electrophoresis* **1999**, *20*, 18-23.
- (46) Zhang, M., El Rassi, Z. *Electrophoresis* **1998**, *19*, 2068-2072.
- (47) Smith, N., Evans, M. B. *J. Chromatogr., A* **1999**, *832*, 41-54.
- (48) Colon, L., Maloney, T., Fermier, A. *J. Chromatogr., A* **2000**, *887*, 43-53.
- (49) Stol, R., Mazereeuw, M., Tjaden, U., van der Greef, J. *J. Chromatogr., A* **2000**, *873*, 293-298.
- (50) Tang, Q., Xin, B., Lee, M. *J. Chromatogr., A* **1999**, *837*, 35-50.
- (51) Adam, M., Colon, L. *J. Microcolumn Sep.* **1998**, *10*, 439-447.

- (52) Kapnissi-christodoulou, C., Zhu, X., Warner, I. *Electrophoresis* **2003**, *24*, 3917-3934.
- (53) Tang, Q., Lee, M. *Trends Anal. Chem.* **2000**, *19*, 648-663.
- (54) Swart, R., Kraak, J., Poppe, H. *Chromatographia* **1995**, *40*, 587-593.
- (55) Pesek, J., Matyska, M., Menezes, S. *J. Chromatogr., A* **1999**, *853*, 151-158.
- (56) Malik, A. *Electrophoresis* **2002**, *23*, 3973-3992.
- (57) Pesek, J., Matyska, M. *J. Chromatogr. Lib.* **2001**, *62*, 241-270.
- (58) Liu, H., Cho, B., Strong, R., Krull, I., Cohen, S., Chan, K., Issaq, H. *Anal. Chim. Acta* **1999**, *400*, 181-209.
- (59) Liu, Z., Wu, R., Zou, H. *Electrophoresis* **2002**, *23*, 3954-3972.
- (60) Sawada, H., Jinno, K. *Electrophoresis* **1999**, *20*, 24-30.
- (61) Constantin, S., Freitag, R. *J. Chromatogr., A* **2000**, *887*, 253-263.
- (62) Hayes, J., Malik, A. *Anal. Chem.* **2001**, *73*, 987-996.
- (63) Koide, T., Ueno, K. *J. Chromatogr., A* **2001**, *909*, 305-315.
- (64) Eeltink, S., Rozing, G., Schoenmakers, P., Kok, W. *J. Chromatogr., A* **2006**, *1109*, 74-79.
- (65) Laemmerhofer, M., Lindner, W. *J. Chromatogr. Lib.* **2003**, *67*, 489-559.
- (66) Hilder, E., Svec, F., Frechet, J. *Electrophoresis* **2002**, *23*, 3934-3953.
- (67) Allen, D., El Rassi, Z. *Electrophoresis* **2003**, *24*, 3962-3976.
- (68) Tanaka, N., Motokawa, M., Kobayashi, H., Hosoya, K., Ikegami, T. *J. Chromatogr. Lib.* **2003**, *67*, 173-196.
- (69) Dabek-zlotorzynska, E., Chen, H., Ding, L. *Electrophoresis* **2003**, *24*, 4128-4149.
- (70) Wistuba, D., Schurig, V. *J. Chromatogr., A* **2000**, *875*, 255-276.

- (71) Chankvetadze, B. *Meths. Mol. Biol.* **2004**, *243*, 387-399.
- (72) Scriba, G. *Electrophoresis* **2003**, *24*, 2409-2421.
- (73) Fu, H., Huang, X., Jin, W., Zou, H. *Curr. Opin. Biotech.* **2003**, *14*, 96-100.
- (74) Scriba, G. *Electrophoresis* **2003**, *24*, 4063-4077.
- (75) Huck, C., Stecher, G., Bakry, R., Bonn, G. *Electrophoresis* **2003**, *24*, 3977-3997.
- (76) Kasicka, V. *Electrophoresis* **2003**, *24*, 4013-4046.
- (77) Svec, F., Peters, E. C., Sykora, D., Frechet, J. J. *J. Chromatogr., A* **2000**, *887*, 3-29.
- (78) Svec, F. In *Capillary Electrochromatography*; Deyl, Z., Svec, F., Ed.; Elsevier: Amsterdam, 2001, pp 183-240.
- (79) Viklund, C., Svec, F., Frechet, Jean, J., Irgum, K. *Chem. Materials* **1996**, *8*, 744-750.
- (80) Lammerhofer, M., Svec, F., Frechet, J., Lindner, W. *J. Chromatogr. A* **2001**, *925*, 265-277.
- (81) Safrany, A., Beiler, B., Laszlo, K., Svec, F. *Polymer* **2005**, *46*, 2862-2871.
- (82) Eeltink, S., Herrero-Martinez, J., Rozing, G., Schoenmakers, P., Kok, W. *Anal. Chem.* **2005**, *77*, 7342-7347.
- (83) Palm, A., Novotny, M. *Anal. Chem.* **1997**, *69*, 4499-4507.
- (84) Xie, S., Svec, F., Frechet, J. J. *J. Chromatogr., A* **1997**, *775*, 65-72.
- (85) Zhang, M., El Rassi, Z. *Electrophoresis* **2001**, *22*, 2593-2599.
- (86) Plieva, F., Andersson, J., Galaev, I., Mattiasson, B. *J. Sep. Sci.* **2004**, *27*, 828-836.
- (87) Wahl, A., Schnell, I., Pyell, U. *J. Chromatogr., A* **2004**, *1044*, 211-222.
- (88) Hoegger, D., Freitag, R. *Electrophoresis* **2003**, *24*, 2958-2972.
- (89) Wang, C., Svec, F., Frechet, J. *Anal. Chem.* **1993**, *65*, 2243-2248.

- (90) Petro, M., Svec, F., Gitsov, I., Frechet, J. *Anal. Chem.* **1996**, 68, 315-321.
- (91) Petro, M., Svec, F., Frechet, J. *J. Chromatogr., A* **1996**, 752, 59-66.
- (92) Gusev, I., Huang, X., Horvath, C. *J. Chromatogr., A* **1999**, 855, 273-290.
- (93) Zhang, S., Zhang, J., Horvath, C. *J. Chromatogr. A* **2001**, 914, 189-178.
- (94) Xiong, B., Zhang, L., Zhang, Y., Zou, H., Wang, J. *J. High Resolut. Chromatogr.* **2000**, 23, 67-72.
- (95) Jin, W., Fu, H., Huang, X., Xiao, H., Zou, H. *Electrophoresis* **2003**, 24, 3172-3180.
- (96) Aoki, H., Kubo, T., Ikegami, T., Tanaka, N., Hosoya, K., Tokuda, D., Ishizuka, N. *J. Chromatogr., A* **2006**, 1119, 66-79.
- (97) Svec, F., Frechet, J. *J. Chromatogr., A* **1995**, 702, 89-95.
- (98) Svec, F., Frechet, J. *Biotech. Bioeng.* **1995**, 48, 476-480.
- (99) Peters, E., Svec, F., Frechet, J. *Adv. Materials* **1997**, 9, 630-633.
- (100) Urban, J., Moravcova, D., Jandera, P. *J. Sep. Sci.* **2006**, 29, 1064-1073.
- (101) Huang, H., Chiu, C., Huang, I., Lee, S. *J. Chromatogr., A* **2005**, 1089, 250-257.
- (102) Huang, H., Chiu, C., Huang, I., Yeh, J. *Electrophoresis* **2004**, 25, 3237-3246.
- (103) Szumski, M., Klodzinska, E., Buszewski, B. *J. Chromatogr. A* **2005**, 1084, 186-193.
- (104) Klodzinska, E., Dahm, H., Jackowski, M., Buszewski, B. *LC-GC Eur.* **2005**, 18, 472-478.
- (105) Okanda, F. M., El Rassi, Z. *Electrophoresis* **2005**, 26, 1988-1995.
- (106) Chung, W., Kim, M., Cho, S., Park, S., Kim, J., Kim, Y., Kim, B., Lee, Y. *Electrophoresis* **2005**, 26, 694-702.

- (107) Yue, G., Balchunas, C., Jeffery, E., Coon, J., Landers, J., Ferrance, J. *Royal Soc. Chem.* **2004**, 297, 291-293.
- (108) Yue, G., Roper, M., Balchunas, C., Pulsipher, A., Coon, J., Shabanowitz, J., Hunt, D., Landers, J., Ferrance, J. *Anal. Chim. Acta* **2006**, 564, 116-122.
- (109) Bedair, M., El Rassi, Z. *J. Chromatogr. A* **2004**, 1044, 177-186.
- (110) Bedair, M., El Rassi, Z. *J. Chromatogr. A* **2005**, 1079, 236-245.
- (111) Okanda, F. M., El Rassi, Z. *Electrophoresis* **2006**, 27, 1020-1030.
- (112) Pan, Z., Zou, H., Mo, W., Huang, X., Wu, R. *Anal. Chim. Acta* **2002**, 466, 141-150.
- (113) Besanger, T., Hodgson, R., Green, J., Brennan, J. *Anal. Chim. Acta* **2006**, 564, 106-115.
- (114) Deng, Q., German, I., Buchanan, D., Kennedy, R. *Anal. Chem.* **2001**, 73, 5415-5421.
- (115) Connor, A., McGown, L. *J. Chromatogr. A* **2006**, 1111, 115-119.
- (116) Wang, Q., Luo, G., Ou, J., Yeung, W. S. B. *J. Chromatogr. A* **1999**, 848, 139-148.
- (117) Slentz, B., Penner, N., Regnier, F. E. *J. Chromatogr. A* **2003**, 984, 97-107.
- (118) Mao, X., Luo, Y., Dai, Z., Wang, K., Du, Y., Lin, B. *Anal. Chem.* **2004**, 76, 6941-6947.
- (119) Phillips, T. M. *Electrophoresis* **2004**, 25, 1652-1659.
- (120) Vizioli, N., Russell, M., Carbajal, M., Carducci, C., Grasselli, M. *Electrophoresis* **2005**, 26, 2942-2948.
- (121) Kotia, R., Li, L., McGown, L. *Anal. Chem.* **2000**, 72, 827-831.
- (122) Clark, S., Remcho, V. *Anal. Chem.* **2003**, 75, 5692-5696.

- (123) Rehder, M., McGown, L. *Electrophoresis* **2001**, 22, 3759-3764.
- (124) Guzman, N. A. *J. Chromatogr. B* **2000**, 749, 197-213.
- (125) Dalluge, J., Sander, L. *Anal. Chem.* **1998**, 70, 5339-5343.
- (126) Thomas, D., Rakestraw, D., Schoeniger, J., Lopez-Avila, V., Van Emon, J. *Electrophoresis* **1999**, 20, 57-66.
- (127) Phillips, T. M., Dickens, B. F. *Electrophoresis* **1998**, 19, 2991-2996.
- (128) Phillips, T., Smith, P. *Biomed. Chromatogr.* **2003**, 17, 182-187.
- (129) Guzman, N. A. *Electrophoresis* **2003**, 24, 3718-3727.
- (130) Guzman, N. *Anal. Bioanal. Chem.* **2004**, 378, 37-39.
- (131) Guzman, N., Phillips, T. *Anal. Chem.* **2005**, 77, 61A-67A.
- (132) Guzman, N., Stubbs, R., Phillips, T. *Drug Discovery Today: Technologies* **2006**, 3, 29-37.
- (133) Vegvari, A., Guttman, A. *Electrophoresis* **2006**, 27, 716-725.
- (134) Rathore, A. *Electrophoresis* **2002**, 23, 3827-3846.
- (135) Rathore, A., Horvath, C. *J. Chromatogr. Lib.* **2001**, 62, 1-38.
- (136) Overbeek, J. In *Colloid Science*; Kruyt, H., Ed.; Elsevier: New York, 1952, pp 115-139 and 194-244.
- (137) Smith, N., Evans, M. *Chromatographia* **1995**, 41, 197-203.
- (138) Li, P., Harrison, J. *Anal. Chem.* **1997**, 69, 1564-1568.
- (139) Giddings, J. *Unified Separation Science*; Wiley: New York, 1991.
- (140) Rathore, A., Horvath, C. *Electrophoresis* **2002**, 23, 1211-1216.
- (141) Wen, E., Horvath, C. *J. Chromatogr. A* **1999**, 855, 203-216.

CHAPTER II

PREPARATION OF NEUTRAL STEARYL-ACRYLATE  
MONOLITHS AND THEIR EVALUATION IN CAPILLARY  
ELECTROCHROMATOGRAPHY OF NEUTRAL  
AND CHARGED SMALL SPECIES  
AS WELL AS PEPTIDES  
AND PROTEINS

Introduction

Polymeric monolithic stationary phases are increasingly employed in capillary and microchip electrochromatography for the separation of various compounds, for recent reviews see Refs [1-3]. This is due primarily to the fact that monolithic stationary phases combine the best features of the two traditional column configurations, namely open tubular capillary columns and particulate packed capillary columns, where in the former case the column is fritless and of high permeability while in the latter case the column is characterized by its high phase ratio and sample capacity. In fact, monolithic

---

*\* The content of this chapter has been published in Electrophoresis, 2005, 26, 1988-1995*



capillary columns offer these four sound features. In addition, monolithic capillary columns can be readily prepared by *in situ* polymerization of a wide variety of monomers thus yielding tailor made stationary phases to solve difficult separation problems.

This investigation is concerned with the preparation of neutral non-polar monoliths with a relatively strong electroosmotic flow (EOF), in order to allow the CEC separation of charged species (e.g., proteins) in the absence of undesirable electrostatic interactions with surface fixed charges and to bring about the rapid elution of charged solutes. Such stationary phases are very desirable for performing reversed-phase CEC of proteins and peptides at neutral pH. While the preparation of monoliths void of fixed charges is rather a straightforward process involving the *in situ* polymerization of neutral monomers, the production of neutral monoliths having strong EOF is rather a delicate task and can only be achieved with particular monoliths the surface of which has the tendency to adsorb electrolyte ions from the mobile phase. These surface adsorbed ions impart the zeta potential thus supporting the EOF necessary for mass transport. In a recent investigation, Bedair and El Rassi developed cationic stearyl-acrylate monoliths (called cationic PEDAS monoliths), which exhibited the ability to adsorb electrolyte ionic components from the mobile phase, a fact that facilitated the alteration of the magnitude and direction of the EOF. This finding triggered the present investigation, which is aimed at producing a viable neutral non-polar PEDAS monolith (see structure of the monomer in Fig. 1) for reversed-phase CEC at zero electrostatic interactions with charged solutes. Previously, two attempts have been made to produce neutral monoliths [4, 5]. In one report, the neutral monolithic column was prepared by the copolymerization of butyl methacrylate (BMA) and ethylene dimethacrylate (EDMA) [4].

This neutral monolith did not exhibit an EOF and allowed the separation of small acidic solutes mainly via their differential electromigration.

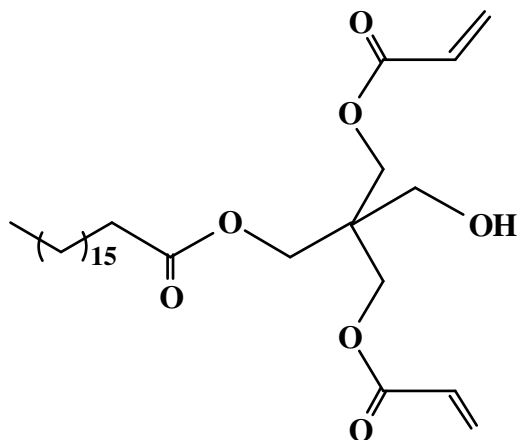


**Figure 1.** Structure of pentaerythritol diacrylate monostearate (PEDAS) used in the preparation of the neutral monolith. Each PEDAS monomer has in addition to the C17 alkyl chain 4 polar functional groups including 3 ester groups and one hydroxyl group.

In a second and more recent report, Horváth and co-workers [5] developed a neutral monolith with annular EOF generation where the inner wall of the capillary was grafted in a two step process with polyethylene imine to form a layer of positively charged amines to support the generation of an annular EOF. The actual monolith was produced in a subsequent polymerization of vinylbenzene chloride and EDMA. The resulting column was demonstrated in the CEC of small peptides at low pH (e.g., pH 2.5) where the peptides carry a net positive charge thus minimizing solute-wall interactions. Thus, while the first monolith obtained by co-polymerization of BMA and EDMA produced no EOF [4], the second monolith with annular EOF generation [5] still has

fixed charges on the capillary wall, which constitute active adsorption sites for charged solutes.

In the aim of reducing solute electrostatic interaction with the fixed charges on the monolith surface, shielded stationary phases consisting of charged AMPS at the monolith surface covered by a top layer of poly(butyl methacrylate) was very recently introduced by Hilder et al. [6]. This is not a neutral monolith but constitutes a viable strategy for reducing electrostatic interaction, which is worth mentioning here.

Thus, it is the aim of this investigation to develop a neutral non-polar monolith at relatively strong EOF and zero electrostatic interactions. As will be shown in this report, such monolithic capillary columns are ideal for the reversed-phase CEC of proteins and peptides at neutral pH.

## Experimental

### Instrumentation

The instrument used for CE/CEC was a P/ACE 2000 CE system from Beckman (Fullerton, CA, USA) equipped with a fixed wavelength UV detector and a personal computer running a Gold P/ACE system. The column temperature was held constant at 23 °C. All samples were injected electrokinetically for 10 s and at various applied voltages, which are stated in the figure captions.

## Reagents and Materials

Pentaerythritol diacrylate monostearate (PEDAS), ethylene dimethacrylate (EDMA), butyl methacrylate (BMA), methyl methacrylate (MMA), ethyl methacrylate (EMA), 2,2'-azobisisobutyronitrile (AIBN) and 3-(trimethoxysilyl)propylmethacrylate, alkyl benzenes and analytical-grade acetone were purchased from Aldrich (Milwaukee, WI, USA). Cyclohexanol and 1,4-butanediol were purchased from J. T. Baker (Phillipsburg, NJ, USA). Ethylene glycol (EG) and HPLC grade acetonitrile (ACN) were from Fisher Scientific (Fair Lawn, NJ, USA). Proteins, peptides and dansyl amino acids (Dns-AA) were purchased from Sigma (St. Louis, MO, USA). Buffer solutions were prepared using sodium phosphate monobasic from Mallinckrodt (Paris, KY, USA), tetrabutylammonium bromide from Fluka, AG (Switzerland) and tris (hydroxymethyl) aminomethane from Fisher. Fused-silica capillaries with an internal diameter (I.D.) of 100  $\mu\text{m}$  and an outer diameter (O.D.) of 360  $\mu\text{m}$  were from Polymicro Technologies (Phoenix, AZ, USA).

## Column Pretreatment

The inner wall of the fused-silica capillary was treated with 1.0 M sodium hydroxide for 30 min, flushed with 0.10 M hydrochloric acid for 30 min, and then rinsed with water for 30 min. The capillary inner wall was then allowed to react twice with a solution of 50% (v/v) of 3-trimethoxysilylpropyl methacrylate in acetone for 20 min each at room temperature to vinylize the inner wall of the capillary. Finally, the capillary was rinsed with acetone and water and dried with a stream of nitrogen.

### *In situ* Polymerization

Polymerization solutions weighing 1.48 g each were prepared from monomers (PEDAS, PEDAS/EDMA, PEDAS/EMA, PEDAS/MMA, PEDAS/BMA or PEDAS/EDMA/EMA) and porogenic solvents in ratios of 30:70 w/w monomers/solvents. The mixtures of monomers were weighed in different ratios, and then dissolved in ternary porogenic solvents consisting of 96.4 wt% of cyclohexanol/ethylene glycol or cyclohexanol/1,4-butanediol in various ratios and at constant 3.6-wt% water. AIBN (1.0 - wt% with respect to monomers) was added to the solution. The solution was then sonicated to obtain a clear solution. A 35 cm or 48 cm pretreated capillary was filled with the polymerization solution up to 24 cm or 33 cm by immersing the inlet of the capillary in the solution vial and applying vacuum to the outlet to prepare a final column of 27 or 37 cm total length, respectively. The capillary ends were then sealed in an oxygen/propane flame, and the capillary submerged in a 60 °C water bath for 18 hrs. The resulting monolith column was washed with an 80:20 v/v acetonitrile: water mixture using an HPLC pump. A detection window was created at 1-2 mm after the end of the polymer bed using a thermal wire stripper. Finally, the column was cut to a total length of either 27 or 37 cm with an effective length of 20 or 30 cm, respectively.

## Results and Discussion

### Choice of Monomers and Porogens

Very recently, Bedair and El Rassi introduced PEDAS-based monoliths with either cationic or anionic sites [7-9] to support a relatively strong EOF. In their work a ternary porogenic solvent made of cyclohexanol (83.2 wt%), ethylene glycol (EG) (13.2 wt%) and water (3.6 wt%) proved to be the optimal porogen for achieving monoliths of high permeability in pressure driven flow, relatively strong EOF and high separation efficiency. The addition of water was essentially in the aim of increasing the solubility of charged monomers. Naturally, this optimal porogen composition was not the best for achieving the most efficient neutral PEDAS monolith (see Fig. 1 for the structure of the PEDAS monomer), which has a different monomer composition. The ratio of PEDAS monomer to porogen was 30:70 (w/w) in the polymerization mixture used for preparing the neutral PEDAS monolith. The highest separation efficiency was achieved with a porogen composed of 79.2-wt% cyclohexanol, 17.2-wt% EG and 3.6-wt% water (monolith referred to as M-1). The neutral monolith required a slightly higher percent of the macroporogen EG and a slightly lower percent of the microporogen cyclohexanol as compared to the charged PEDAS monoliths reported earlier [7-9]. Replacing EG by a less polar macroporogen, e.g., 1,4-butanediol, yielded a monolith with lower permeability in pressure-driven flow. Increasing the EG further to 21.2 wt% while decreasing the percentage of cyclohexanol and keeping the water constant resulted in a monolith of much lower separation efficiency. While water was needed to increase the solubility of charged monomers in the case of charged PEDAS monoliths [7-9], omitting water in the

case of neutral PEDAS monolith prepared here and increasing the percentage of the microporogen cyclohexanol yielded a monolith of poor efficiency. This is an indication that water in small amount contributes to the pore morphology and is a suitable porogen in a ternary or binary solvent mixture.

To further modulate the properties of the neutral PEDAS monoliths, monofunctional monomers having short alkyl chains e.g., methyl, ethyl or butyl methacrylate (MMA, EMA or BMA) were added in small quantities (0.5 – 4 wt%) to the polymerization mixture composed essentially of PEDAS while keeping the nature of the porogen the same (i.e., a ternary porogen of cyclohexanol, EG and water) and the ratio of monomers to porogen constant (i.e., 30:70). However, the wt% of cyclohexanol: EG were varied e.g., 83.2:13.2%, 79.2:17.2% and 75.2:21.2% while that of water was kept constant at 3.6 wt%. These attempts resulted in the majority of cases in either no improvement of flow characteristics or reduction in separation efficiency at low wt% of short alkyl monomer (< 2%), and to low permeability at higher wt% monomer (> 2%). Another set of PEDAS monoliths was prepared with a small amount of either EDMA (2 – 8 wt%) alone or a mixture of EDMA:EMA (0.5: 1 wt%, 1:1 wt%, 2:1 wt% and 4:1 wt%). The PEDAS-EDMA polymerization mixtures yielded monoliths with either low separation efficiency in CEC and/or low permeability for pressure-driven flow. The PEDAS-EDMA-EMA monomer mixtures yielded monoliths with good permeability in pressure-driven flow and the monolith with the best separation efficiency was the one with the composition: 28.0 wt% PEDAS, 1.0 wt% EDMA and 1.0 wt% EMA in the presence of the porogen at 75.2 wt% cyclohexanol, 21.2 wt% EG and 3.6 wt% water (monolith referred to as M-2). However, under the same elution conditions the M-2

column exhibited 18% less plates than the M-1 column. In the rest of this study the M-1 column with the optimal performance was the only one considered further.

#### Characterization of the Optimal Neutral Monolith

EOF. The M-1 monolith is void of fixed charges, and therefore it has no zeta potential with respect to water. Despite this inherent property, the monolith produced a relatively strong EOF over a certain pH range as shown in Fig. 2. Uracil was used as the EOF inert tracer. The observed EOF can be explained by the adsorption of electrolyte ionic components to the monolithic surface thus becoming the zeta potential determining ions (i.e., determining the sign of the surface zeta potential). This behavior was also observed with a cationic PEDAS monolith reported recently by Bedair and El Rassi [8] where the magnitude and direction of the EOF can be conveniently altered by the composition of the mobile phase electrolyte. The ability of the acrylic PEDAS monolith to adsorb ions from the mobile phase was attributed to the presence of ester and hydroxyl groups in the PEDAS structure (see Fig. 1) [8]. The effect of the adsorption of ions on the zeta potential of solid phases has been previously observed for non-ionized and ionizable solids [10].



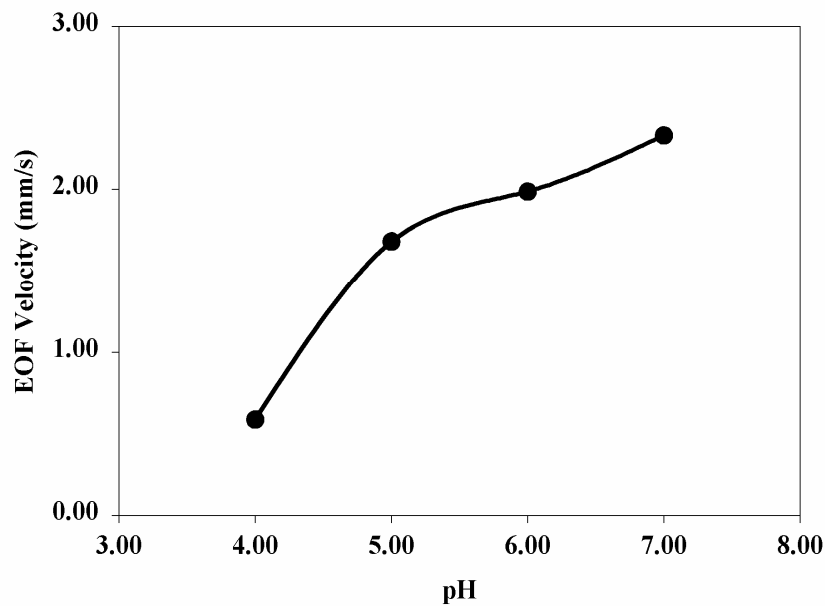


**Figure 2.** *Plot of the apparent EOF velocity versus the pH of the mobile phase.*  
*Capillary column, M-1, 20 cm (effective length), 27cm (total length) x 100  $\mu$ m I.D.*  
*Mobile phase, 5.0 mM sodium phosphate, pH 7.0, at 60 % (v/v) ACN; running voltage,*  
*25 kV; EOF, tracer, uracil; electrokinetic injection for 10 s at 10 kV.*

The EOF reported in Fig. 2 indicates that the neutral monolith adsorbs a sufficient amount of ions from the mobile phase and consequently acquires the zeta potential necessary for supporting the EOF. The direction of the EOF is from anode to cathode (i.e., cathodal EOF) indicating that the zeta potential is negative and that the adsorbed ions are essentially phosphate ions under the mobile phase conditions used. The EOF increases sharply from pH 4 to pH 5 (see Fig. 1) and then somewhat levels off in the pH range 6 – 7. This can be attributed to the fact that the adsorbed phosphate ions are more ionized (doubly charged) at pH 6 and 7 than at pH 4.0 (singly charged).

In fact, the PEDAS monolith also has polar functions (e.g., ester and hydroxyl groups, see Fig. 1), which can establish hydrogen bonding with the phosphate ions of the mobile phase. Despite the fact that increasing the percent ACN decreases the dielectric constant of the mobile phase, the concomitant decrease in the viscosity of the mobile phase would also favor the observed increase in the magnitude of the EOF at elevated percent ACN. In brief, the amphiphilic character of the PEDAS monomer, which is exhibited by the presence of a non-polar C17 chain and polar ester and hydroxyl functions in its structure (see Fig. 1), is an important development in the design of monolithic stationary phases void of fixed charges but still can yield a relatively strong EOF for moving the mobile phase across the CEC column.

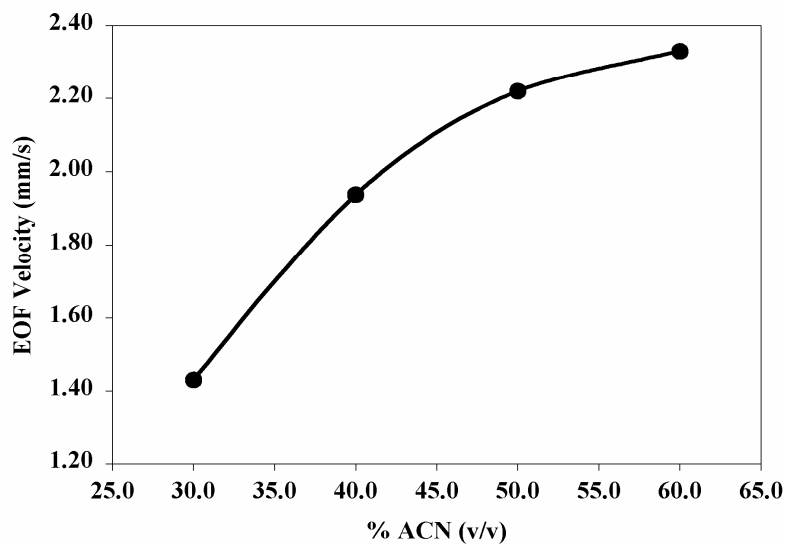


**Figure 3.** *Effect of percent ACN (v/v) in the mobile phase on the apparent EOF velocity of the M-1 monolithic column. Conditions are the same as in Fig 2.*

Under this condition, while the C17 chain functions as the non-polar ligand for solute retention by a reversed-phase mechanism, the polar functions constitute the sites for the attachment of electrolyte ionic components for EOF generation. Other kinds of monolithic columns in this category of stratified stationary phases are being developed in our laboratory.

Retention of Homologous Series. The M-1 monolithic stationary phase was evaluated for its retentive properties toward non-polar solutes using model homologous series such as alkyl benzenes (ABs). Fig. 4 shows the dependence of the  $\log k'$  on the percent ACN (v/v) in the mobile phase for ABs. It can be seen that  $\log k'$  linearly decreases with increasing concentration of ACN, and the slope of the line increases with

the size of the solute which reflects the hydrophobic contact area between the non-polar solute and the non-polar stationary phase ligand (i.e., C17 ligand). These retention data are indicative of a true reversed phase electrochromatography behavior involving neutral non-polar solutes.

As expected, plots of  $\log k'$  versus the carbon number in the homologous solutes are linear with slopes of 0.32, 0.28, 0.23 and 0.20 at 30%, 40%, 50% and 60 % ACN in the mobile phase, respectively. These slopes represent the logarithmic methylene group selectivity ( $\log \alpha_{\text{CH}_2}$ ), which corresponds to a methylene group retention increment (i.e., hydrophobic increment) of 2.08, 1.92, 1.69 and 1.57 at 30%, 40%, 50% and 60 % ACN in the mobile phase, respectively.

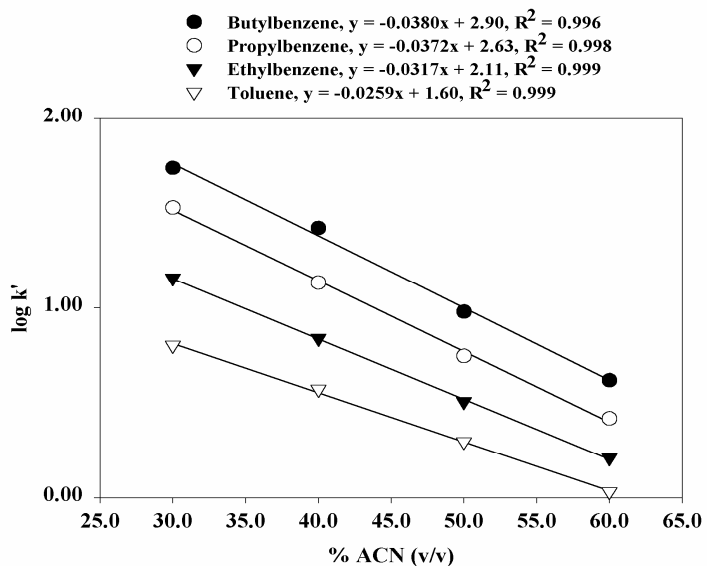


**Figure 4.** Plots of  $\log k'$  for alkyl benzene homologous series versus percent ACN (v/v) in the mobile phase. Conditions are the same as in Fig. 2.

Also the effect of pH values of the mobile phase on the retention factor  $k'$  of ABs was determined as shown in Fig. 5. The  $k'$  values slightly decrease with increasing the pH of the mobile phase. This can be attributed to the increase in the ionization of the adsorbed ions (i.e., phosphate ions) with increasing pH leading to decreasing retention. The %RSD ( $n = 5$ ) of the retention times from run-to-run for the alkyl benzene homologous series were 0.34, 0.31, 0.27 and 0.22 for toluene, ethylbenzene, propylbenzene and butylbenzene, respectively. This reproducibility was achieved by implementing a washing step with the mobile phase prior to subsequent injections.

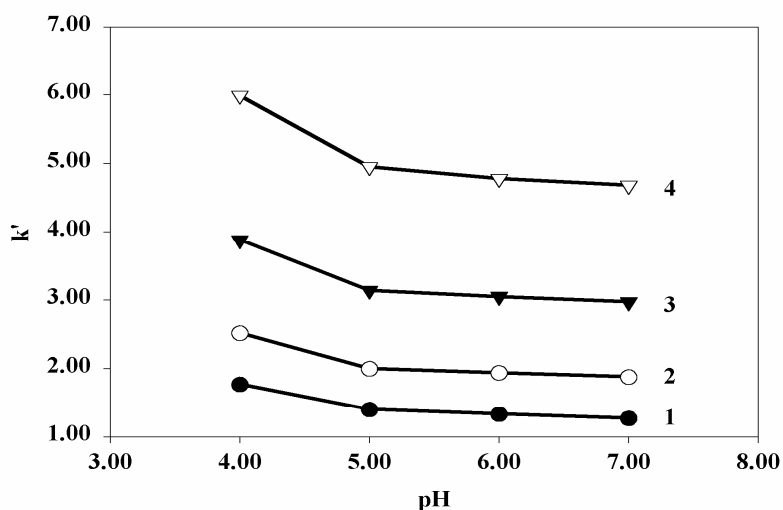


**Figure 5.** Plots of the retention factor  $k'$  of alkyl benzene homologous series obtained on the M-1 monolithic column versus the pH of the mobile phase at 60% (v/v) ACN. Solutes: 1, toluene; 2, ethylbenzene; 3, propylbenzene; 4, butylbenzene. Other conditions are the same as in Fig. 2.

Migration and Retention of Charged Solutes – Ion-Pair CEC. The retention and migration of a group of Dns-AA were studied on the M-1 monolithic stationary phase under evaluation. The results in terms of retention and velocity factors are grouped in Table 1. In CEC, both the electrophoretic mobility and the chromatographic partitioning control the migration of charged solutes. Under this circumstance, the dimensionless retention factor  $k^*$  for charged solutes is given by the equation [11, 12]:

$$k^* = \frac{t_m(1 + k_e^*) - t_0}{t_0} \quad (1)$$

where  $k_e^*$  is the velocity factor,  $t_m$  is the migration time of the analyte and  $t_0$  is the migration time of the EOF marker in the CEC column.  $k_e^*$  describes the contribution of electrophoretic mobility to the separation of a charged species in CEC and is given by:

$$k_e^* = \frac{\mu_{ep}}{\mu_{eo}} \quad (2)$$

$k^*$  and  $k_e^*$  are measured under conditions used in the CEC experiments. The electrophoretic mobility  $\mu_{ep}$  is obtained from separate capillary zone electrophoresis (CZE) measurements in an open tube using the same mobile phase and other conditions as in the CEC experiment. The electroosmotic mobility (i.e., mobile phase mobility)  $\mu_{eo}$ , is the actual “interstitial” EOF mobility in the monolithic column, which is equal to the apparent EOF mobility  $\mu_{eo}^*$  within the CEC column multiplied by the ratio of current in the open tube to that in the monolithic or packed column [13]. For neutral solutes,  $k_e^* = 0$ , and consequently  $k^* = k'$ , the retention factor normally encountered in chromatography.

**Table 1.** Dimensionless retention parameters of Dns-AA in the presence and absence of TBAB in the mobile phase. Column, M-1, 20/27 cm x 100  $\mu$ m I.D.; mobile phases, 4 mM tris, pH 7.0, at 5% ACN (v/v) containing various mM TBAB; running voltage, 20 kV.

	0 mM TBAB			2 mM TBAB				7 mM TBAB				10 mM TBAB			
	$k_c^*$	$k_e^*$	$k^*$	$k_c^*$	$k_e^*$	$k^*$	$\eta$	$k_c^*$	$k_e^*$	$k^*$	$\eta$	$k_c^*$	$k_e^*$	$k^*$	$\eta$
Lys	-0.01	0.13	0.18	-0.25	0.00	0.10	0.53	-0.41	0.07	0.16	0.88	-0.54	0.006	0.16	0.84
Arg	-0.009	0.13	0.20	-0.25	0.05	0.16	0.79	-0.41	0.05	0.16	0.80	-0.53	0.006	0.17	0.84
Pro	0.35	-0.20	0.15	1.53	-0.13	1.01	14.63	2.85	-0.42	3.19	21.12	2.34	-0.32	4.63	17.73
Ile	0.36	-0.15	0.24	1.09	-0.15	1.58	6.68	2.54	-0.45	2.62	11.06	2.26	-0.33	4.45	19.96
Met	0.36	-0.15	0.24	1.27	-0.13	1.89	7.88	2.46	-0.42	2.70	11.28	1.63	-0.42	2.81	11.74
Leu	0.40	-0.16	0.26	1.03	-0.15	1.51	5.77	2.49	-0.42	2.78	10.67	2.25	-0.32	4.48	16.96
Val	0.44	-0.18	0.26	1.01	-0.15	1.49	5.65	2.29	-0.39	2.71	10.25	2.25	-0.33	4.38	18.46
Trp	0.47	-0.22	0.22	5.58	-0.35	5.28	23.66	9.31	-0.34	11.71	52.40	14.72	-0.33	25.06	63.37
Ala	0.49	-0.24	0.22	1.03	-0.23	1.28	5.88	2.27	-0.45	2.34	10.77	2.06	-0.37	3.77	17.34
Phe	0.51	-0.24	0.22	2.40	-0.06	3.63	16.29	6.00	-0.43	6.37	28.53	NM			
Thr	0.55	-0.16	0.39	0.59	-0.22	0.81	2.05	1.64	-0.40	1.95	4.92	1.01	-0.36	2.18	14.45
Ser	0.62	-0.20	0.38	1.25	-0.24	1.50	3.93	1.48	-0.41	1.73	4.53	1.05	-0.37	2.23	5.82
Asn	0.68	-0.22	0.41	1.23	-0.25	1.43	3.51	1.32	-0.41	1.57	3.84	0.82	-0.42	1.61	3.95
Gly	0.69	-0.31	0.24	1.62	-0.23	1.94	8.10	2.23	-0.45	2.28	9.52	2.05	-0.38	3.71	15.51
Gln	0.72	-0.28	0.32	1.15	-0.19	1.54	4.78	1.28	-0.39	1.60	4.97	1.04	-0.37	2.18	9.75
Glu	2.18	-0.44	0.92	1.44	-0.43	1.01	1.10	NE				NE			

NM: not measured; NE: not eluted

Because of the presence of  $k^*_e$  in eq. 1 which reflects the electrophoretic process the  $k^*$  does not serve as a useful peak locator as its counterpart  $k'$  in chromatography. To reflect the elution order of charged solutes in CEC, a peak locator,  $k^*_c$ , based on chromatographic formalism, has been suggested [12]:

$$k^*_c = \frac{t_m - t_0}{t_0} \quad (3)$$

Despite the fact that  $k^*_c$  is devoid of any mechanistic insight, and has limited utility, it proved useful for calculating resolution [12]. Its value increases with the migration time as  $k'$  in chromatography.  $k^*_c$  is negative for components migrating faster than the EOF tracer.

Other expressions have been developed for the retention of charged solutes in CEC [14]. However, these equations require the measurement of the retention factors of the charged solutes in liquid chromatography in addition to their electrophoretic mobility in capillary electrophoresis in order to estimate the retention factor in CEC.

As can be seen in Table 1,  $k^*$  is in the range of 0.15 – 0.41 except for the doubly charged amino acid, i.e., Glu. This may indicate that the migration of this negatively charged solute is primarily influenced by its electrophoretic mobility and to a lesser extent by their chromatographic partitioning. Lys and Arg elute before the  $t_0$  ( $k^*_c < 0$ ) indicating that the net charge of these amino acids is positive. As can be seen in Table 1  $k^*_e$  has a negative value in all cases, which means that the electrophoretic mobility is opposite in direction to the electroosmotic mobility, and the absolute value of  $k^*_e$  is  $< 1$  indicating that the magnitude of  $\mu_{ep}$  is less than that of  $\mu_{eo}$ . This fact portrays the utility of neutral PEDAS monoliths in CEC whereby the mobility of the mobile phase is of



sufficient magnitude to facilitate the differential migration of charged solutes down the column and consequently separation.

On the basis of the above results, the chromatographic partitioning of Dns-AA seems to be rather weak under the mobile phase conditions used. In order to enhance the retention of Dns-AA, the ion-pairing agent TBAB was added to the mobile phase. As in chromatography, whether the mechanism of action of TBAB is ion-pair formation or dynamic ion-exchange or a mixture of both, all these possible mechanisms can lead to an increase in  $k^*$  and  $k^*_c$ . In fact, in all cases, both  $k^*$  and  $k^*_c$  increased with increasing TBAB concentration in the mobile phase (see Table 1). In order to express the enhancement factor of solute retention, the retention modulus  $\eta$ , which is defined as the ratio of  $k^*$  in the presence of TBAB to that in the absence of TBAB in the mobile phase, is introduced:

$$\eta = \frac{k^*_{presence}}{k^*_{absence}} \quad (4)$$

Ion-pairing is occurring when  $\eta > 1$  and is absent when  $\eta \leq 1$ . As can be seen in Table 1, with the exception of Lys and Arg where  $\eta < 1$ , all other Dns-AA associated with TBAB to a varying extent and the value of their  $\eta$  is greater than 1. The doubly charged Dns-Glu did not elute from the column at 7 mM and 10 mM TBAB in the mobile phase (i.e.,  $\eta$  is very large) indicating strong association with TBAB. The Dns-AA with non-polar side chains (e.g., Trp, Phe, Val, Leu, Ile) exhibited much larger  $\eta$  values than Dns-AA with polar side chains (e.g., Gly, Gln, Asn, Ser). This fact may indicate the formation of an ion pair (i.e., solute-TBAB ion-pair) in the mobile phase, which binds stronger to the PEDAS column than the free Dns-AA.

Peptides and Proteins. The neutral M-1 monolith was evaluated in the separation of peptides and proteins. Figure 6 shows the simultaneous separation of 7 peptides, namely Lys-Cys-Thr-Cys-Cys-Ala, L-ala-DL-phe, Gly-L-Trp, insulin chain B; Val-Gly-Ser-Glu, Val-Gly-Asp-Glu and Phe-Leu-Glu-Glu-Val, with an average of 121,000 plates/m. For the migration time window (5 min to 22 min) of the electrochromatogram in Fig. 6, the peak capacity is ~ 72. Typical %RSD (n = 3) of the migration times from run-to-run for the peptides were 0.20, 0.14, 0.30 and 0.21 for Ala-Phe, Gly-Trp, insulin chain B and Val-Gly-Ser-Glu, respectively.

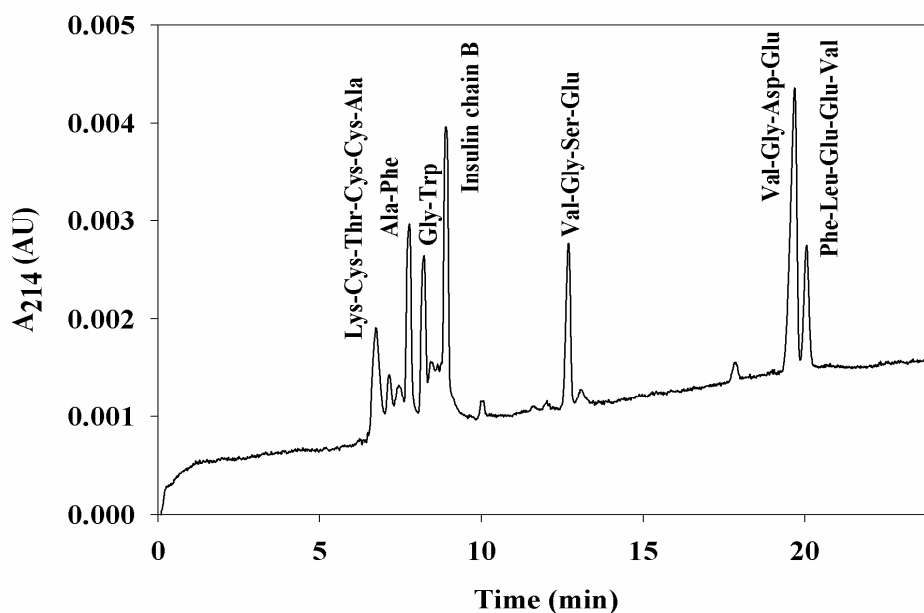


**Figure 6.** *Electrochromatogram of some peptides. Conditions: hydro-organic mobile phase, 40% ACN (v/v), 20 mM sodium phosphate monobasic, pH 7.0; capillary column, M-1, 30 cm effective length, 37 cm total length x 100  $\mu$  m I.D.; voltage, 10 kV.*

Under the same elution conditions, six proteins of widely differing size and charges (i.e., isoelectric points), namely cytochrome C, ribonuclease A, carbonic anhydrase,  $\beta$ -lactoglobulin B,  $\alpha$ -lactalbumin and trypsin inhibitor, were separated with an average separation efficiency of 255,000 plates/m, see Fig. 7.

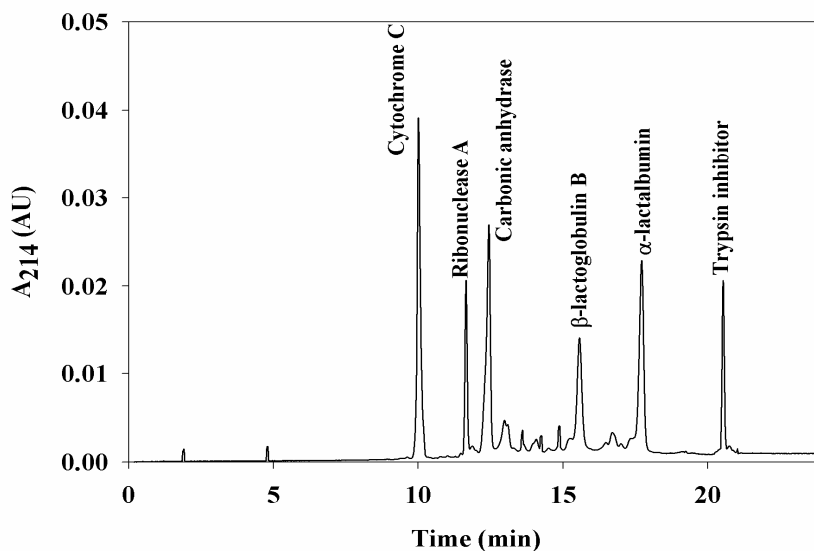


**Figure 7.** *Electrochromatogram of some proteins. Conditions are the same as in Fig. 6.*

For the time frame (5 min to 22 min) of the electrochromatogram in Fig. 7, the protein peak capacity is  $\sim 103$ , a value that clearly demonstrates the high resolving power of these neutral monoliths. To the best of our knowledge, this is the first protein separation ever reported at pH 7.0 in reversed phase CEC. The observed cathodal EOF at 10 kV is about 1.34 mm/s using a mobile phase containing 20 mM sodium phosphate, pH 7.0, and 40% v/v ACN. This EOF can be as high as 2.35 mm/s at 25 kV using a mobile phase containing 5 mM sodium phosphate, pH 7.0, and 60% v/v ACN (see Figs 2 and 3). Typical %RSD ( $n = 3$ ) of the migration times from run-to-run for cytochrome C.

ribonuclease A, carbonic anhydrase and  $\beta$ -lactoglobulin B, were 1.12, 0.17, 0.91 and 0.66, respectively.

### Conclusions

The present investigation has introduced a novel neutral PEDAS monolith that belongs to the stratified type of stationary phases whereby the surface top layer is essentially the non-polar C17 ligands for chromatographic partitioning/adsorption of solutes by a reversed phase retention mechanism and the surface sub-layer contains polar functional groups for ion binding which impart the monolith with a given zeta potential to generate the EOF. This inherent property of the PEDAS monolith yielded a stationary phase with “zero” electrostatic attraction toward charged solutes but with the ability of generating an EOF of relatively high magnitude thus allowing the rapid and efficient RP-CEC of peptides and proteins at neutral pH.

## References

- (1) Eeltink, S., Rozing, G. P., Kok, W. T., *Electrophoresis*, **2003**, *24*, 3935-3961.
- (2) Hilder, E. F., Svec, F., Fréchet, J. M. J., *J. Chromatogr. A*, **2004**, *1044*, 3-22.
- (3) Bedair, M., El Rassi, Z., *Electrophoresis*, **2004**, *25*, 4110-4119.
- (4) Zhang, L., Ping, G., Zhang, L., Zhang, W., Zhang, Y., *J. Sep. Sci.*, **2003**, *26*, 331-336.
- (5) Li, Y., Xiang, R., Horváth, C., Wilkins, J. A., *Electrophoresis*, **2004**, *25*, 545-553.
- (6) Hilder, E. F., Svec, F., Fréchet, J. M. J., *Anal. Chem.*, **2004**, *76*, 3887-3892.
- (7) Bedair, M., El Rassi, Z., *Electrophoresis*, **2002**, *23*, 2938-2948.
- (8) Bedair, M., El Rassi, Z., *J. Chromatogr. A*, **2003**, *1013*, 35-45.
- (9) Bedair, M., El Rassi, Z., *J. Chromatogr. A*, **2003**, *1013*, 47-56.
- (10) Morris, C. J. O. R., Morris, P., *Separation Methods in Biochemistry*. 2nd ed. **1976**, New York: John Wiley and Sons. 718-724.
- (11) Rathore, A. S., Horváth, C., *J. Chromatogr. A*, **1996**, *743*, 231-246.
- (12) Rathore, A. S., Horváth, C., *Electrophoresis*, **2002**, *23*, 1211-1216.
- (13) Rathore, A. S., Wen, E., Horváth, C., *Anal. Chem.*, **1999**, *71*, 2633-2641.
- (14) Dittmann, M. M., Masuch, K., Rozing, G. P., *J. Chromatogr. A*, **2000**, *887*, 209-221.

## CHAPTER III

# POLYMETHACRYLATE MONOLITHS WITH IMMOBILIZED LECTINS FOR GLYCOPROTEIN SEPARATION BY AFFINITY CAPILLARY ELECTROCHROMATOGRAPHY AND AFFINITY NANO-LIQUID CHROMATOGRAPHY IN EITHER A SINGLE COLUMN OR COLUMNS COUPLED IN SERIES

### Introduction

It is well established that covalent linkages between carbohydrates and proteins (called glycosylation) do occur in all domains of life, i.e., in eukaryotes, prokaryotes and viruses [1, 2]. The human genome project has yielded large amounts of DNA sequence data, which would provide the sequence of 80,000 to 100,000 proteins without the efficient prediction of all the post-translational modification (PTM) of which the majority of proteins are the targets. Several PTM (e.g., acetylation, methylation, phosphorylation, glycosylation, etc.) are currently known and many more are yet to be discovered. The most common, but also the most complex PTM of proteins is glycosylation.

---

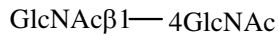
*\*The content of this chapter has been published in Electrophoresis, 2006, 27, 1020-1030*

specificities to the core portion of *N*-linked sugar chains, i.e., *N*-glycans. In fact, WGA has a strong affinity for *N,N'*-diacetylchitobiose, the tetrasaccharide GlcNAc $\beta$ 1-4Man $\beta$ 1-4GlcNAc $\beta$ 1-4GlcNAc and bisected hybrid-type glycans [13, 14], see Fig. 1. Also glycoconjugates with clustered sialic acid residues have strong affinity to immobilized WGA [15]. In fact, the binding of WGA to glycopeptides has been shown to decrease after treatment with neuraminidase [16], an exoglycosidase that removes sialic acids from the non-reducing terminal of glycans [17]. Oligosaccharides with poly-*N*-acetylglucosamine chains have weak affinity and are retarded by the WGA column (i.e., elute with the binding mobile phase) [13]. The specificity of a given lectin is often expressed in terms of the best monosaccharide inhibitor, i.e., hapten sugar. The hapten sugar for WGA is *N*-acetyl-D-glucosamine (GlcNAc) [7, 13, 14].

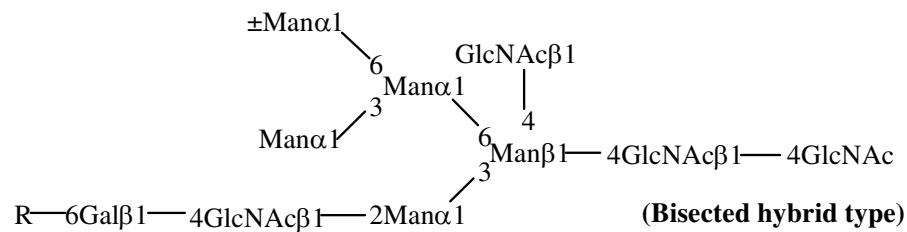
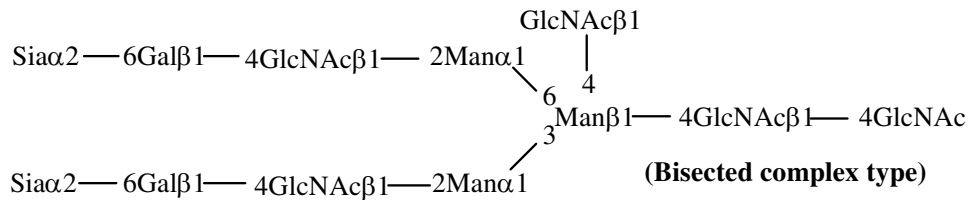
*Lens culinaris* agglutinin (LCA) on the other hand recognizes sequences containing  $\alpha$ -linked mannose residues of *N*-glycans, but *N*-acetylglucosamine residues at the reducing terminals should be in pyranose form and substitution of its C-6 hydroxyl group with fucose is required [13, 18, 19]. In addition to biantennary *N*-glycans, C-2, C-2,6 branched triantennary sugar chains with fucosylated cores bind to LCA (see Fig. 1) [20]. Presence of bisecting GlcNAc does not alter the affinity of an oligosaccharide [13]. By recognizing additional sugars as part of the receptor structure, LCA has a narrower specificity than WGA. For example, a  $\alpha$ -linked fucose residue attached to the *N*-acetylchitobiose portion of the core oligosaccharide markedly

**Immobilized WGA**

⇒ Structures exhibiting strong binding and requiring 0.1M N-acetylglucosamine for elution



GlcNAcβ1—4Manβ1—4GlcNAcβ1—4GlcNAc, structural determinant for lectin recognition



Cluster of sialic acid residues

⇒ Structures having weak binding

Poly-N-acetylglucosamine chains

**Immobilized LCA**

⇒ Structures exhibiting strong binding and requiring 0.2 M α-methylmannopyranoside for elution

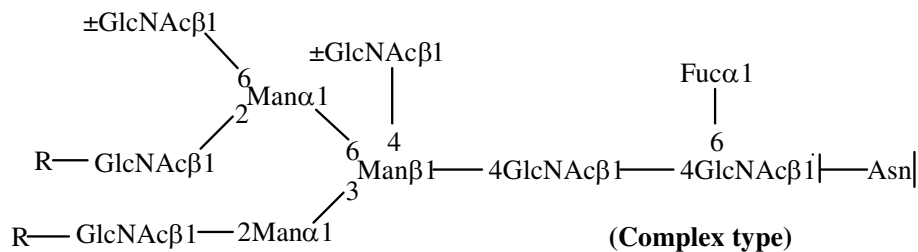


**Figure 1.** Specificity of WGA and LCA toward N-glycans. R = H or sugar residues; ± = present or not.



enhances affinity. The hapten monosaccharide for LCA is the methyl- $\alpha$ -D-mannopyranoside (Me- $\alpha$ -D-Man).

In this investigation the WGA-monolith and LCA-monolith were demonstrated in the isolation of glycoproteins by either a single capillary column format or coupled capillary columns in series. These two formats were evaluated in both nano-LC and CEC. In both formats, CEC proved superior to nano-LC.

## Experimental

### Instrumentation

The instrument used was an HP<sup>3D</sup>CE system from Agilent Technologies (Waldbronn, Germany) equipped with a photodiode array detector. Chromatograms were recorded with a personal computer running an HP<sup>3D</sup>CE ChemStation. The chromatograms shown in this report are representative of the data, which in most cases involved two or more replicate measurements. Column temperature was held constant at 15 °C, and an external pressure of 10 bars (1.0 MPa) was applied to the column inlet for sample injection and separation in both nano-LC and CEC.

### Reagents and Materials

Glycidyl methacrylate (GMA), ethylene glycol dimethacrylate (EDMA), [2-(methacryloyloxy)ethyl]trimethyl ammonium chloride (MAETA), [2-(acryloyloxy)ethyl]trimethylammonium methyl sulfate (AETA), 2,2'-

azobisisobutyronitrile (AIBN), 3-(trimethoxysilyl)propyl methacrylate, 1-dodecanol, ethylenediamine (EDA), diethylenetriamine (DETA) and triethylenetetramine (TETA) tetrahydrochloride were from Aldrich (Milwaukee, WI, U.S.A.). Cyclohexanol, ethylene glycol and acetonitrile (HPLC grade) were from Fisher Scientific (Fair Lawn, NJ, U.S.A.). Wheat germ agglutinin (WGA) and *Lens culinaris* agglutinin (LCA) were obtained from Vector Laboratories Inc. (Burlingame, CA, U.S.A.). Horse skeletal muscle myoglobin, bovine milk  $\beta$ -lactoglobulin B ( $\beta$ -Lac B), ovalbumin (OVA), human  $\alpha_1$ -acid glycoprotein (AGP), bovine milk  $\alpha$ -lactalbumin, human transferrin (HT), glucose oxidase (GO) from *Aspergillus niger*, collagen type VI from human placenta, soy bean lipoxidase,  $\kappa$ -casein from bovine milk, fetal calf serum III fetuin, bovine erythrocytes carbonic anhydrase (CA), soy bean trypsin inhibitor (TI) type 1-S, bis-Tris, *N*-acetyl-D-glucosamine (GlcNAc) and methyl- $\alpha$ -D-mannopyranoside (Me- $\alpha$ -D-Man) were from Sigma (St. Louis, MO, U.S.A.). Avidin from egg white was from EMD Biosciences Inc. (San Diego, CA, U.S.A.). Sodium phosphate monobasic was from Mallinckrodt (Hazelwood, MO, U.S.A.). Fused-silica capillaries with an internal diameter of 100  $\mu\text{m}$  and an outer diameter of 360  $\mu\text{m}$  were from Polymicro Technology (Phoenix, AZ, U.S.A.).

### Column Pretreatment

The inner wall of the fused-silica capillary was treated with 1.0 M sodium hydroxide for 30 min, flushed with 0.10 M hydrochloric acid for 30 min, and then rinsed with water for 30 min. The capillary inner wall was then allowed to react with a 50% (v/v) solution of 3-(trimethoxysilyl)propyl methacrylate in acetone for 12 h to vinylize

the inner wall of the capillary after which the capillary was rinsed with methanol and water and then dried with a stream of nitrogen.

### *In situ* Polymerization

For neutral monoliths, polymerization solutions weighing 2 g each were prepared from GMA 18 wt%, EDMA 12 wt%, cyclohexanol 58.8 wt% and dodecanol 11.2 wt%. For the positively charged monoliths, MAETA 1wt% or AETA 2 wt% were added to the polymerization solution (2 g) consisting of GMA 17 wt% or 16 wt%, EDMA 12 wt%, cyclohexanol 59.5 wt% and dodecanol 10.5 wt%, respectively. In all cases, AIBN (1% with respect to monomers) was added to the polymerization solutions as initiator. Thereafter, the solution was degassed by purging with nitrogen for 5 min. A 40 cm pretreated capillary was filled with the polymerization solution up to 30 cm by immersing the inlet of the capillary in the solution vial and applying a vacuum to the outlet. The capillary ends were then plugged with GC septum, and the capillary submerged in a 50 °C water bath for 24 h. The resulting monolith was washed with acetonitrile and then with water using an HPLC pump. The monolith was again filled with the porogen (cyclohexanol and dodecanol) and put in a GC oven for 16.5 hrs, with a temperature gradient from 30°C to 70°C at a rate 0.5 °C/min. Then, the resulting monolith was rinsed with acetonitrile and water using an HPLC pump.

### Immobilization of Lectins

The glycidyl methacrylate monolith was first rinsed thoroughly with water and then filled with either 0.1 M HCl solution and heated at 50 °C for 12 h or 0.2 M H<sub>2</sub>SO<sub>4</sub> and heated at 80 °C for 3 h to hydrolyze the epoxy groups. The column was then rinsed with water followed by a freshly prepared solution of 0.1 M sodium periodate for 1 h to oxidize the ethylene glycol on the surface of the column to an aldehyde. Lectin was then immobilized to the monolithic column by pumping a solution of LCA at 4.0 mg/mL in 0.1 M sodium acetate buffer pH 6.4 containing 1 mM of CaCl<sub>2</sub>, MgCl<sub>2</sub>, MnCl<sub>2</sub>, 0.1 M Me- $\alpha$ -D-Man and 50 mM sodium cyanoborohydride through the column overnight at room temperature. WGA was immobilized using the same procedure at 5.0 mg/mL in 0.1 M sodium acetate buffer, pH 6.4, containing only 0.1 M GlcNAc and 50 mM sodium cyanoborohydride. The resulting columns were then rinsed for 3 h at room temperature with a solution of 0.4 M Tris/HCl, pH 7.2 containing 50 mM sodium cyanoborohydride to react Tris with any unreacted aldehyde group. The column was then rinsed with water and cut to the desired length.

### Results and Discussion

There are four essential criteria for producing an affinity monolith for simultaneous or independent use in both CEC and nano-LC. The monolith should provide (i) high EOF velocity, (ii) high permeability, (iii) high reactivity with the analyte of interest, and (iv) minimum non-specific interactions. The next section uses these criteria for assessing the usefulness of a given lectin affinity monolith. The findings should also be applicable to any other type of affinity monoliths. In the remaining

sections that follow, single lectin affinity columns as well as serially coupled lectin affinity columns are demonstrated in the separation of mixtures of glycoproteins.

#### Evaluation of EOF and Pressure Driven Flow of the Various Monoliths

Criterion (iii) stated above is met by ensuring a monolith with a relatively high surface density in affinity ligands, which in this investigation are lectin ligands. Poly(glycidyl methacrylate-co-ethylene dimethacrylate) monolith should in principle provide the ground for achieving high surface density in affinity ligands due to the presence of reactive epoxy functions on its surface [12, 21-23]. However, the conversion of the epoxy functions to aldehyde groups, which are subsequently used in the immobilization of a given lectin becomes a critical step (i.e., limiting step) in the process of the preparation of an active lectin affinity monolith. In this investigation, the hydrolysis of the epoxy ligands to diol functions with two strong acidic solutions, namely 0.1 M HCl and 0.2 M H<sub>2</sub>SO<sub>4</sub>, were compared (see Experimental section). The quantitative conversion of epoxy groups to diol functions will insure a surface rich in aldehyde groups in the subsequent step of periodate oxidation. With the LCA monolith which was prepared by the immobilization of LCA to the aldehyde monolith, most of the glycoproteins known for their affinity to this lectin exhibited a spill out, i.e., a major amount of the glycoprotein did not retain and eluted in the column breakthrough, when the column was hydrolyzed with HCl prior to periodate oxidation. Conversely, the epoxy monolith, which was hydrolyzed by sulfuric acid prior to periodate oxidation, did not yield a significant spill out of the injected glycoproteins. This seems to be dependent on the nature of the immobilized lectins. In fact, and in a previous work published from this

laboratory with concanavalin and WGA, the hydrolysis with HCl yielded robust lectin affinity monoliths, which did not exhibit significant spillage [11]. In the rest of this investigation hydrolysis with sulfuric acid was adopted since sulfuric acid hydrolysis seems to lead to quantitative conversion of epoxide to diol [24].

Another criterion that must be met is to generate a monolith with both high EOF in CEC and high permeability in nano-LC, i.e., criteria (i) and (ii) listed above. In the class of positive monoliths, column AP1, which incorporates the MAETA monomer in its structure, exhibited the highest flow velocity in nano-LC. However, there was no detectable EOF with the use of bis-Tris buffer, pH 6.0. To produce an acceptable EOF, 10 mM ethylenediamine (EDA), pH 6.0, was required to produce an EOF velocity of 1.74 mm/sec at  $-25.0$  kV. However, the current gradually increased to more than  $100 \mu\text{A}$ , which denatured the immobilized protein (i.e., lectin) by the resultant high Joule heating and hence destroyed the lectin affinity after a few CEC runs. Column AP2, whose structure incorporates the AETA monomer, though yielded a lower flow velocity in nano-LC, it exhibited a faster EOF with the 10 mM EDA than MAETA, however, the current was again too high ( $>100 \mu\text{A}$ ).

To further improve on criteria (i), (ii) and (iii), neutral monoliths were also tested. In this class of monoliths, the flow velocity in the nano-LC mode was relatively slow compared to the positive monoliths. Although the current through the column during the CEC run was still high when 10 mM EDA, pH 6.0, was used at an applied voltage of  $-25$  kV, the neutral monoliths were more robust and could withstand several runs without significant glycoprotein spill out in CEC, more so when  $0.2 \text{ M H}_2\text{SO}_4$  was used to hydrolyze the epoxy groups. To alleviate the problem of high current and at the same

time achieve high EOF velocity in CEC, other buffers were tested including diethylenetriamine (DETA) and sodium phosphate. The best eluting buffer then used for the CEC was 2.5 mM sodium phosphate buffer at pH 3, which resulted in an EOF as high as 3.06 mm/sec at an applied voltage of -30 kV and a resultant relatively low current (~40  $\mu$ A) was observed.

The incorporation of a charged monomer in a given monolith is a common approach to generate a relatively strong EOF in CEC with monolithic columns [25-29]. However, the incorporation of an anionic monomer such as AMPS may lead to strong electrostatic interactions with proteins. This is relevant in the case of lectin affinity chromatography of glycoproteins. Although the introduction of a cationic monomer in a given monolith such as described above and elsewhere [11, 29] may not interfere with the actual and intended underlying retention mechanism of a given monolith, the resulting monolith undergoes strong ion adsorption from the running mobile phase a phenomenon that strongly alters the magnitude and direction of the EOF [29]. In fact, it has been shown that in the pH range 3 to 8 the EOF can be switched from anodal to cathodal and even zeroed by simply changing the nature of the mobile phase ions [29] but it is not a straight forward task to predict the response of the monolith to the nature of the mobile phase ions and this may necessitate several trial and error experiments. On the other hand, very recently we have shown that a neutral monolith can be used in CEC with a relatively strong EOF whose direction is predictable by simply controlling the nature and concentration of ions in the mobile phase [30].

From the above discussion it is very reasonable to state that cationic monoliths are promising for lectin affinity chromatography by nano-LC and less so for affinity CEC,

with little or no electrostatic interactions (i.e., non-specific interactions) with glycoproteins. Neutral monoliths are a good compromise for achieving both nano-LC and CEC affinity separation by providing acceptable permeability and predictable EOF with virtually no electrostatic interactions with proteins.

#### Lectin Affinity Nano-LC and CEC with Single Lectin Monolithic Columns

Both the neutral and positive monolithic columns with immobilized LCA or WGA were evaluated for their affinity for different glycoproteins. The results are summarized in the following sections.

Nano-LC and CEC with LCA Monoliths. Positive-LCA monolith (based on AP1 monolith) yielded a good permeability and flow velocity (1.46 mm/sec at  $\Delta P = 10$  bars = 1.0 MPa) as compared to neutral monoliths (0.53 mm/sec) in nano-LC. Figure 2 shows the affinity of a glycoprotein lipoxidase to the immobilized LCA in the presence of other non-glycosylated proteins. While lipoxidase was eluted with the hapten sugar (i.e., Me- $\alpha$ -D-Man), the other non-glycosylated proteins were not retained and were eluted in the dead volume of the column with the binding mobile phase. This is an indication of the absence of non-specific interactions with the LCA monolith. Lipoxidase, an oxidoreductase (also called lipoxygenase), is a glycoprotein of  $M_r$  ca. 94,000 found in leaves of soybean (*Glycine max* [L.] Merr.) [31, 32]. The oligosaccharide chains of lipoxidase have not been well characterized yet. The presence of the monosaccharides glucosamine and galactose and to a lesser extent mannose has been reported [33]. The



binding of lipoxidase to the immobilized LCA would suggest the presence of  $\alpha$ -mannosyl residues, which are required for the LCA recognition of glycans. Neutral LCA monoliths

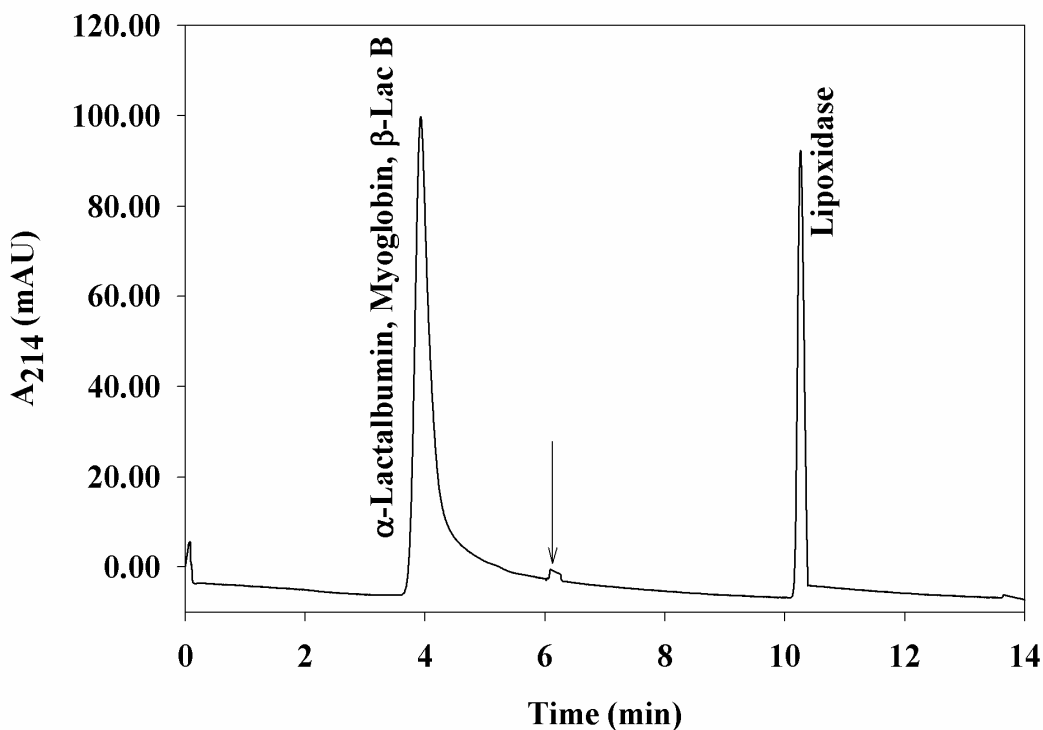


**Figure 2.** Chromatogram of lipoxidase in the presence of non-glycosylated proteins, e.g.,  $\alpha$ -lactalbumin, myoglobin and  $\beta$ Lac B, using LCA-monolith based on the positive API monolithic column. Column dimensions, 25 cm effective length, 33.5 cm total length x 100  $\mu$ m I.D.; binding mobile phase, 20 mM bis-Tris, pH 6.0, containing 100 mM NaCl, 1 mM CaCl<sub>2</sub>, 1 mM MnCl<sub>2</sub> and 1 mM MgCl<sub>2</sub>; eluting mobile phase: 0.2 M Me- $\alpha$ -D-Man in binding mobile phase introduced at 6.0 min as indicated by the arrow;  $\Delta P$ , 1.0 MPa for both running mobile phase and sample injection; sample injection, 6 s.

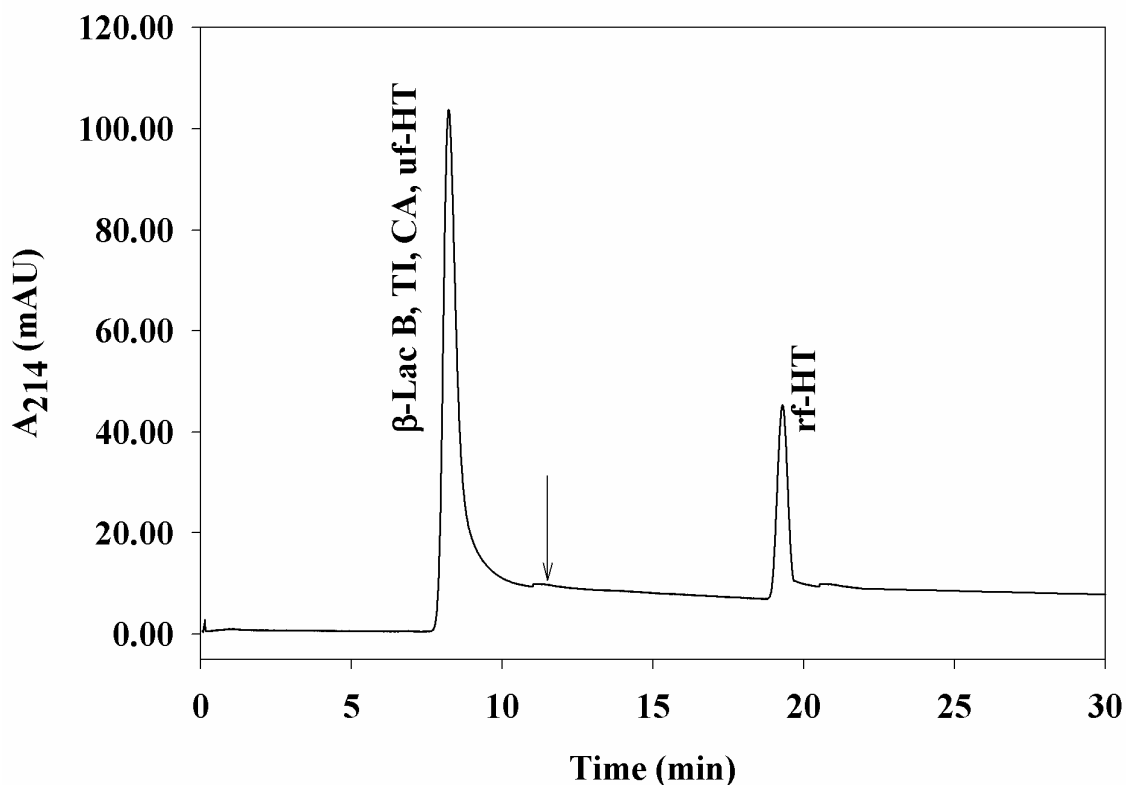


**Figure 3.** *Chromatogram of human transferrin (HT) in the presence of non-glycosylated proteins, e.g.,  $\alpha$ -lactalbumin, trypsin inhibitor (TI) and carbonic anhydrase (CA), using LCA immobilized on a neutral monolithic column. Conditions as in Fig. 2 except that the eluting mobile phase was introduced at 11.0 min as indicated by the arrow.*

exhibited the same behavior toward lipoxidase with the difference that the flow velocity was ca. three-fold slower than that with the positive monolith at the behavior toward lipoxidase with the difference that the flow velocity was ca. three-fold slower than that with the positive monolith at the same inlet pressure. As with the positive LCA-

monolith, the neutral LCA-monolith did not exhibit non-specific interactions for the proteins studied.

This is shown in Fig. 3 where three non-glycosylated proteins [e.g.,  $\beta$ -lactoglobulin B ( $\beta$ -Lac B), trypsin inhibitor (TI) and carbonic anhydrase (CA)] pass through the column with no retention and elute at the dead time of the column while the glycoprotein human transferrin (HT) is captured by the column and elutes upon applying a step gradient of the hapten sugar, Me- $\alpha$ -D-Man.

Human transferrin is known to have two glycosylation sites at Asn-413 and 611, which may be occupied either by di-, tri- or tetra-antennary glycans of the *N*-acetylglucosaminic type (i.e., complex type glycans) [34-36] at different degrees of sialylation [37, 38]. Despite the fact that LCA would require fucosylated complex type glycans for recognition, the LCA column binds the HT whose complex type glycans are non-fucosylated except in trace amounts in human cerebrospinal fluid [39]. This agrees with the observation that whereas glycans and glycopeptides interact specifically with lectins, and can be fractionated on the basis of actual affinity chromatography, a glycoprotein, having two or more glycosylation sites (e.g., HT) each of which can be occupied by more than one type of glycan, can interact with more than one lectin since lectins are able to recognize different saccharidic sequences belonging to the same glycan class [7]. It should be noted that HT exhibited two fractions one is retained (rf-HT) by the LCA column and another fraction is unretained (uf-HT) by the LCA column. While the rf-HT would have the carbohydrate motif or determinant recognized by LCA, the uf-HT is the glycosylated fraction without the carbohydrate motif recognized by the LCA.

In CEC, the positive-LCA monolith allowed not only the capture of the glycoproteins but also their separation. This is seen in Fig. 4 which shows the separation of AGP and lipoxidase in a three-step process involving first a nano-LC elution step to elute unretained species followed by a second nano-LC step to change from a high ionic strength to a low ionic strength mobile phase and a final CEC step for debinding the retained glycoproteins and achieve their separation. This represents a superiority of affinity CEC over affinity nano-LC in the sense that in the later all captured glycoproteins will co-elute by applying the hapten sugar whereas in the former once the glycoproteins are released from the immobilized lectin they move differentially down the column according to their charge-to-mass ratio and separate under the influence of the applied electric field.  $\alpha$ -Acid glycoprotein (AGP) has a high-carbohydrate content (~ 40%) with five *N*-glycosylation sites at asparagine residues in positions 15, 38, 54, 75 and 85 of the 181 amino acid long polypeptide chains. To these five glycosylation sites various sialylated bi-, tri- and tetra-antennary complex-type *N*-glycans with and without fucose residues [40] as well as tetra-antennary chains with repeating lactosamine blocks are attached [41]. It should be noted that AGP yields an unretained fraction (uf-AGP) and a retained fraction (rf-AGP) on the LCA-monolith.

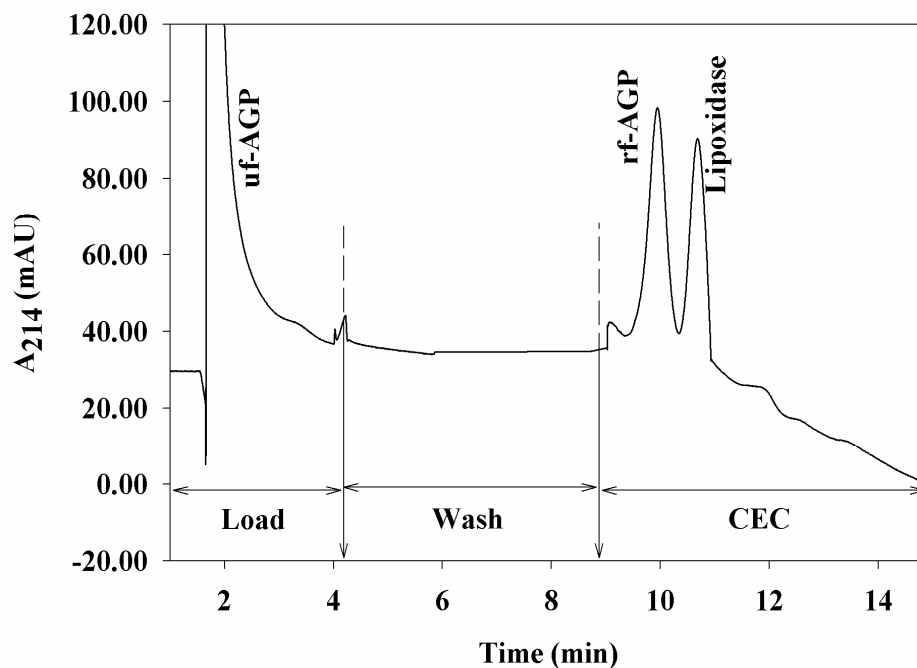


**Figure 4.** *Electrochromatogram of lipoxidase and AGP obtained on an LCA-monolith based on the positive API monolithic column by a three-step process. Column dimensions, 25 cm effective length, 33.5 cm total length x 100  $\mu\text{m}$  I.D.; binding mobile phase, 20 mM bis-Tris, pH 6.0, containing 100 mM NaCl, 1 mM  $\text{CaCl}_2$ , 1 mM  $\text{MnCl}_2$  and 1 mM  $\text{MgCl}_2$ ; washing mobile phase, 20 mM bis-Tris, pH 6.0; eluting mobile phase, 0.2 M Me- $\alpha$ -D-Man in 2.0 mM TETA pH 6.0;  $\Delta P$ , 1.0 MPa for both binding and washing mobile phases as well as sample injection; running voltage, -20 kV for eluting mobile phase; sample injection 6 s.*

Returning to Fig. 4, the three-step process recently introduced by Bedair and El Rassi [12], is essential for achieving affinity CEC in the third step. The binding mobile phase, which has a relatively high salt concentration and other divalent metal ions, is necessary for capturing the glycoconjugates by the immobilized lectin.

This first step can only be carried out by nano-LC due to the relatively high ionic strength, which would produce prohibitively high current in CEC. To perform CEC in the third step, a washing step (second step) with a low ionic strength mobile phase is necessary to prepare the column for CEC elution with a mobile phase containing the hapten sugar in a relatively low ionic strength mobile phase.

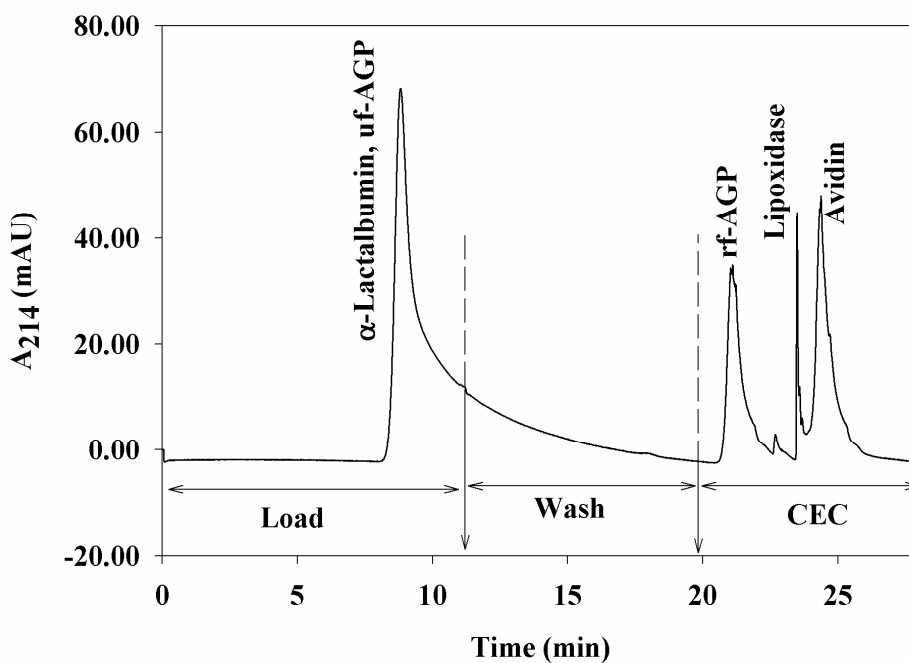


**Figure 5.** *Electrochromatogram of lipoxidase, AGP and avidin, using LCA immobilized on a neutral monolithic column. Conditions as in Fig. 4, except washing mobile phase, 4.0 mM EDA, pH 6.0.*

Affinity CEC was also performed on a neutral LCA monolith. As can be seen in Fig. 5, while the non-glycosylated protein  $\alpha$ -lactalbumin eluted with no retention in the

column dead volume with the binding mobile phase, the three glycoproteins AGP, lipoxidase and avidin were captured and eluted with the hapten sugar as three separated peaks thus again showing the superiority of affinity CEC. The eluting mobile phase incorporated EDA to boost the EOF. Avidin is a basic tetrameric glycoprotein (pI ~ 10.5) of  $M_r = 68,000$  composed of four identical subunits each of which consists of a single polypeptide chain bearing 128 amino acids. Of the 10-asparagine residues of each subunit, only Asn 17 is glycosylated. The carbohydrate moiety accounts for ~19% of the molecular weight of the protein and exhibits extensive microheterogeneity [42]. Avidin contains at least 3 distinct *N*-glycans composed of four *N*-acetyl-glucosamines and five mannoses [43].

Nano-LC and CEC with WGA Monoliths. Again, the inclusion of a positively charged monomer in the polymerization reaction yielded a WGA-monolith of relatively high permeability as in the case of positive LCA-monolith. Figure 6 shows the nano-LC on the positive WGA-monolith (i.e., based on AP1 monolith) of a non-glycosylated protein  $\alpha$ -lactalbumin and a glycoprotein fetuin. As expected, only the glycoprotein fetuin was retained by the column and eluted by a step gradient with the hapten sugar, *N*-acetylglucosamine (GlcNAc). Fetuin has three *N*-linked sites that contain bi- [44, 45] and tri-antennary [46, 47] complex glycan structures. In addition, three *O*-linked sites are present that are occupied with sialylated di- and tetra-saccharides [48, 49]. The high degree of sialylation and the presence of complex *N*-glycans may be responsible for the strong binding of fetuin to the immobilized WGA

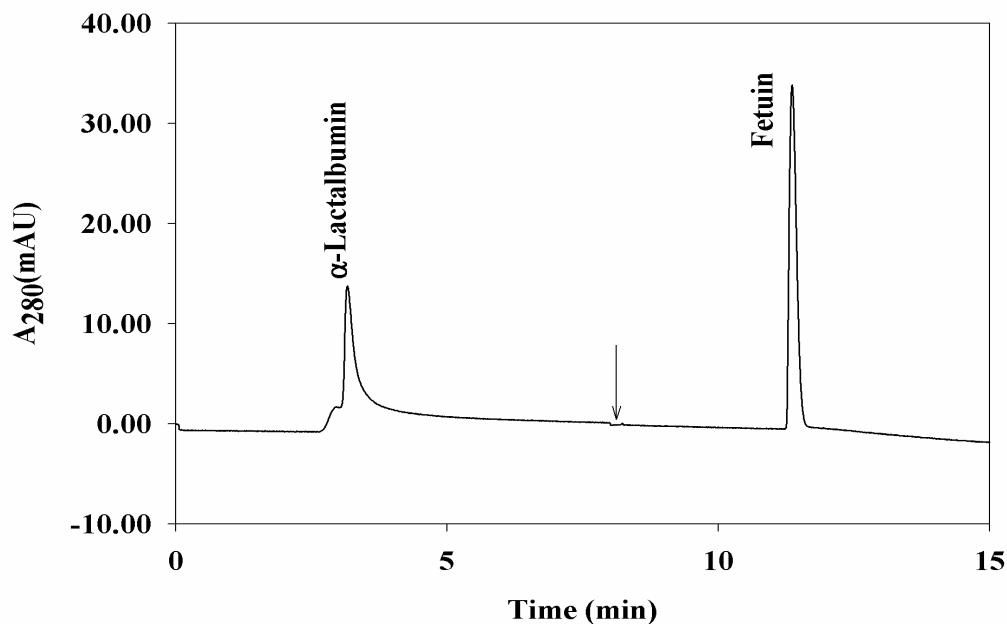


**Figure 6.** *Chromatogram of fetuin in the presence of non-glycosylated  $\alpha$ -lactalbumin, using WGA immobilized on a positive monolithic column of the AP1 type. Column dimensions, 25 cm effective length, 33.5 cm total length x 100  $\mu$ m I.D.; binding mobile phase, 10 mM EDA, pH 6.0, containing 100 mM NaCl; eluting mobile phase, 0.2 M GlcNAc in 1 mM EDA introduced at 8.0 min as indicated by the arrow;  $\Delta P$ , 1.0 MPa for both running mobile phase and sample injection; sample injection, 6 s.*

Similar to the neutral LCA-monolith, the neutral WGA-monolith exhibited a relatively low permeability. Figure 7 shows the affinity of the immobilized WGA to the glycoprotein AGP and in major part the absence of it to ovalbumin (OVA). A small fraction of OVA was retained (rf-OVA) by the WGA column and co-eluted with AGP (rf-AGP) upon a step gradient with the hapten sugar. As discussed in the preceding section AGP possess *N*-glycans at various degrees of sialylation and this may explain its affinity to the immobilized WGA.



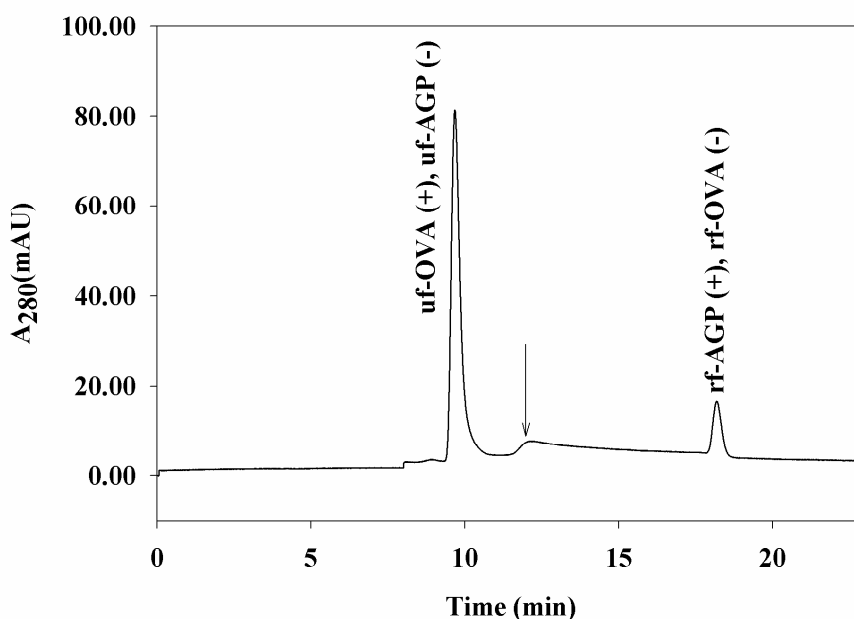


**Figure 7.** Chromatogram of AGP in the presence of ovalbumin, using WGA immobilized on a neutral monolithic column. Conditions as in Fig. 6, except for the eluting mobile phase, which was introduced at 11.0 min as indicated by the arrow. (-), Signifies minor component while (+) signifies major component.

One small fraction of AGP (~ 20% of injected protein) passes through the column unretained (uf-AGP). OVA has a single *N*-glycosylation site (Asn 292) to which various high mannose type or hybrid type *N*-glycans are attached [50, 51]. This explains the non-binding of OVA (uf-OVA) in major fraction to the WGA column, and the elution of which occurred at the dead time of the column with the binding mobile phase. The much smaller retained fraction of OVA (rf-OVA) may be the fraction of the protein glycosylated with hybrid glycans to which WGA has an affinity (see Fig. 1). While Fig. 6 demonstrates the absence of a non-specific interaction of the monolith with non-

glycosylated protein (e.g.,  $\alpha$ -lactalbumin), Fig. 7 shows the reactivity of WGA with glycoproteins having the oligosaccharides, which interact selectively with WGA.

In CEC, the neutral monolith yielded the simultaneous separation of three glycoproteins as shown in Fig. 8. In this figure, a three step process was conducted including a binding step by nano-LC followed by a second nano-LC step with a mobile phase of lower ionic strength to prepare the column for the third elution step by CEC with a mobile phase containing the hapten sugar GlcNAc. As can be seen in Fig. 8, the non-glycosylated protein trypsin inhibitor (TI) along with the unretained fraction of HT (uf-HT) pass unretained through the column in the void volume with the binding mobile phase while the glycosylated proteins glucose oxidase (GO), fetuin and rf-HT are captured by the column and elute into three separated zones upon the application of a step gradient elution with the hapten sugar GlcNAc. The carbohydrate content of the enzyme GO from *A. niger* consists mainly of D-mannose (about 14% of the enzyme by mass) but it also contains D-glucosamine (2.3%) and D-galactose (0.3%) [52, 53]. Its affinity to WGA may be attributed to the presence of *N*-acetylglucosamine saccharides in its glycan moiety.

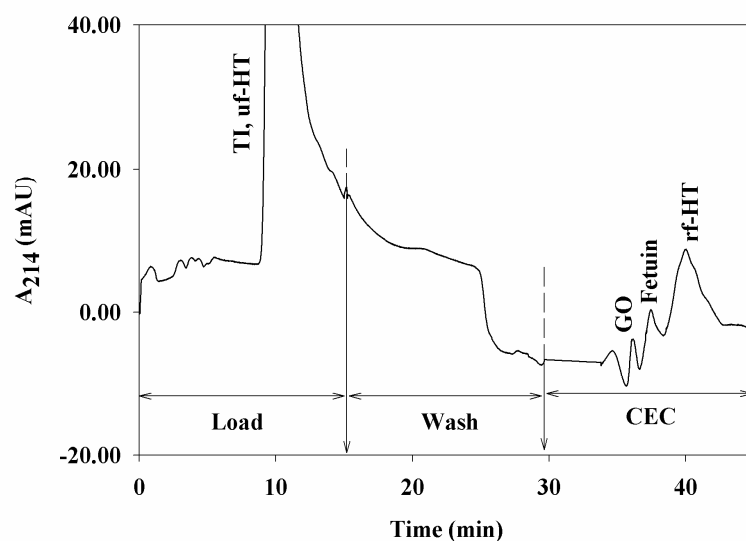


**Figure 8.** *Electrochromatogram of glucose oxidase (GO), fetuin and HT in the presence of non-glycosylated TI, obtained on WGA immobilized on a neutral monolithic column by a three-step process. Binding mobile phase: 10 mM EDA, pH 6.0, containing 100 mM NaCl; washing mobile phase: 4.0 mM EDA, pH 6.0; eluting mobile phase: 0.2 M GlcNAc in 2.0 mM EDA, pH 6.0;  $\Delta P$ , 1.0 MPa for binding mobile phase and washing mobile phase as well as sample injection; running voltage, -20 kV for eluting mobile phase; sample injection 6 s. Column dimensions as in Fig. 6.*

## Nano-LC and CEC with Coupled Lectin Affinity Monolithic Columns

Nano-LC with LCA-Monolith → WGA-Monolith Coupled in Series. Four glycoproteins were injected onto two neutral lectin monolithic columns, namely LCA- and WGA-monoliths coupled in series in the order LCA → WGA. The four glycoproteins yielded two separate peaks as shown in Fig. 9 each of which representing the glycoproteins reactive with the corresponding lectin. The elution of the glycoproteins captured by a given lectin was affected independently by the corresponding hapten sugar. In this case, the elution was affected successively by Me- $\alpha$ -D-Man and GlcNAc. AGP was found in both peaks indicating the presence of two distinct fractions one with affinity to LCA and another one with affinity to WGA. Avidin which is equally retained by both lectin columns eluted in the second peak while lipoxidase with affinity only to LCA eluted in the first peak and fetuin with affinity only to WGA eluted in the second peak. In summary, in nano-LC one peak is generated for each lectin column; that is two peaks for two lectin columns coupled in series, three peaks for three columns and so on. Since different lectins usually have different hapten sugars, two, three or more lectin columns can be coupled in series to fractionate a mixture of glycoproteins (also glycopeptides and glycans) into two, three or more fractions in nano-LC. These affinity schemes are being investigated in our laboratories, and their potentials will be described in upcoming articles.

CEC with LCA-Monolith  $\leftrightarrow$  WGA-Monolith Coupled in Series. Figure 10 shows the CEC separation of six different glycoproteins in about 35 min using two-lectin columns coupled in series in the order WGA → LCA.

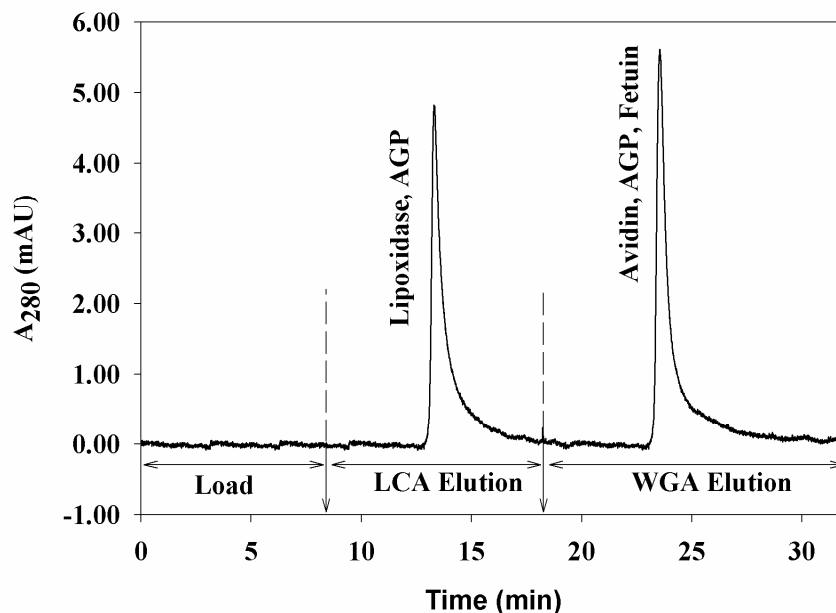


**Figure 9.** Chromatogram of AGP, lipoxidase, avidin and fetuin, obtained on coupled lectin columns in the order LCA →WGA where the lectins were immobilized on a neutral monolith. Column dimension, 25 cm effective length, 33.5 cm total length x 100 μm I.D. composed of two segments connected butt-to-butt with zero dead volume teflon tubing, where the LCA-monolith occupies the first segment (12.5 cm) and the WGA-monolith the second segment and has an effective length of 12.5 cm and an open portion of 8.5 cm; binding mobile phase: 10 mM EDA, pH 6.0, containing 100 mM NaCl, 1 mM CaCl<sub>2</sub>, 1 mM MnCl<sub>2</sub> and 1 mM MgCl<sub>2</sub>; eluting mobile phase: 0.2 M GlcNAc and 0.2 M Me-α-D-Man in 1 mM EDA introduced at 8.0 and 18.0 min respectively as indicated by the two arrows; ΔP, 1.0 MPa for both running mobile phase and sample injection; sample injection, 6 s.

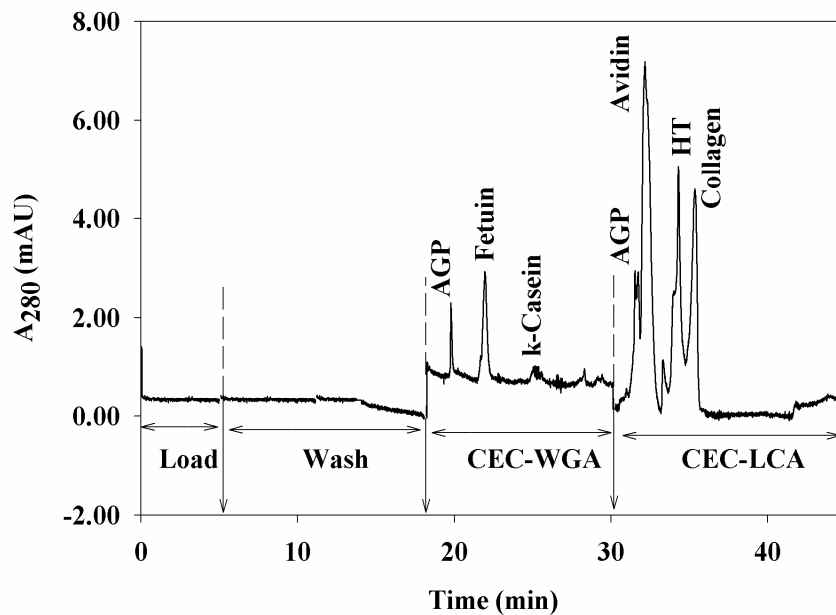


**Figure 10.** *Electrochromatogram of AGP, HT, collagen,  $\kappa$ -casein, avidin and fetuin, obtained on coupled lectin columns in the order WGA→LCA where the lectins were immobilized on a neutral monolith. Column dimension, 25 cm effective length, 33.5 cm total length x 100  $\mu$ m I.D. composed of two segments connected butt-to-butt with zero dead volume teflon tubing, where the WGA-monolith occupies the first segment (12.5 cm) and the LCA-monolith the second segment and has an effective length of 12.5 cm and an open portion of 8.5 cm; binding mobile phase: 10 mM DETA, pH 6.0, containing 100 mM NaCl, 1 mM CaCl<sub>2</sub>, 1 mM MnCl<sub>2</sub> and 1 mM MgCl<sub>2</sub>; washing mobile phase, 2.5 mM DETA, pH 6.0 introduced at 5 min; eluting mobile phase: 0.1 M Me- $\alpha$ -D-Man and 0.1 M GlcNAc in 2.5 mM phosphate, pH 3.0 introduced at 18.0 and 30.0 min, respectively, as indicated by the arrows;  $\Delta P$ , 1.0 MPa for both running mobile phase and sample injection; running voltage, -20 kV for eluting mobile phases,; sample injection, 6 s.*

As in the preceding section, each lectin column is eluted with its hapten sugar. The first eluting mobile phase contains GlcNAc while the second has Me- $\alpha$ -D-Man. In this case, the separation requires four distinct steps, two of which are nano-LC involving loading and washing mobile phases, and the last two steps are CEC requiring two eluting mobile phases. In CEC, once the glycoproteins are released from the lectin by the hapten sugar, the glycoproteins undergo differential electromigration by virtue of differences in charge-to-mass ratio. AGP yields 3 peaks corresponding to different glycoforms. One peak has affinity to WGA while the other two peaks correspond to glycoforms with affinity to LCA. This is a typical example demonstrating the potentials of coupled lectin columns to separate the glycoforms of a given glycoprotein. This is shown again in Fig. 11 but in the reverse order LCA  $\rightarrow$  WGA where one can see first the two glycoforms with affinity to LCA as two separate peaks and then the glycoforms with affinity to WGA appearing as a single peak.

Returning to Fig. 10, since only WGA exhibits affinity toward fetuin and  $\kappa$ -casein, these two glycoproteins are eluted first from WGA column as two separate peaks whereas avidin, collagen and HT, which have affinity to both WGA and LCA, are eluted in the fourth step from the LCA column as three separate peaks.

Milk  $\kappa$ -casein is a glycoprotein [54] of 169 amino acid residues with a  $M_r \sim 19,000$  [55]. The glycan part of  $\kappa$ -casein is constituted of only three different monosaccharides: galactose (Gal), *N*-acetylgalactosamine (GalNAc) and *N*-acetylneuraminic acid, i.e., sialic acid (NeuAc). At least five *O*-glycans have been identified in  $\kappa$ -casein including GalNAc, Gal-GalNAc disaccharide, NeuAc-Gal-GalNAc trisaccharide, Gal-(NeuAc)GalNAc trisaccharide, and NeuAc-Gal-(NeuAc)GalNAc

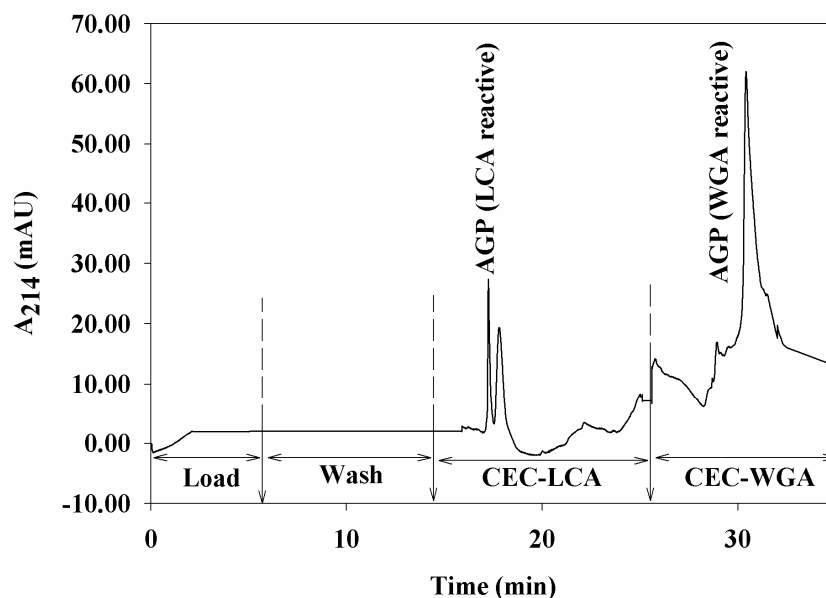


**Figure 11.** *Electrochromatogram of AGP glycoforms, obtained on coupled lectin columns in the order LCA→WGA where the lectins were immobilized on a neutral monolith. Column dimension, 25 cm effective length, 33.5 cm total length x 100 μm I.D. composed of two segments connected butt-to-butt with zero dead volume teflon tubing, where the LCA-monolith occupies the first segment (12.5 cm) and the WGA-monolith the second segment and has an effective length of 12.5 cm and an open portion of 8.5 cm; binding mobile phase: 10 mM EDA, pH 6.0, containing 100 mM NaCl, 1 mM CaCl<sub>2</sub>, 1 mM MnCl<sub>2</sub> and 1 mM MgCl<sub>2</sub>; washing mobile phase: 5 mM EDA, pH 6.0 introduced at 5 min; eluting mobile phase: 0.1 M Me-α-D-Man and 0.1 M GlcNAc in 1.0 mM EDA, pH 6.0 introduced at 15.0 and 25.0 min, respectively, as indicated by the arrows. ΔP, 1.0 MPa for both running mobile phase and sample injection; running voltage, -20 kV for eluting mobile phase; sample injection, 6 s.*



At least five *O*-glycans have been identified in  $\kappa$ -casein including GalNAc, Gal-GalNAc disaccharide, NeuAc-Gal-GalNAc trisaccharide, Gal-(NeuAc)GalNAc trisaccharide, and NeuAc-Gal-(NeuAc)GalNAc. The sialylated nature of the *O*-glycans of  $\kappa$ -casein may explain its affinity to WGA and not to LCA.

On the other hand, the collagen type VI glycoprotein from human placenta is a heterotrimer with 19 potential sites for attachment of *N*-glycans. The oligosaccharide is a heterogeneous biantennary *N*-acetylglucosamine type. The heterogeneity reflects the presence or absence of five Gal residues at the non-reducing end and the presence of a fucose residue at the reducing end [59]. The high degree of glycosylation of the type VI collagen and heterogeneity of its *N*-glycans may explain the affinity of this glycoprotein to both WGA and LCA.

## Conclusions

In this investigation, we have shown that lectin monolithic columns are very effective tools for glycoprotein isolation and separation. While lectin affinity nano-LC results in an enrichment of classes of different glycoproteins having similar *N*-glycans recognized by the immobilized lectin, lectin affinity CEC provides the simultaneous capturing and separation of different glycoproteins due to differences in charge-to-mass ratio, thus emerging as a very suitable microcolumn separation technique for nano glycomics/proteomics. This investigation has demonstrated for the first time the coupling of lectin capillary columns in series for enhanced separation by LAC using the CEC modality. In the coupled columns format, glycoforms of a given glycoprotein are readily separated without sample loss since the species are transferred from column-to-column while staying in the liquid phase. These schemes are expected to find general use in nano glycoproteomics.

## References

- (1) Wnag, I., Li, Y., Que, Q., Bhattacharya, M., Lane, L. C., Chaney, W. G., Etten, J. L. V., *Proc. Natl. Acad. Sci. USA*, **1990**, *90*, 3840-3844.
- (2) Roberts, P. C., Garten, W., Klenk, K. D., *J. Virol.*, **1993**, *67*, 3048-3060.
- (3) van den Steen, P., Rudd, P. M., Dwek, R. A., Opdenakker, G., *Crit. Rev. Biochem. Mol. Biol.*, **1998**, *33*, 151-208.
- (4) Apweiler, R., Hermjakob, H., Sharon, N., *Biochim. Biophys. Acta*, **1999**, *1473*, 4-8.
- (5) Cummings, R. D., in: Gabius, H.-J., Gabius, S. (Eds), *Glycosciences. Status and Perspectives* Chapman & Hall, London, **1997**, pp. 191-199.
- (6) Carlsson, S. R., in: Fukuda, M., Kobata, A. (Eds), *Glycobiology. A Practical Approach*, IRL Press, Oxford, **1993**, pp. 1-26.
- (7) Montreuil, J., S. B., Debray, H., Fournet, B., Spik, G., Strecker, G., in: Chaplin, M. F., Kennedy, J. F. (Eds), *Carbohydrate Analysis. A Practical Approach* IRL Press, Oxford. **1986**, pp. 143-204.
- (8) Qiu, R., Regnier, F. E., *Anal. Chem.*, **2005**, *77*, 2802-2809.
- (9) Yang, Z., Hancock, W. S., *J. Chromatogr. A*, **2005**, *1070*, 57-64.
- (10) Madera, M., Mechref, Y., Novotny, M., *Anal. Chem.*, **2005**, *77*, 4081-4090.
- (11) Bedair, M., El Rassi, Z., *J. Chromatogr. A*, **2005**, *1079*, 236-245.
- (12) Bedair, M., El Rassi, Z., *J. Chromatogr. A*, **2004**, *1044*, 177-186.
- (13) Kobata, A., Yamashita, K., in: Fukuda, M., Kobata, A. (Eds), *Glycobiology. A Practical Approach*, IRL Press, Oxford, **1993**, pp. 103-125.

- (14) Debray, H., Montreuil, J., in: Breborowicz, J., Mackiewicz, A. (Eds), *Affinity Electrophoresis: Principles and Application* CRC Press, Boca Raton. , **1991**, pp. 23-57.
- (15) Bhavanandan, V. P., Umemoto, J., Banks, J. R., Davidson, E. A., *Biochemistry*, **1977**, *16*, 4426-4437.
- (16) Osawa, T., Tsuji, T., *Ann. Rev. Biochem.*, **1987**, *56*, 21-42.
- (17) Prime, S., Merry, T., in: Hounsell, E. F. (Ed), *Glycoanalysis Protocols Humana* Press Inc., Totowa, **1998**, pp. 53-69.
- (18) Kornfeld, K., Reitman, M. L., Kornfeld, R., *J. Biol. Chem.*, **1981**, *256*, 6633-6640.
- (19) Debray, H., Decout, D., Strecker, G., Spik, G., Montreuil, J., *Eur. J. Biochem.*, **1981**, *117*, 41-55.
- (20) Tsuji, T., Irimura, T., Osawa, T., *J. Biol. Chem.*, **1981**, *256*, 10497-10502.
- (21) Tennikova, T. B., Belenkii, B. G., Svec, F., *J. Liq. Chromatogr.*, **1990**, *13*, 63-70.
- (22) Petro, M., Svec, F., Frechet, J. M. J., *Biotech. Bioeng.*, 1996, *49*, 355-363.
- (23) Pan, Z., Zou, H., Mo, W., Huang, X., Wu, R., *Anal. Chim. Acta*, **2002**, *466*, 141-150.
- (24) Pavlinek, V., Quadrat, O., Sába, P., Benes, M. J., Trlica, J., *Colloid Polym. Sci.*, **1998**, *276*, 690-697.
- (25) Svec, F., Peters, E. C., Sykora, D., Frechet, J. M. J., *J. Chromatogr. A*, 2000, *887*, 3-29.

- (26) Svec, F., *Capillary column technology: Continuous polymer monoliths*, in *Capillary Electrochromatography*, Deyl, Z. and Svec, F., (Eds) **2001**, Elsevier: Amsterdam. p. 183-240.
- (27) Bedair, M., El Rassi, Z., *J. Chromatogr. A*, **2003**, *1013*, 35-45.
- (28) Bedair, M., El Rassi, Z., *Electrophoresis*, **2002**, *23*, 2938-2948.
29. Bedair, M., El Rassi, Z., *J. Chromatogr. A*, **2003**, *1013*, 47-56.
- (30) Okanda, F., El Rassi, Z., *Electrophoresis*, **2005**, *26*, 1988-1995.
- (31) Wittenbach, V. A., *Plant Physiol.*, **1983**, *73*, 125-129.
- (32) Tranbarger, T. J., Franceschi, V. R., Hildebrand, D. F., Grimes, H. D., *The Plant Cell*, **1991**, *3*, 973-987.
- (33) Franceschi, V. R., Giaquinta, R. T., *Planta*, **1983**, *157*, 422-431.
- (34) Hatton, M. W. C., Marz, L., Berry, L. R., BDebanne, M. T., Regoeczi, E., *Biochem. J.*, **1979**, *181*, 633-638.
- (35) Marz, L., Hatton, M. W. C., Berry, L. R., Regoeczi, E., *Can. J. Biochem.*, **1982**, *60*, 624-630.
- (36) Montreuil, J., Spik, G., Mazurier, J., in: Montreuil, J., Vliegenthart, J. F. G., Schachter, H., (Eds), *Glycoproteins II* Elsevier, Amsterdam, **1997**, pp. 203-242.
- (37) Spik, G., Coddeville, B., Montreuil, J., *Biochimie*, **1988**, *70*, 1459-1469.
- (38) Yamashita, K., Koide, N., Endo, T., Iwaki, Y., Kobata, A., *J. Biol. Chem.*, **1989**, *264*, 2415-2423.
- (39) Hoffmann, A., Nimtz, M., Getzlaff, R., Conradt, H.S., *FEBS Lett.*, **1995**, *359*, 164-168.

- (40) Clemetson, K. J., in: Montreuil, J., Vliegenthart, J. F. G., Schachter, H., (Eds), *Glycoproteins II* Elsevier, Amsterdam, **1997**, pp. 173-201.
- (41) Shiyan, S. D., Bovin, N. V., *Glycoconjugate J.*, **1997**, *14*, 631-638.
- (42) Bruch, R. C., White, H. B., *Biochemistry*, **1982**, *21*, 5334-5341.
- (43) DeLange, R., Huang, T., *J. Biol. Chem.*, **1971**, *246*, 698-709.
- (44) Green, E. D., Adelt, G., Baenziger, J. U., Wilson, S., Van Halbeek, H., *J. Biol. Chem.*, **1988**, *263*, 18253-18268.
- (45) Townsend, R. R., Hardy, M. R., Wong, T. C., Lee, Y. C., *Biochemistry*, **1986**, *25*, 5725-5731.
- (46) Cumming, D. A., Hellerqvist, C. G., Harris-Brandts, M., Michnick, S. W., Carver, J. P., Bendiak, B., *Biochemistry*, **1989**, *28*, 6500-6512.
- (47) Bendiak, B., Harris-Brandts, M., Michnick, S. W., Carver, J. P., Cumming, D. A., *Biochemistry*, **1989**, *28*, 6491-6499.
- (48) Edge, A. S. B., Spiro, R. G., *J. Biol. Chem.*, **1987**, *262*, 16135-16141.
- (49) Spiro, R. G., Bhoyroo, V. D., *J. Biol. Chem.*, **1974**, *249*, 5704-5717.
- (50) An, H. J., Peavy, T. R., Hedrick, J. L., Lebrilla, C. B., *Anal. Chem.*, **2003**, *75*, 5628-5637.
- (51) Ohyama, Y., Kasai, K., Nomoto, H., Inoue, Y., *J. Biol. Chem.*, **1985**, *260*, 6882-6887.
- (52) Wilson, R., Turner, A. P. F., *Biosensors & Bioelectronics*, **1992**, *7*, 165-185.
- (53) Pazur, J. H., Kleppe, K., Ball, E. M., *Arch. Biochem.*, **1963**, *103*, 513-516.
- (54) Wheelock, J., Sinkinson, G., *Biochim. Biophys. Acta*, **1969**, *194*, 597.

- (55) Mercier, J. C., Brignon, G., Ribadeau-Dumas, B., *Eur. J. Biochem.*, **1973**, 35, 222-231.
- (56) Saito, T., Itoh, T., *J. Dairy Sci.*, **1992**, 75, 1768-1774.
- (57) Saito, T., Yamaji, A., Itoh, T., *Biochim. Biophys. Acta*, **1981**, 673, 487-494.
- (58) Fiat, A. M., P. J., *Mol. Cell. Biol.*, **1989**, 87, 5-30.
- (59) Noelken, M. E., Hudson, B. G., in: Montreuil, J., Schachter, H., Vliegenthart, J.F.G. (Eds), *Glycoproteins* Elsevier, Amsterdam, **1995**. pp. 589-616.

CHAPTER IV

PEPTIDE MAPPING BY REVERSED-PHASE CAPILLARY  
ELECTROCHROMATOGRAPHY USING  
A NEUTRAL MONOLITHIC  
STATIONARY PHASE

Introduction

Capillary electrochromatography (CEC), which combines both electrokinetic phenomena (electroosmosis and electrophoresis) and chromatographic distribution between two phases, provides a unique selectivity for achieving the separation of complex mixtures such as tryptic digests of proteins also called peptide mapping of proteins. However, the exploitation of the full potential of CEC in peptide mapping has been hampered by the lack of suitable stationary phases, which exhibit one single and predominant retention mechanism rather than a mixed mode retention mechanism which renders the optimization of peptide mapping a complicated process.

Most of the stationary phases that have been designed for CEC bear the interactive chromatographic ligand of interest (e.g., nonpolar ligands) and fixed charges (e.g., sulfonic acid groups, carboxylic acid groups, amine functionalities, etc.) on their surface [1-8]. The fixed charges are usually intentionally introduced into the stationary



phase to support the electroosmotic flow (EOF) necessary to move the mobile phase across the capillary column. Under this condition, a mixed mode retention mechanism will be readily established for charged solutes *via* the interactive ligands and the fixed charges. Typical examples of these mixed mode stationary phases used in peptide and proteins separation include microparticulate silica bonded with octadecyl functions and strong cation exchange groups [8, 9] or embedded cationic quaternary amine in a dodecyl chain [10]. Also, a monolithic stationary phase based on *N,N*-dimethylacrylamide-piperazine diacrylamide bearing sulfonic acid groups [11] and poly(glycidyl methacrylate-co-ethylene dimethacrylate) bearing the ionic *N*-ethylbutylamine moiety [12] were shown to be useful in the separation of peptides. The current state-of-the-art of CEC of peptides is summarized in recent a monograph [13] and several review articles [14-18].

In this chapter, the full potential of the neutral C17 monolith, which was developed and characterized in Chapter II, is further demonstrated here in peptide mapping. As shown in Chapter II, the neutral monolith produced sufficient EOF for driving the mobile phase across the capillary column and allowed the CEC of charged species including peptides and proteins in the absence of electrostatic interactions. Under this condition, the main retention mechanism of charged species is a reversed phase electrochromatography (RP-CEC) and differential electromigration under the influence of the applied electric field. As will be shown in this chapter, the optimization of the RP-CEC peptide mapping with C17 monolith is a simple process, and the same mobile phase composition proved to be optimal for achieving the peptide map of various proteins including glycosylated and phosphorylated proteins.

## Experimental

### Instrumentation

The instrumentation used was described in the previous chapter.

### Reagents and Materials

Pentaerythritol diacrylate monostearate (PEDAS), 2,2'-azobisisobutyronitrile (AIBN), 3-(trimethoxysilyl)propylmethacrylate were from Aldrich (Milwaukee, WI, U.S.A.). Cyclohexanol, ethylene glycol (EG) and ACN (HPLC grade) were from Fisher Scientific (Fair Lawn, NJ, U.S.A.). Human  $\alpha_1$ -acid glycoprotein (AGP), human transferrin, ovalbumin (egg albumin), cytochrome C from bovine heart, myoglobin from horse skeletal muscle, ribonuclease B from bovine pancreas, iodoacetamide and 2-mercaptoethanol were from Sigma (St. Louis, MO, U.S.A.). Sodium phosphate monobasic was from Mallinckrodt (Hazelwood, MO, U.S.A.) and sodium octyl sulfate salt (HPLC grade) from Acros Organics (NJ, U.S.A.). Sequencing grade-modified trypsin was obtained from Promega (Madison, WI, U.S.A.). Fused-silica capillaries with an internal diameter of 100  $\mu\text{m}$  and an outer diameter of 360  $\mu\text{m}$  were from Polymicro Technology (Phoenix, AZ, U.S.A.).

### Column Pretreatment

The inner wall of the fused-silica capillary was treated with 1.0 M sodium hydroxide for 30 min, flushed with 0.1 M hydrochloric acid for 30 min, and then rinsed

with water for 30 min. The capillary inner wall was then allowed to react with 50% (v/v) solution of 3-(trimethoxysilyl) propylmethacrylate in acetone for 12 h to vinylize the inner wall of the capillary and lastly the capillary was rinsed thoroughly with methanol then water and dried under a stream of nitrogen.

### *In situ* Polymerization

Polymerization solutions weighing 1.48 g were prepared from PEDAS and porogenic solvents in ratios of 30:70 (w/w) monomers/solvents. The ternary porogenic solvents consisted of 79.2 wt% cyclohexanol, 17.2 wt% EG, and 3.6 wt% water. AIBN (1% (w/w) with respect to monomer was added and the mixture was then sonicated to give a clear solution [19]. A 60 cm pretreated capillary was filled with the polymerization solution up to 50 cm by immersing the inlet of the capillary in the solution vial and applying a vacuum to the outlet. The capillary ends were then plugged with GC septa, and the capillary was submerged in a 60 °C water bath for 18 h. The resulting monoliths were rinsed thoroughly with 80:20 v/v ACN:water mixture using an HPLC pump.

### Sample Preparation

The preparation of the samples of glycopeptides/peptides was done by tryptic digestion of the given proteins after reduction and alkylation following the Promega protocol [20]. Five milligrams of a given protein was dissolved in 100 mM NH<sub>4</sub>HCO<sub>3</sub>, pH 8, and denatured using 6 M urea for 1h at 37 °C. The denatured protein was further

reacted with 50 mM mercaptoethanol for 1 h at 56 °C. Cysteinyl residues in the protein were subsequently alkylated with 100 mM iodoacetamide for 1 h at 37 °C. The solution was diluted with 100 mM NH<sub>4</sub>CO<sub>3</sub> (pH 8) and 1 mM CaCl<sub>2</sub> until the urea concentration was below 1 M. Thereafter, 1 µg/µL of modified trypsin was added and kept at 37 °C overnight to complete digestion of protein. Finally, 0.1 % TFA was added to the digestion and sonicated in water bath for 20 min to increase extraction and stop reaction [21, 22]

## Results and Discussion

### CEC Peptide Mapping of Proteins

Case of Myoglobin. Myoglobin is a well-studied standard protein, whose peptide chain consists of 153 amino acids with a nominal mass of about 17 kDa and a pI of 7.36 [23-25]. The tryptic digest of myoglobin yields 21 fragments including three free lysines, three dipeptides, one tripeptide and the remaining 14 fragments are longer peptides of varying lengths as shown in Table 2. Thus, myoglobin is a simple model protein for studying the effects of the various operating CEC parameters and demonstrating the potential of RP-CEC in peptide mapping.

Since peptides are charged species, it was necessary to study the effect of the ionic strength of the mobile phase on the migration of the peptides. Also, the concentration of the organic modifier of the mobile has a profound effect on the magnitude of retention in RP-CEC. Ionic pairing agents such as octyl sulfate can

**Table 1.** *Amino acid names, three and one-letter standard abbreviations [44].*

Non-polar side chains amino acids (Hydrophobic)

<b>Amino acid</b>	<b>Letter code</b>	<b>Single letter code</b>	<b>Other features</b>
Glycine	Gly	G	
Alanine	Ala	A	
Valine	Val	V	
Leucine	Leu	L	
Isoleucine	Ile	I	
Methionine	Met	M	
Phenylalanine	Phe	F	
Tryptophan	Trp	W	
Proline	Pro	P	

Polar uncharged and charged side chains amino acids (Hydrophilic)

<b>Amino acid</b>	<b>Letter code</b>	<b>Single letter code</b>	<b>Other features</b>
Serine	Ser	S	
Threonine	Thr	T	
Cysteine	Cys	C	
Tyrosine	Tyr	Y	
Asparagine	Asn	N	
Glutamine	Gln	Q	
Aspartic acid	Asp	D	Negatively charged
Glutamic acid	Glu	E	Negatively charged
Lysine	Lys	K	Positively charged
Arginine	Arg	R	Positively charged
Histidine	His	H	Positively charged

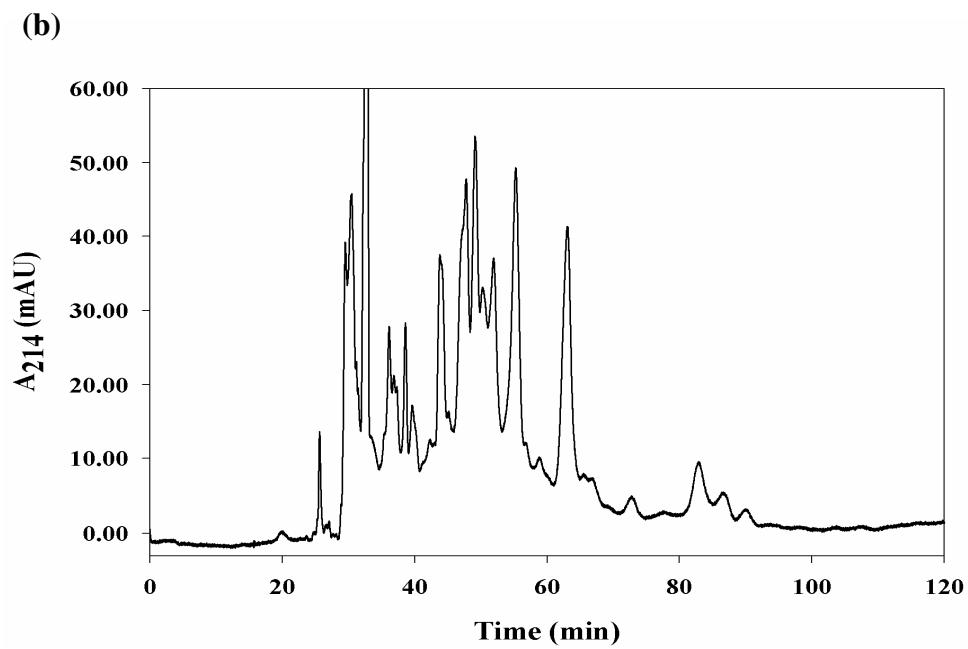
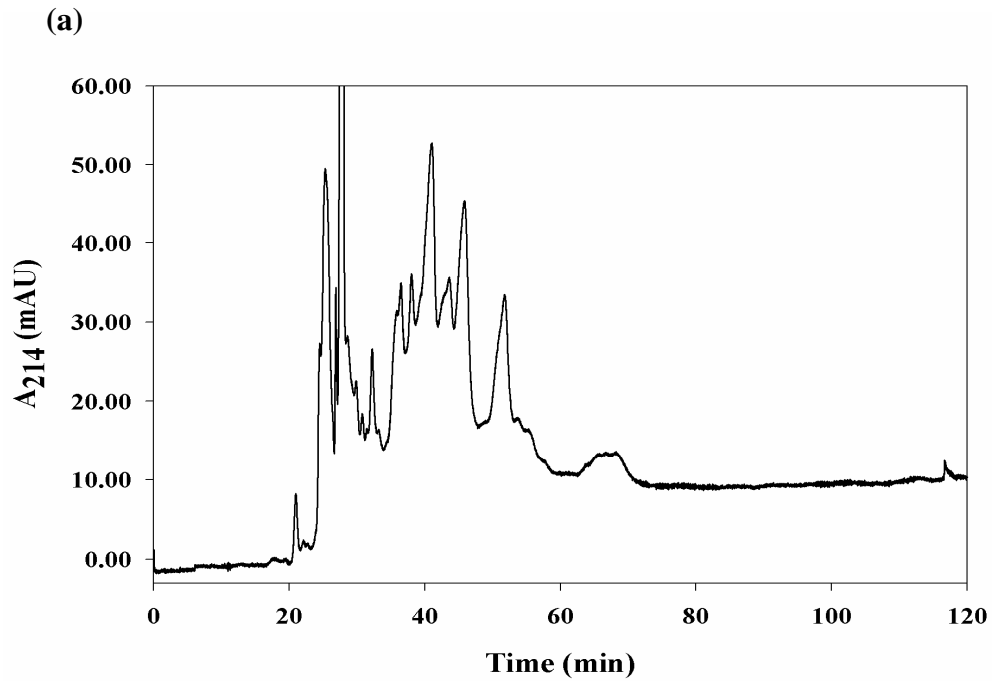
**Table 2.** Amino acid sequence and tryptic fragments of myoglobin as well as the net charge and L/W ratio of the various peptide fragments [23]

No	Fragment	Sequence	L/W	Net charge
1	1-16	GLSDGEWQQVLNVWGK	1.29	1-
2	17-31	VEADIAGHGQEVLR	1.5	1-
3	32-42	LFTGHPETLEK	0.83	1-
4	43-45	FDK	0.5	0
5	46-47	FK	1	1+
6	48-50	HLK	0.5	2+
7	51-56	TEAEMK	0.5	1-
8	57-62	ASEDLK	0.5	1-
9	63-63	K	0	1+
10	64-77	HGTVVLTALGGILK	2.5	2+
11	78-78	K	0	1+
12	79-79	K	0	1+
13	80-96	GHHEAELKPLAQSHATK	0.7	+3
14	97-98	HK	0	2+
15	99-102	IPIK	3	1+
16	103-118	YLEFISDAIIHVLHSK	1.43	1+
17	119-133	HPGNFGADAQGAMTK	1.5	0
18	134-139	ALELFR	2	0
19	140-145	NDIAAK	1	0
20	146-147	YK	0	1+
21	148-153	ELGFQG	1	1-

associate with charged solutes such as peptides and consequently affect their retention and migration in CEC. On this basis, the ionic strength and concentration of organic modifier and ion-pairing agent in the mobile phase were varied in order to determine the optimal mobile phase composition to achieve the best peptide mapping. However, it should be kept in mind that it is often difficult to resolve every peptide in a mixture, even with careful optimization of the running conditions.

The effect of the ionic strength of the mobile phase on myoglobin peptide mapping in RP-CEC was examined by varying the concentration of sodium phosphate in mobile phases composed of water/ACN (70:30 v/v) at pH 7.0. The results in terms of electrochromatograms at 30, 70, 100 and 150 mM sodium phosphate, pH 7, are shown in Fig. 1. As can be seen in and as expected, the retention time increased with increased sodium phosphate concentration in the mobile phase. The best resolution of the peptides was at 100 mM as shown in Fig. 1c, and any increase in the concentration did not improve the resolution significantly, but just led to a higher electric current and a longer analysis time. First, increasing the ionic strength decreased the EOF from 0.48 mm/sec at 30 mM to 0.41 mm/sec at 70 mM, to 0.29 mm/sec at 100 mM and to 0.22 mm/sec at 150 mM sodium phosphate. The observed increase in the migration time at high buffer concentrations is due to the screening effect of the electrolyte counter ions [26]. As the ionic strength is increased the screening effect becomes more pronounced and the solute effective charge is decreased, a fact that leads to more pronounced hydrophobic interactions between the peptides and the nonpolar C17 monolith. Since the magnitude of the screening effect of the running electrolyte varies among various ionic species, the

net result is a marked difference in the extent of the retention of the peptides, thus affecting differently the selectivity and resolution of the complex peptide digest





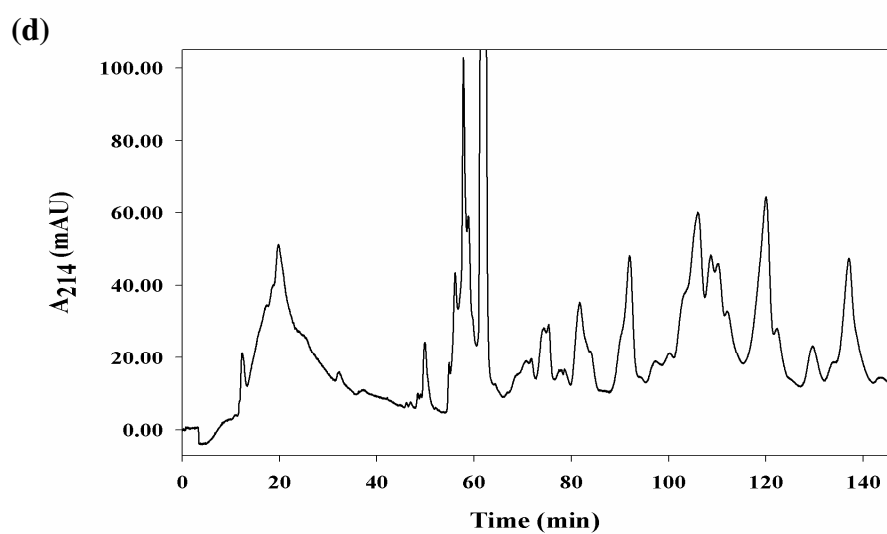
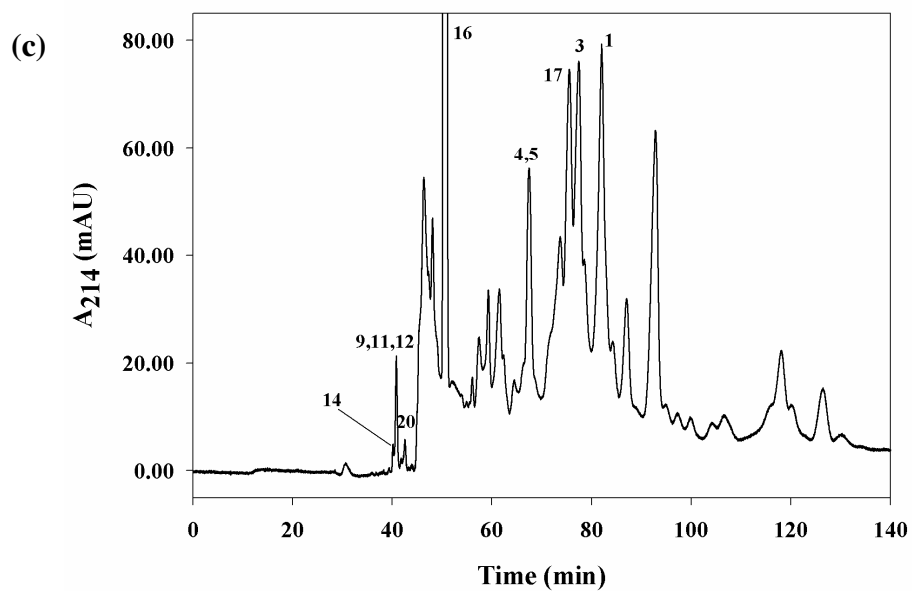
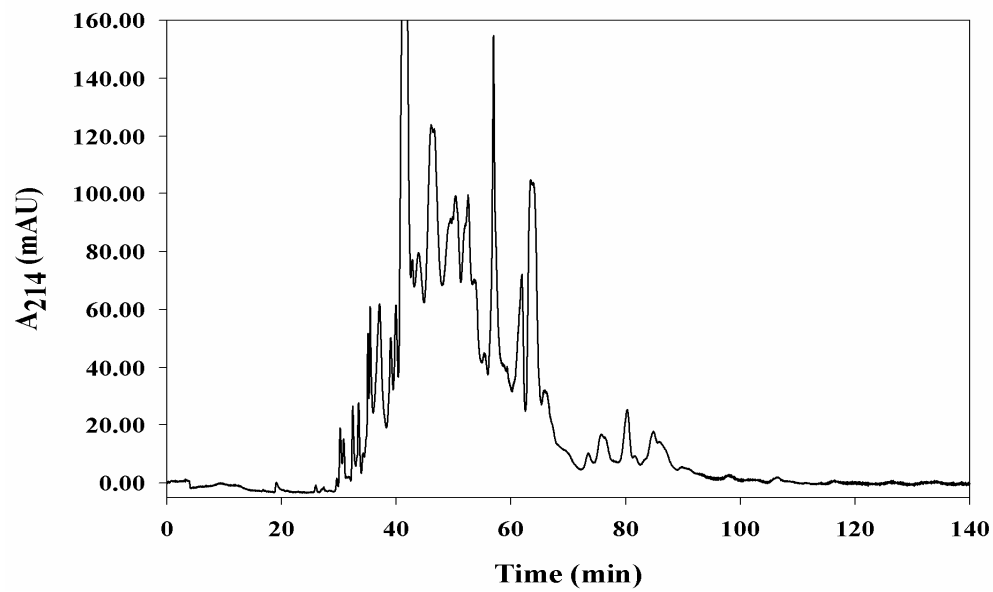


**Figure 1.** Electrochromatogram of the tryptic digest of myoglobin. Conditions: hydro-organic mobile phase, 30 % v/v ACN, (a) 30 mM, (b) 70 mM, (c) 100 mM and (d) 150 mM sodium phosphate, pH 7; capillary column, 50 cm effective length, 57 cm total length x 100  $\mu$ m ID; voltage, 10 kV.

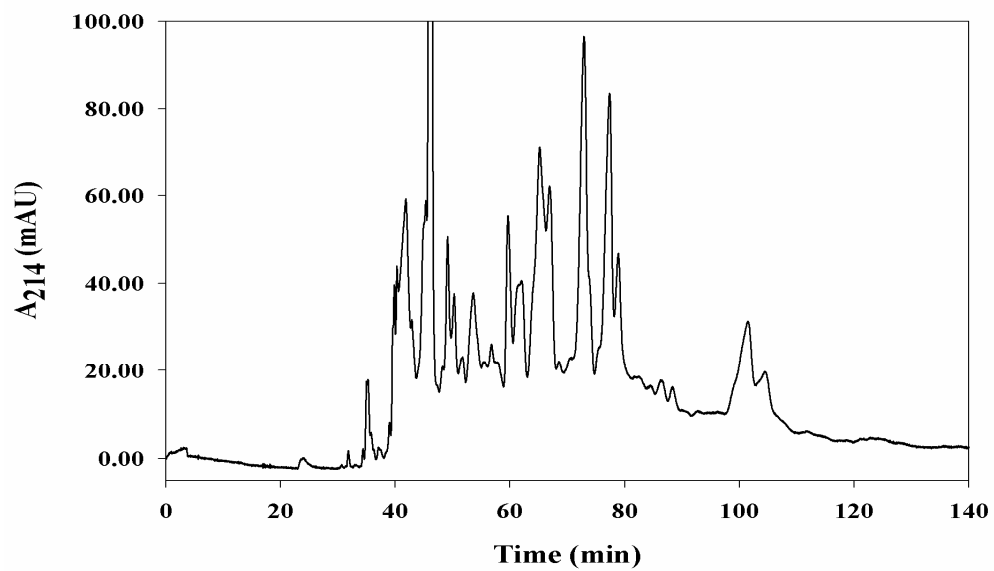
The influence of the ACN content of the mobile phase on the retention and resolution of the tryptic digest of myoglobin was evaluated at different percentages of ACN in mobile phases containing 100 mM phosphate buffer, pH 7. With reversed-phase stationary phases, a low content of organic solvent in the mobile phase is expected to favor hydrophobic interactions, and consequently higher retention while the converse is expected at higher organic content in the mobile phase. While this behavior is followed by uncharged non-polar solutes [19], the effect of organic modifier on the retention of charged solutes such as the peptides under investigation is a rather complex behavior as shown in Fig. 2 and Fig. 1c in terms of typical electrochromatograms obtained at different ACN concentration in the mobile phase. It has been observed recently that the net charge of dipeptides varied significantly with the organic content of the running electrolytes [27]. The effect of organic solvent on the ionization of charged solutes and consequently their electrophoretic migration in CZE is well documented [28, 29]. Furthermore, increasing the organic modifier content of the mobile phase seems to decrease the magnitude of EOF from 0.44 mm/sec at 10% to 0.35 mm/sec at 20%, to 0.29 mm/sec at 30% and to 0.27 mm/sec at 40% v/v ACN.

As can be seen in Fig. 2 and Fig. 1c, increasing the ACN concentration in the mobile phase from 10% to 30% caused the retention times of most peaks to increase while the reverse happened for from 30% to 40% ACN with no significant improvement in the overall separation. The electrochromatographic behavior of peptides in the presence of an organic modifier is a complex phenomenon, and the reversed-phase retention might not be the predominant mechanism for the separation. The selectivity and

(a)



(b)



(c)

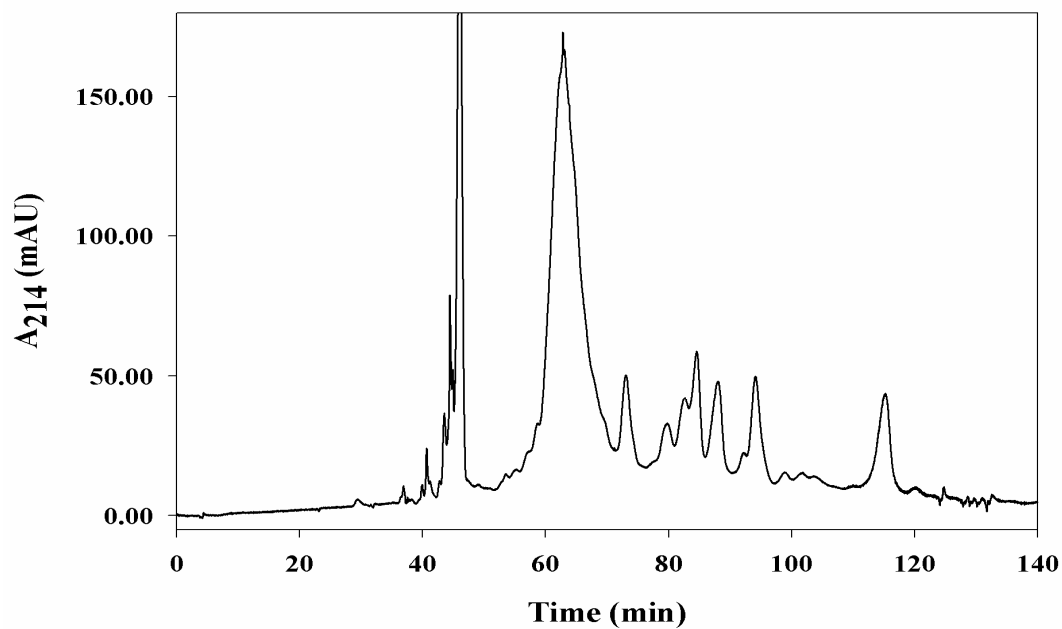


**Figure 2.** *Electrochromatogram of the tryptic digest of myoglobin. Conditions: hydro-organic mobile phase, (a) 10%, (b) 20% and (c) 40% v/v ACN, 100 mM sodium phosphate, pH 7; capillary column, 50 cm effective length, 57 cm total length x 100  $\mu$ m ID; voltage, 10 kV.*

resolution are widely altered by varying the ACN composition of the mobile phase. The optimum percent ACN for maximum resolution among the various peptides is 30% v/v.

The spectra of certain amino acids such as tyrosine, phenylalanine and tryptophan obtained by the CEC instrument diode array detector were used to assess the peptide fragments that contain such amino acid residues. Also, using the net electric charge on each fragment and the ratio of the number of hydrophobic (i.e., lipophilic, L) amino acid residues to the number of hydrophilic (water like, W) amino acid residues (L/W) in the peptide fragments would allow the tentative assignment of the nature of some of the peptide fragments on the CEC peptide map. Table 1 lists all the amino acids and their classification as either hydrophobic or hydrophilic which was used for the above calculations. The peptide fragment no. 1 which contains two tryptophan residues and has a ratio  $L/W = 1.3$  and a net negative charge of  $-1$  was tentatively identified in Fig 1c. The peptide fragment no. 3 which has a phenylalanine residue, a ratio of  $L/W = 0.84$  and a net negative charge of  $1-$  has been also tentatively identified on the CEC peptide map. Similarly, the peptide fragments no. 4 and 5 which have phenylalanine residues, a ratio of  $L/W = 0.5$  and  $1$ , and a net charge of  $0$  and  $1+$ , respectively, are indicated tentatively on the CEC peptide map. The peptide no. 17 is characterized by a net zero charge, a ratio of  $L/W = 1.5$  and a phenylalanine residue is shown in Fig 1c. Using the same approach, the peptide fragment no. 16, which has one tyrosine and phenylalanine residue, a net positive charge of  $1+$ , and a ratio  $L/W = 1.4$  is tentatively indicated on the CEC peptide map. The fragments 9, 11 and 12, which are the free lysine amino acid resulting of the myoglobin tryptic digest, eluted first on the map as a single peak. Fragments 14 and 20, which are dipeptides with lysine residue in their structures are very hydrophilic ( $L/W = 0$ ) with a net positive charge of  $2+$  and  $1+$ , respectively, are eluted around the free lysine peak.

Case of Cytochrome C. Cytochrome C from bovine heart was selected as another model protein, with 105 amino acid residues and a mass of about 12 kDa [25, 30, 31]. The tryptic digest of cytochrome C yields 6 free lysine, 3 dipeptides, 2 tripeptides and 10 larger peptides as can be seen in Table 3. Thus, a fully resolved peptide map of cytochrome C should exhibit 16 peaks. The CEC peptide shown in Fig. 4 contains at least 14 well-resolved peaks under the same mobile phase conditions as those, which yielded the best resolution for myoglobin tryptic digest. Thus, it seems that a mobile phase consisting of 100 mM sodium phosphate, pH 7, at 30% ACN is a mobile phase that offers the optimal CEC peptide map for non-glycosylated and simple proteins such as myoglobin and cytochrome C.

Following the same evaluation of the spectra of the various fragments and relying on their net charges and L/W ratios, one can tentatively identify the various fragments on the peptide map shown in Fig. 3. The peptide fragments 14 and 19 having each a tyrosine residue and possessing a net charge of 1+ and 1-, respectively, and the same L/W ratio of 1 can be indicated as shown on the peptide map. Peptide fragment no. 12 has one tryptophan residue and one tyrosine residue, an L/W = 0.78, and a net negative charge of 3-. It is assigned tentatively on the map at elution time of ~ 50 min. Peptide fragments 4, 8 and 15 each have one phenylalanine residue and net positive charges of 1+, 2+ and 1+, respectively, and L/W ratios of 1.5, 1.75 and 6, respectively, are designated on the peptide map. Peptide fragment no. 10 has one phenylalanine residue and one tyrosine residue with a zero net charge and an L/W ratio of 0.86 appears tentatively at ~65 min on the peptide map. The free lysine amino acid, which corresponds to fragments

**Table 3.** Amino acid sequence and tryptic fragments of cytochrome C as well as the net charge and L/W ratio of the various peptide fragments [30]

No	Fragment	Sequence	L/W	Net charge
1	1-6	MGDVEK	1	1-
2	7-8	GK	1	1+
3	9-9	K	0	1+
4	10-14	IFVQK	1.5	1+
5	15-23	CAQCHTVEK	0.29	1+
6	24-26	GGK	2	1+
7	27-28	HK	0	2+
8	29-39	TGPNLHGLFGR	1.75	2+
9	40-40	K	0	1+
10	41-54	TGQAPGFSYTDANK	0.86	0
11	55-56	NK	1	1+
12	57-73	GITWGEETLMEYLENPK	1	3-
13	74-74	K	0	1+
14	75-80	YIPGTK	1	1+
15	81-87	MIFAGIK	6	1+
16	88-88	K	0	1+
17	89-89	K	0	1+
18	90-92	GER	0	0.5
19	93-100	EDLIAYLK	1	1-
20	101-101	K	0	1+
21	102-105	ATNE	0.33	0

3, 9, 13, 16, 17 and 20, is also identified on the map as they coincide with the peak of the standard lysine. Peptide fragments 2, 7 and 11 are dipeptides containing lysine. They are labeled on the electrochromatogram in Fig. 3.

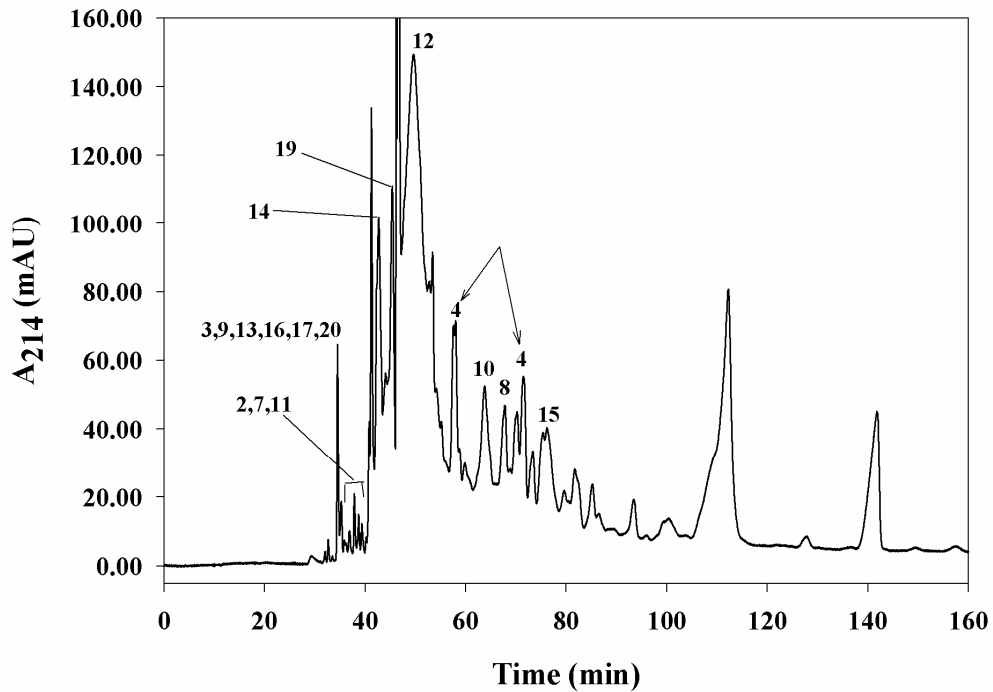


**Figure 3.** *Electrochromatogram of the tryptic digest of cytochrome C. Conditions: hydro-organic mobile phase, 30 % v/v ACN, 100 mM sodium phosphate, pH 7; capillary column, 50 cm effective length, 57 cm total length x 100  $\mu$ m ID; voltage, 10 kV.*



### CEC Peptide Mapping of Glycoproteins

Case of AGP. AGP has high carbohydrate content (the highest in plasma proteins), a very acidic pI due to the high sialylation of the glycans chains (12%) and a mass of 42 kDa. It has 183 amino acid residues and five glycosylation sites at Asn-15, Asn-38, Asn-54, Asn-75 and Asn-85 in the *N*-terminal [25, 32, 33]. The tryptic digestion of AGP yields two free lysine and 20 peptide fragments of varying lengths, see Table 4. The peptide map obtained under optimal mobile phase conditions (Fig. 4) yields more peptide peaks due to the different glycoforms arising from the heterogeneity of the glycosylation sites. The variation in the terminal sialic acid causes charge heterogeneity in the glycopeptide fragments cleaved at the same location by trypsin, the differences in the extent of glycosylation among a population of the protein molecules lead to fragments having the same peptide backbone but with or without carbohydrate chains and the variation in the nature of the oligosaccharide chains at each glycosylation site yields several glycopeptides that have the same peptide backbone, but different in their oligosaccharide structures. This observation corroborates earlier finding by Nashabeh and El Rassi in capillary electrophoresis of the tryptic digest of human AGP [34].

Returning to Fig. 4 one can draw the conclusion that the optimal conditions established for non-glycosylated proteins (e.g., cytochrome C and myoglobin) are also suitable for glycosylated proteins such as AGP. In order to assess the most suitable peptide mapping conditions, octyl sulfate a potential ion-pairing agent was added to the mobile phase containing 40 mM sodium phosphate, pH 7.0, with and without organic modifier. The amount of octyl sulfate was also fixed at 100 mM while the percent ACN

**Table 4.** Amino acid sequence and tryptic peptide fragments of AGP as well as the net charge and L/W ratio of the various peptide fragments [33]. N\* indicates the glycosylation site(s).

No	Fragment	Sequence	L/W	Net charge
1	1-24	EIPLCANLVPVPITN*ATLDQITGK	1.4	1-
2	25-33	WFYIASAFR	2	1+
3	34-39	NEEYN*K	0	1-
4	40-55	SVQEIQATFFYFTPN*K	0.88	0
5	56-63	TEDTIFLR	0.75	1-
6	64-68	EYQTR	0	0
7	69-83	QDQCIYN*TTYLNVQR	0.25	0
8	84-90	EN*GTISR	0.4	0
9	91-105	YVGGQEHFHLLILR	0.56	2+
10	106-108	DTK	0	0
11	109-120	TYMLAFDVNDEK	0.71	2-
12	121-135	NWGLSVYADKPETTK	0.67	0
13	136-149	EQLGEFYEALDCLR	0.75	3-
14	150-152	IPK	2	1+
15	153-161	SDVVYTDWK	0.5	1-
16	162-162	K	0	1+
17	163-164	DK	0	0
18	165-170	CEPLEK	0.5	1-
19	171-174	QHEK	0	1+
20	175-176	ER	0	0
21	177-177	K	0	1+
22	178-183	QEEGES	0.2	2-

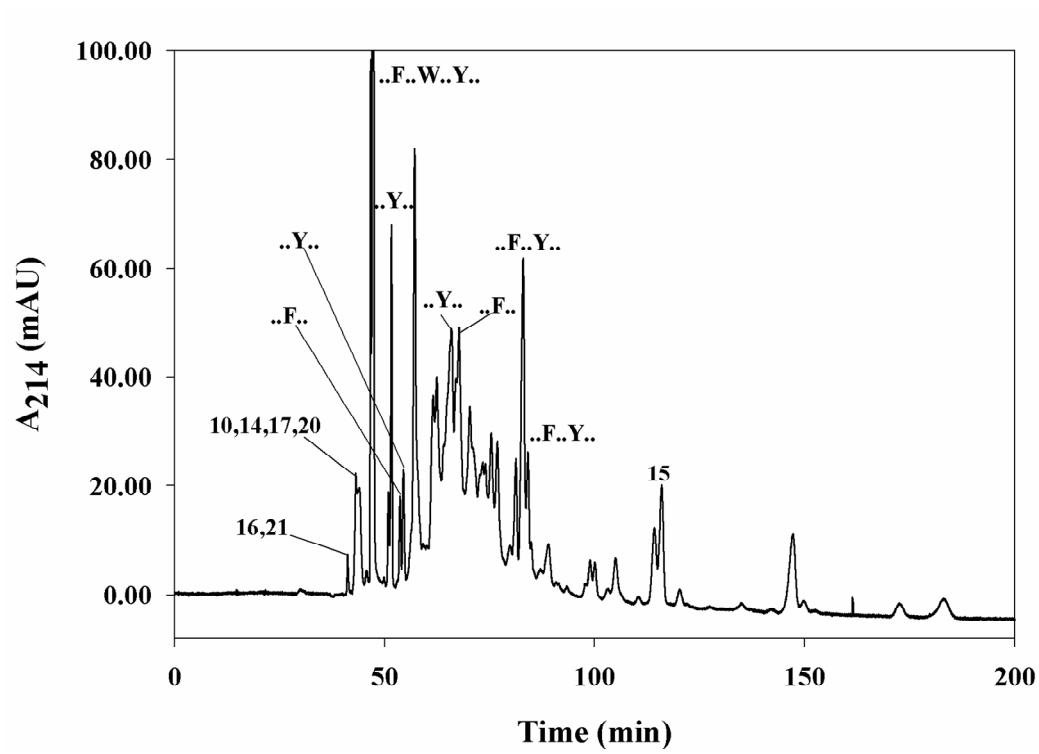
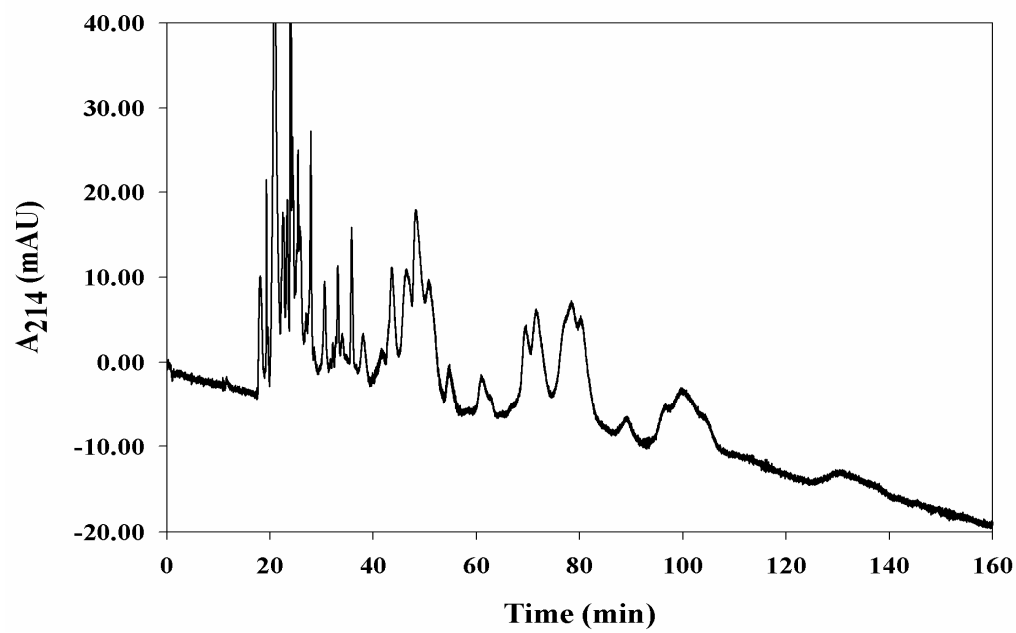


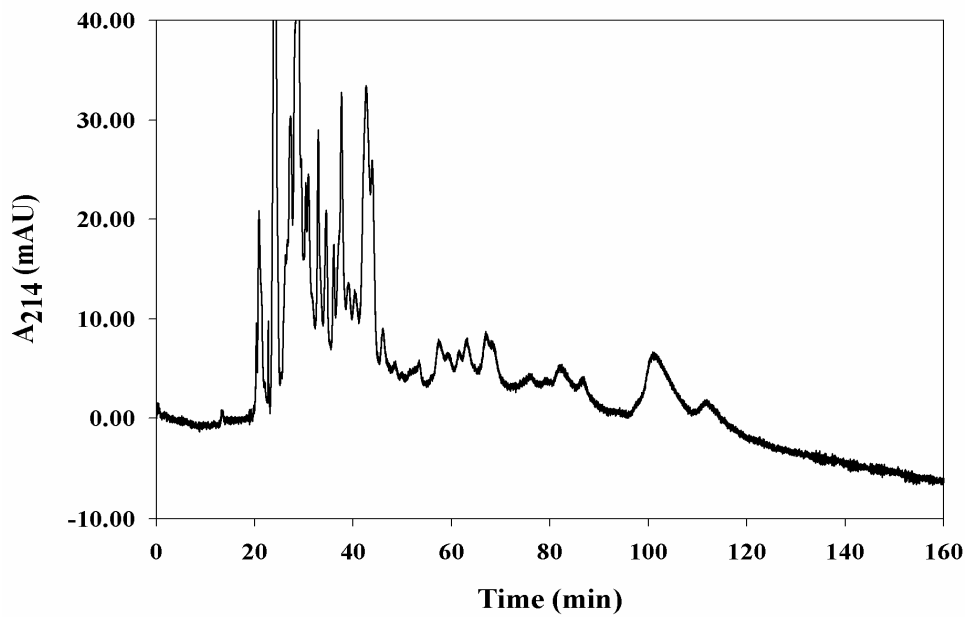
**Figure 4.** *Electrochromatogram of the tryptic digest of AGP. Conditions as in Fig.3.*

was varied from 0 to 20% (v/v). As can be seen in Fig. 5, the addition of octyl sulfate served as an eluting agent for the peptides. Besides peptide fragments 2, 9 and 19, which have a net positive charge due to the presence of the histidine and arginine residues, all other fragments have either a net negative charge (e.g., peptide fragments 1, 3, 5, 11, 13, 15, 18 and 22) or a net zero charge (e.g., peptide fragments 4, 6, 7, 8, 10, 12, 17 and 20). Glycosylated fragments such as 4, 7 and 8 would have a net negative charge because of the sialylation of their sugar chains. The negatively charged octyl sulfate would coat the surface of the C17 monolith, thus transforming it to a cation exchanger. Also, the octyl sulfate can form an ion pair with the peptides having net positive charges. The coating of the surface of the C17 monolith with octyl sulfate would make it repulsive for the binding of the peptide fragments with net negative charges, and in turn allow them to separate via their differential migration under the influence of the applied electric field. For the peptides of zero net charge, the octyl sulfate would serve as an organic modifier thus allowing their elution from the columns and consequently their differential migration due to differences in their partitioning between the stationary phase and the mobile phase. For the peptide fragments of net positive charge, both ion-pair formation in the mobile phase as well as ion exchange mechanism and differences in charge-to-mass ratio would be the parameters that control their differential migration. Increasing the amount of ACN in the mobile phase yielded a decrease in the retention and resolution among the various peptide fragments. Thus, a neat aqueous mobile phase consisting of 40 mM sodium phosphate, 100 mM octyl sulfate, pH 7.0, seems to be the best mobile phase composition for peptide mapping. The only drawback of including octyl sulfate is the broadening of

(a)



(b)



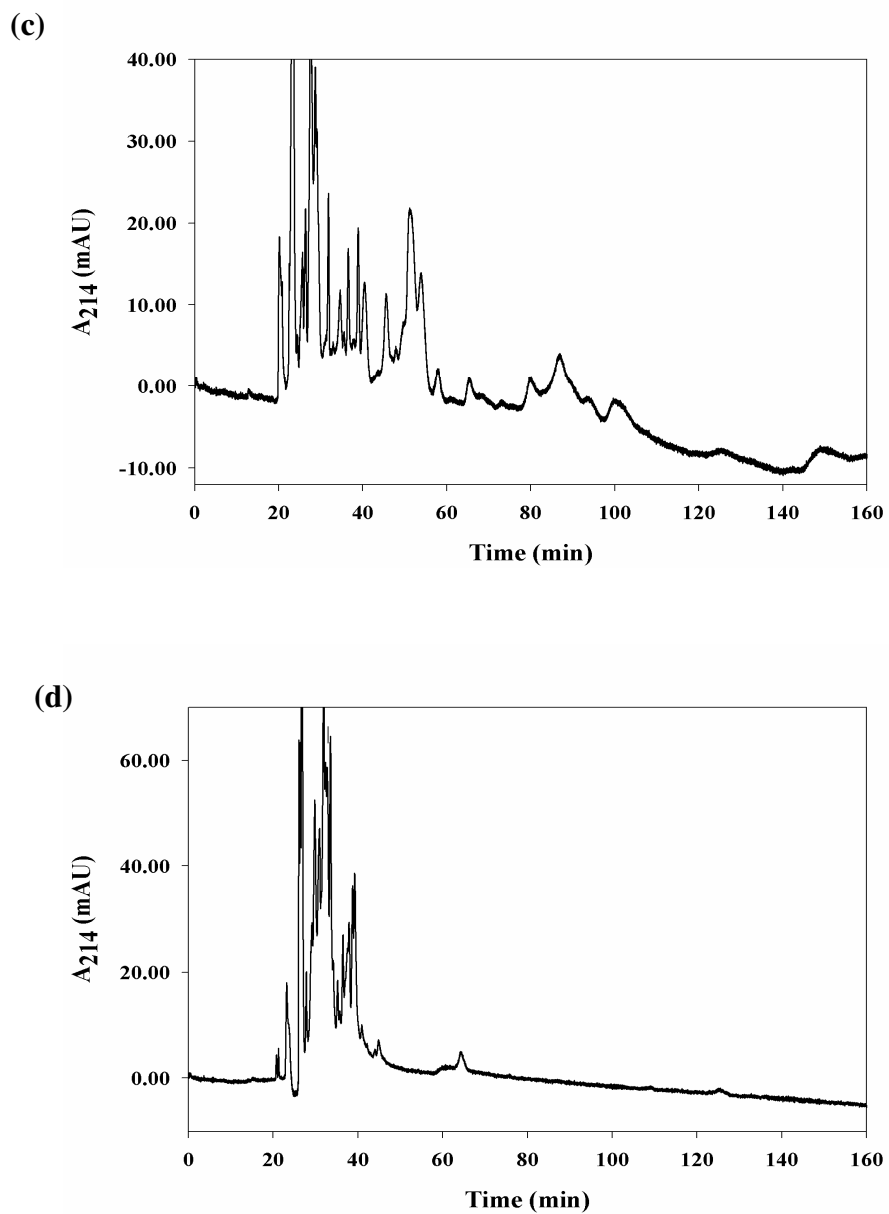


**Figure 5.** *Electrochromatograms of the tryptic digest of AGP. Conditions: hydro-organic mobile phase, (a) 0%, (b) 5%, (c) 10% and (d) 20 % v/v ACN, 40 mM sodium phosphate and 100 mM octyl sulfate, pH 7; capillary column, 50 cm effective length, 57 cm total length x 100  $\mu$ m ID; voltage, 8 kV.*

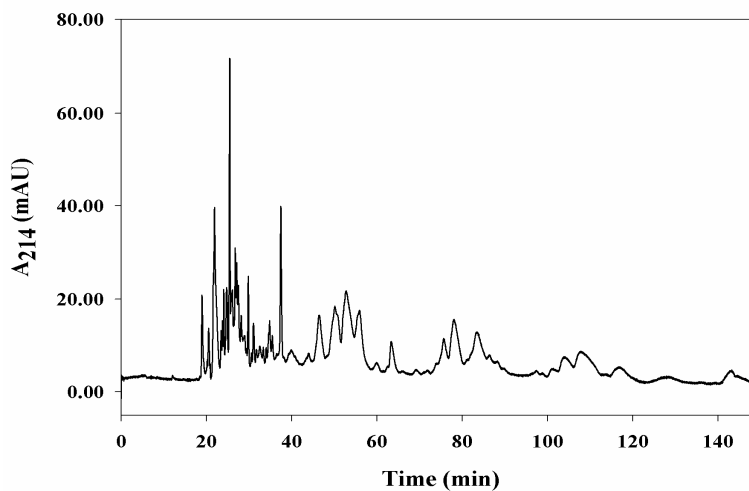


**Figure 6.** *Electrochromatogram of the tryptic digest of AGP. Conditions: 40 mM sodium phosphate and 100 mM octyl sulfate, pH 7; capillary column, 50 cm effective length, 57 cm total length x 100  $\mu$ m ID; voltage, 8 kV.*

the late eluting peak, which may have been the fragments of net positive charge (see Fig. 6). Using the same approach as for the other protein tryptic digests (i.e. DAD spectra, L/W ratio and the net charge of the peptide fragment); the identity of some peptide fragments were tentatively indicated on the peptide map, see Fig. 4. Fragments 16 and 21 are free lysine. They eluted as a single peak at about 40 min, which coincides with the retention time of the standard lysine. Fragments 2 and 4 have the amino acid residues of tryptophan, phenylalanine and tyrosine, and are designated “..F.W.Y..” on the peptide map. “..Y..” designates the peptide fragments 3, 6 and 7, which have each a tyrosine residue in their structures, while “..F..” designates the peptide fragments 5 and 9, which have a phenylalanine residue.

The designation “..F..Y..” is used to indicate the peptide fragments 11 and 13, which contain each phenylalanine and tyrosine residues. The peptide fragment 15 has the tryptophan residue, and is tentatively identified on the peptide map.

Case of Ribonuclease B. Ribonuclease B is a well-studied glycoprotein containing high mannose oligosaccharides. The peptide chain contains 150 amino acids with a nominal mass of 13.7 kDa and a single glycosylation site at Asn-60 [25, 35] The sequence and tryptic fragments are shown in Table 5. The tryptic digest yields 16 peptide fragments of varying lengths including 2 dipeptides. Besides the peptide fragments 4, 5, 9, 12 and 16, which have zero net charge, the remaining 11 peptide fragments each possess a net charge of 1+. Furthermore, the peptide fragments 1, 2, 3, 4 and 16 with L/W of 3, 4.34, 1.34, 1 and 1.23, respectively, possess some hydrophobic shade and may be more retarded than the remaining 11 fragments on the peptide map, which are relatively more hydrophilic peptides. The glycosylated peptide fragment no. 8 (a tetrapeptide) is the most hydrophilic due to its sugar moiety and has a net charge of 1+. This makes the various peptide fragments vary in size, charge and polarity over a wide range, thus yielding the observed high selectivity, see Fig. 7.

The relatively high selectivity shown in Fig 7 for the tryptic peptide map of ribonuclease B was obtained again with the mobile phase consisting of 100 mM sodium phosphate, pH 7.0 at 30% ACN. This mobile phase condition yielded superior separation capability and better peak shape than the inclusion of octyl sulfate as an ion pairing agent in the mobile phase.



**Table 5.** Amino acid sequence or fragment of ribonuclease B as well as the net charge and L/W ratio of the various peptide fragments [35]. N\* indicates the glycosylation site(s).

No	Fragment	Sequence	L/W	Net charge
1	1-4	MALK	3	1+
2	5-20	SLVLLSLLVLVLLLVR	4.33	1+
3	21-27	VQPSLGK	1.33	1+
4	28-33	ETAAAK	0	1
5	34-36	FER	0.5	0
6	37-56	QHMDSS TSAASSSNYCQMMK	0.33	1+
7	57-58	SR	0	1+
8	59-62	N*LTK	0.33	1+
9	63-66	DRCK	0	1+
10	67-86	PVNTFVHESLADVQAVCSQK	0.75	0
11	87-91	NVACK	0.66	1+
12	92-110	NGQTNCYQSYSTMSITDCR	0.3	0
13	111-116	ETGSSK	0.2	0
14	117-123	YPNCA YK	0.4	1+
15	124-129	TTQANK	0.2	1+
16	130-150	HIIVACEGNPYVPVHFDASV	1.22	0

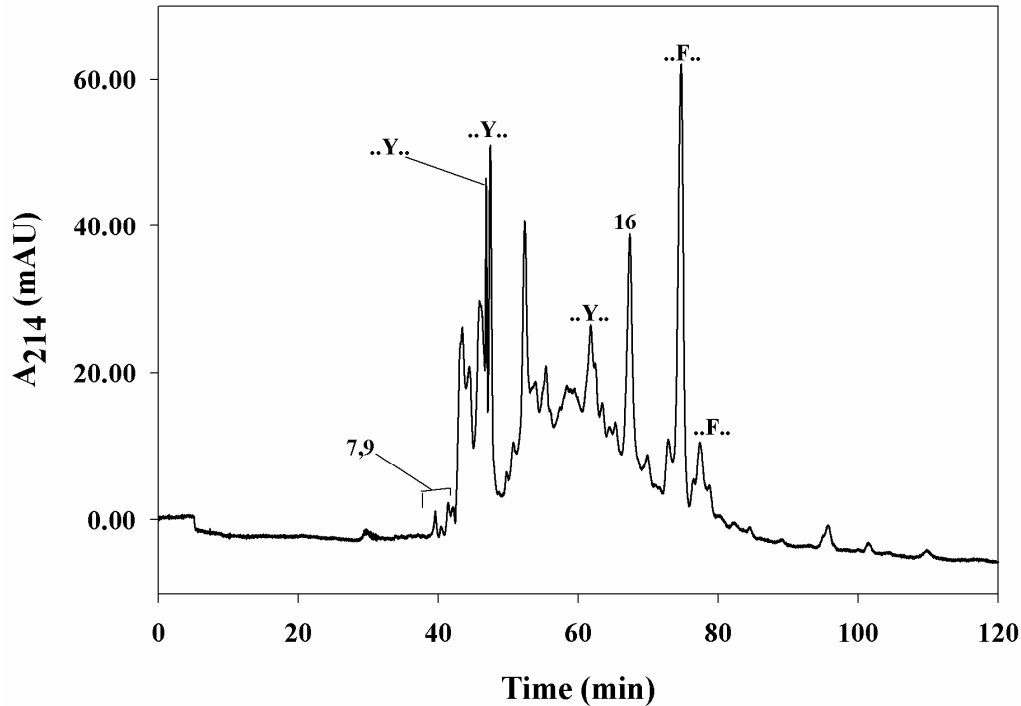


**Figure 7.** *Electrochromatogram of the tryptic digest of ribonuclease B. Conditions as in Fig.3.*

The fact that octyl sulfate caused some band broadening may be attributed to the net positive charge of most of the peptide fragments, which by virtue of their cationic nature may undergo an additional cation exchange separation mechanism with the C17 monolith that is dynamically coated with the negatively charged octyl sulfate.

Based on DAD spectral data of some amino acids, the peptide fragments 6, 12 and 14 were tentatively identified as having tyrosine residue and they are labeled “..Y..” on the map. The dipeptide fragments 7 and 9 have an arginine residue and they are identified on the peptide map. The peptide fragments 5 and 10 each have a phenylalanine

residue are labeled “..F.. “ on the peptide map. The peptide fragment 16 has both tyrosine and phenylalanine residues and is tentatively identified on the electrochromatogram, see Fig. 7.

Case of Ovalbumin. Ovalbumin with a mass of 43 kDa consists of 385 amino acid residues with two glycosylation sites at Asn-293 and Asn-312 [35]. The amino acid sequence and tryptic fragments are shown in Table 6. The digest yields one free lysine and 32 peptide fragments of varying lengths including two MK dipeptides, one IK dipeptide, and three tripeptides. An additional feature of ovalbumin is its phosphorylation [36-39]. The glycosylation and phosphorylation of ovalbumin, which introduce heterogeneity to the protein, may explain the presence of the many small peaks on the peptide map as can be seen in Fig. 8. Our results show that the peak capacity of RP-CEC is comparable if not better than that of HPLC and CE [40]

Using the spectral DAD data, the values of L/W ratio and the net charge of the peptide fragments, it was possible to tentatively identify some of the fragments on the peptide map. For instance, the peptide fragment no. 3 which has phenylalanine and tyrosine residues was assigned at a migration time of ~45 min. The designation “..F..” is used to label the peaks on the peptide map that correspond to peptide fragments that contain phenylalanine residue while the designation “..Y..” is used to label those peaks that are tyrosine containing peptide fragments. The peak designated by “..W..” is to signify a peptide fragment containing tryptophan. The tripeptides 2, 6 (zero net charge) and 17 (a 1+ net positive charge) are tentatively assigned on the peptide map in Fig. 8.

**Table 6.** Amino acid sequence or fragment of ovalbumin B as well as the net charge and L/W ratio of the various peptide fragments [35]. N\* indicates the glycosylation site(s).

No	Fragment	Sequence	L/W	Net charge
1	1-16	GSIGAASMEFCFDVFK	1.67	1-
2	17-19	ELK	0.5	0
3	20-46	VHHANENIFYCPIAIMSALAMVYLGAK	1.7	2+
4	47-50	DSTR	0	0
5	51-55	TQINK	0.25	1+
6	56-58	VVR	2	1+
7	59-61	FDK	0.5	0
8	62-84	LPGFGDSIEAQCGTSVNVHSSLR	0.92	0
9	85-104	DILNQITKPNDVYSFSLASR	0.67	0
10	105-110	LYAEER	0.5	1-
11	111-122	YPILPEYLQCVK	1.2	0
12	123-126	ELYR	0.33	0
13	127-142	GGLEPINFQTAADQAR	0.89	1-
14	143-158	ELINSWVESQTNGIIR	0.78	1-
15	159-181	NVLQPSSVDSQTAMVLVNAIVFK	1.3	0
16	182-186	GLWEK	1.5	0
17	187-189	AFK	2	1+
18	190-199	DEDTQAMPFR	0.67	2-
19	200-218	VTEQESKPVQMMYQIGLFR	0.9	0
20	219-226	VASMASEK	1	0
21	227-228	MK	1	1+
22	229-263	ILELPPASGTMSMLVLLPDEVSGLEQLESIIN FEK	1.5	5-
23	264-276	LTEWTSSNVMEER	0.44	2-
24	277-277	K	0	1+
25	278-279	IK	1	1+
26	280-284	VYLPR	1.5	1+
27	285-286	MK	1	1+
28	287-290	MEEK	0.33	1-
29	291-321	YN*LTSVLMAMGITDVFSSAN*SGISSAESL K	0.94	1-
30	322-338	ISQAVHAAHAEINEAGR	1.29	1+
31	339-358	EVVGSAAEAGVDAASVSEEFR	1.38	4-
32	359-368	ADHPFLFCIK	1.5	1+
33	369-381	HIATNAVLFGR	2	2+
34	381-385	CVSP	1	0

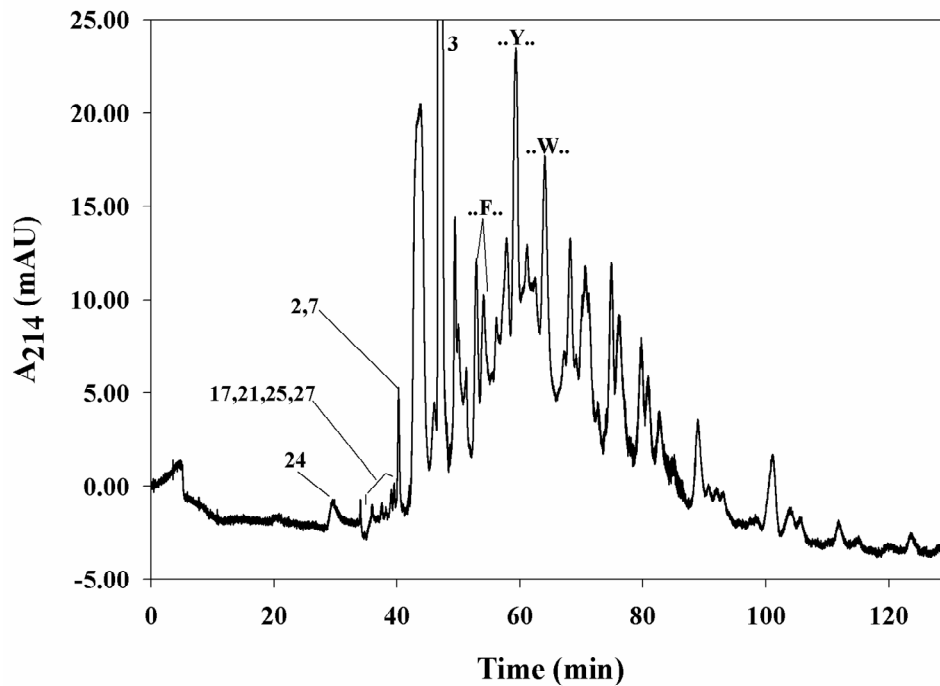


**Figure 8.** *Electrochromatogram of the tryptic digest of ovalbumin. Conditions as in Fig.3.*

The dipeptides 21, 25 and 27, which contain lysine residue are also shown on the map.

The free lysine, which eluted first, is designated on the peptide map in Fig. 8.

Unlike in the case of the AGP tryptic peptide map, the addition of octyl sulfate to the mobile phase did not yield the selectivity required to achieve the resolution among the various peptide fragments of ovalbumin. First, the trypsin digestion of ovalbumin yields 12 more peptide fragments than that of AGP (34 peptides versus 22). Second, the trypsin digestion of ovalbumin yields almost as many peptide fragments with net positive charge as the peptide fragments with net negative charge as well as the peptide fragments of zero net charge (11 positively charged peptides, 10 negatively charged peptide and 12 neutral

peptides). The addition of octyl sulfate may have obliterated the differences among the various peptide fragments such that the positively charged peptides which ion-pair with octyl sulfate will acquire similar retention to those of neutral peptides while it decreased the retention of the negatively charged peptides in commensurate way due to electrostatic repulsion from the surface coated with octyl sulfate.

Case of Transferrin. Transferrin is a glycoprotein containing 698 amino acid residues with a mass of 80 kDa, with *N*-glycosylation at Asn-413 and Asn-611 [25, 41-43]. The trypsin digestion of transferrin yields 80 fragments, 8 of which are free lysine, see Table 7. Thus the tryptic digest has 72 peptide fragments of varying lengths including 8 dipeptides and 3 tripeptides. The tryptic peptide map shown in Fig. 9 has about 50 peaks, which indicates that most of the peptide fragments are well resolved.

Using the spectra from the DAD we could infer that the peaks with designation “..W..” are the fragments with tryptophan residues. The designation “..Y..F..” on the peptide map is used to identify peptide fragments that contain tyrosine and phenylalanine residues. The labeling “..Y..” on the peptide map is to indicate peptide fragments with tyrosine residues, while the labeling with “..W..F..” is to indicate peptide fragments with tryptophan and tyrosine residues. The fragments 8, 12, 15, 46, 49, 54, 66 and 78 are a single lysine amino acid and they are eluted at ~42 min on the map. The di and tripeptides with a lysine residue are peaks 14, 29, 30, 40, 48 and 67.

**Table 7.** Amino acid sequence or fragment of transferrin as well as the net charge and L/W ratio of the various peptide fragments [42, 43, 45]. N\* indicates the glycosylation site(s).

No	Fragment	Sequence	L/W	Net charge
1	1-2	MR	1	1+
2	3-23	LAVGALLVCAVLGLCLAVPDK	4.5	0
3	24-26	TVR	0.5	1+
4	27-37	WCAVSEHEATK	0.57	0
5	38-42	CQSFR	0.25	1+
6	43-46	DHMK	0.33	1+
7	47-60	SVIPSDGPSVACVK	1.33	0
8	61-61	K	0	1+
9	62-69	ASYLDCIR	0.6	0
10	70-107	AIAANEADAVTLDAGLVYDAYLAPN NLKPVVAEFYGSK	1.47	3-
11	108-121	EDPQTFYYAVAVVK	1	1-
12	122-122	K	0	1+
13	123-132	DSGFQMNQLR	0.67	0
14	133-134	GK	1	1+
15	135-135	K	0	1+
16	136-143	SCHTAVGR	0.6	2+
17	144-162	SAGWNIPIGLLYCDLPEPR	1.71	1-
18	163-167	KPLEK	0.67	1+
19	168-212	AVANFFSGSCAPCADGTDFPQLCQLC PGCGCSTLNQYFGTSGAFK	1.09	1-
20	213-215	CLK	0.5	1+
21	216-225	DGAGDVAFVK	2.67	1-
22	226-236	HSTIFENLANK	0.57	1+
23	237-239	ADR	0.5	0
24	240-251	DQYELLCLDNTR	0.33	2+
25	252-258	KPVDEYK	0.4	0
26	259-273	DCHLAEVPSHTVVAR	1	1+
27	274-278	SMGGK	1.5	1+
28	279-295	EDLIWELLNQAQEHFGK	0.87	2-
29	296-297	DK	0	0
30	298-299	SK	0	1+
31	300-310	EFQLFSSPHGK	0.83	1+
32	311-315	DLLFK	1.5	0
33	316-323	DSAHGFLK	1	1+
34	324-327	VPPR	3	1+
35	328-331	MDAK	1	0

36	332-343	MYLGYEYVTAIR	1	0
37	344-346	NLR	0.5	1+
38	347-362	EGTCPEAPTDECK	0.67	2-
39	363-371	WCALSHHER	0.5	2+
40	372-373	LK	0	2+
41	374-384	CDEWSVSDVGK	0.57	1-
42	385-399	IECVSAETTEDCIAK	0.5	3-
43	400-420	IMNGEADAMSLDGGFVYIAGK	2	2-
44	421-433	CGLVPVLAE*NYMK	1.17	0
45	434-452	SDNCEDTPEAGYFAVAVVK	1	3-
46	453-453	K	0	1+
47	454-464	SASDLTWDNLK	0.57	1-
48	465-466	GK	1	1+
49	467-467	K	0	1+
50	468-475	SCHTAVGR	0.6	2+
51	476-489	TAGWNIPMGLLYNK	2.25	1+
52	490-494	INHCR	0.25	2+
53	495-508	FDEFFSEGCAPGSK	1	2-
54	509-509	K	0	1+
55	510-515	DSSLCK	0.2	0
56	516-530	LCMGSGNLNCEPNNK	0.88	0
57	531-541	EGYYGYTGAFR	0.83	0
58	542-546	CLVEK	0.67	0
59	547-553	GDVAFVK	2.5	0
60	554-564	HQTVTQNPGGK	0.57	1+
61	565-571	NPDPWAK	1.33	0
62	572-576	NLNEK	0.25	0
63	577-587	DYELLCLDGTR	0.57	1-
64	588-600	KPVQEYANCHLAR	0.63	2+
65	601-609	APNHAVVTR	1.25	2+
66	610-610	K	0	1+
67	611-612	DK	0	0
68	613-618	EACVHK	0.5	1+
69	619-621	ILR	2	1+
70	622-642	QQHLFGS*NVTDCSGNFCLFR	0.62	1+
71	643-646	SETK	0	0
72	647-651	DLLFR	1.5	0
73	652-659	DDTVCLAK	0.6	1-
74	660-663	LHDR	0.33	1+
75	664-668	NTYEK	0	0
76	669-676	YLGQEYVK	0.6	1-
77	677-682	AVGNLR	2	1+
78	683-683	K	0	1+
79	684-696	CSTSSLLEACTFR	0.44	0
80	697-698	RP	1	1+



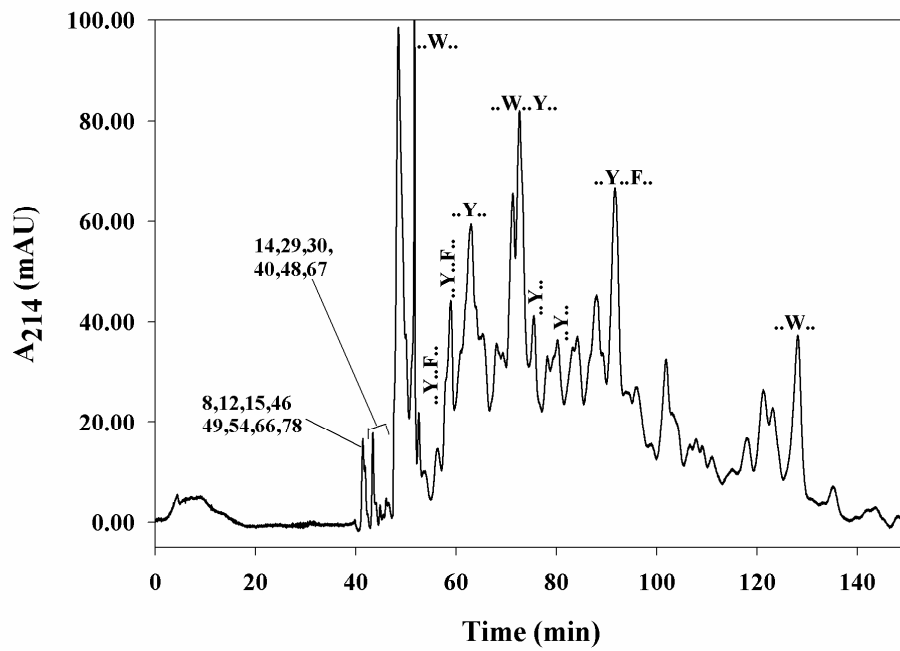


**Figure 9.** *Electrochromatogram of the tryptic digest of transferrin. Conditions as in Fig.3.*

## Conclusions

In this chapter, the use of neutral C17 monolith at neutral pH has been further exploited in the tryptic peptide mapping of standard proteins including glycosylated proteins. Independent of the nature of the protein and its size, the best mobile phase conditions to achieve the maximum resolution for the peptide fingerprint prove to be 100 mM sodium phosphate, pH 7.0 at 30% (v/v) ACN. The relatively high ionic strength of the mobile phase was necessary to affect the maximum charge screening of the peptide fragments and bring about their separation by RP-CEC. Although the addition of an ion-pairing agent to the mobile phase helped in modulating retention and selectivity in some cases by superimposing an ion-pair and an ion exchange separation mechanisms, some of the peptide fragments yielded broad peaks, a phenomenon that decreased resolution among the strongly retained peptide fragments.

## References

- (1) Zhang, M., El Rassi, Z. *Electrophoresis* **1998**, *19*, 2068-2072.
- (2) Zhang, M., El Rassi, Z. *Electrophoresis* **2000**, *21*, 3135-3140.
- (3) Allen, D., El Rassi, Z. *Analyst* **2003**, *128*, 1249-1256.
- (4) Bedair, M., El Rassi, Z. *Electrophoresis* **2002**, *23*, 2938-2948.
- (5) Bedair, M., El Rassi, Z. *J. Chromatogr. A* **2003**, *1013*, 35-45.
- (6) Zhang, S., Huang, X., Zhang, J., Horvath, C. *J. Chromatogr. A* **2000**, *887*, 465-477.
- (7) Zhang, S., Zhang, J., Horvath, C. *J. Chromatogr. A* **2001**, *914*, 189-200.
- (8) Walhagen, K., Unger, K. K., Olsson, A. M., Hearn, M. T. W. *J. Chromatogr. A* **1999**, *853*, 263-275.
- (9) Walhagen, K., Unger, K. K., Hearn, M. T. W. *Anal. Chem.* **2001**, *73*, 4924-4936.
- (10) Progent, F., Taverna, M. *J. Chromatogr. A* **2004**, *1052*, 181-189.
- (11) Hoegger, D., Freitag, R. *J. Chromatogr. A* **2003**, *1004*, 195-208.
- (12) Szucs, V., Freitag, R. *J. Chromatogr. A* **2004**, *1044*, 201-210.
- (13) Svec, F., Deyl, Z. *Monolithic Materials*; Elsevier: Amsterdam, **2003**.
- (14) Kasicka, V. *Electrophoresis* **2003**, *24*, 4013-4046.
- (15) Kasicka, V. *Electrophoresis* **2006**, *27*, 142-175.
- (16) Bedair, M., El Rassi, Z. *Electrophoresis* **2004**, *25*, 4110-4119.
- (17) Hilder, E. F., Svec, F.; Fréchet, J. M. J. *J. Chromatogr. A* **2004**, *1044*, 3-22.
- (18) Svec, F. *J. Sep. Sci.* **2005**, *28*, 729-745.
- (19) Okanda, F. M., El Rassi, Z. *Electrophoresis* **2005**, *26*, 1988-1995.
- (20) www.promega.com, **2006**.
- (21) Matsunaga, H., Sadakane, Y., Haginaka, J. *Anal. Biochem.* **2004**, *331*, 358-363.

- (22) Mao, X., Wang, K., Du, Y., Lin, B. C. *Electrophoresis* **2003**, *24*, 3273-3278.
- (23) Wu, J. T., Huang, P., Li, M. X., Qian, M. G., Lubman, D. M. *Anal. Chem.* **1997**, *69*, 320-326.
- (24) Marie, G., Serani, L., Laprevote, O. *Anal. Chem.* **2000**, *72*, 5423-5430.
- (25) <http://ca.expasy.org/tools/peptide-mass.html>, **2006**.
- (26) Mechref, Y., Ostrander, G. K., El Rassi, Z. *J. Chromatogr. A* **1997**, *792*, 75-82.
- (27) Zhong, H., El Rassi, Z. *J. Sep. Sci.* **2006**, *29*, 2023-2030.
- (28) Porras, S. P., Riekkola, M.-L., Kenndler, E. *J. Chromatogr. A* **2001**, *905*, 259-268.
- (29) Psurek, A., Scriba, G. K. E. *Electrophoresis* **2003**, *24*, 765-773.
- (30) Hennessy, T. P., Boysen, R. I., Huber, M. I., Unger, K. K., Hearn, M. T. W. *J. Chromatogr. A* **2003**, *1009*, 15-28.
- (31) Young, P. M., Wheat, T. E. *Peptide Research* **1990**, *3*, 287-292.
- (32) Treuheit, M., Costello, C., Halsall, B. *Biochem. J.* **1992**, *283*, 105-112.
- (33) Dage, J. L., Ackermann, B. L., Halsall, H. B. *Glycobiology* **1998**, *8*, 755-760.
- (34) Nashabeh, W., El Rassi, Z. *J. Chromatogr.* **1991**, *536*, 31-42.
- (35) An, H. J., Peavy, T. R., Hedrick, J. L., Lebrilla, C. B. *Anal. Chem.* **2003**, *75*, 5628-5637.
- (36) Hunzinger, C., Schrattenholz, A., Poznanovic, S., Schwall, G. P., Stegmann, W. *J. Chromatogr. A* **2006**, *1123*, 170-181.
- (37) Nisbet, A. D., Saundry, R. H., Moir, A. J. G., Fothergill, L. A., Fothergill, J. E. *Eur. J. Biochem.* **1981**, *115*, 335-345.
- (38) Stein, P. E., Tewkesbury, D. A., Carrell, R. W. *Biochem. J.* **1989**, *262*, 103-107.

- (39) Vogel, H. J., Bridger, W. A. *Biochemistry* **1982**, *21*, 5825-5831.
- (40) Charlwood, J., Birrell, H., Bouvier, E., Langridge, J., Camilleri, P. *Anal. chem.* **2000**, *72*, 1469-1474.
- (41) Montreuil, J., Spik, G., Mazurier, J. In *Glycoproteins II*; Schachter, J. M. J. V. H., Ed.; Elsevier, **1997**, pp 203-242.
- (42) MacGillivray, R. T. A., Mendez, E., Sinha, S. K., Sutton, M. R., Lineback-Zins, J., Brew, K. *Proc. Nat. Acad. Sci., USA* **1982**, *79*, 2504-2508.
- (43) MacGillivray, R. T. A., Mendez, E., Shewale, J. G., Sinha, S. K., Lineback-Zins, J., Brew, K. *J. Biol. Chem.* **1983**, *258*, 3543-3553.
- (44) <http://www.bio.davidson.edu/courses/molbio/aatable.html>, **2006**.
- (45) Thevis, M., Loo, R. R. O., Loo, J. A. *J. Proteome Res.* **2003**, *2*, 163-172.

## CHAPTER V

# GLYCOPEPTIDES SEPARATION BY SINGLE AND TANDEM LECTIN AFFINITY MONOLITHIC CAPILLARY COLUMNS AND BY SERIAL LECTIN AFFINITY NANO LIQUID CHROMATOGRAPHY AND REVERSE-PHASE CAPILLARY ELECTROCHROMATOGRAPHY

### Introduction

In Chapter III, lectin monolithic capillary columns in various arrangements and mode of operations, i.e., single lectin columns and tandem lectin columns operated in affinity capillary electrochromatography (CEC) and/or nano liquid chromatography (nano-LC), have been introduced to the separation of glycoproteins. The investigation reported in Chapter III was very recently published in the journal *Electrophoresis* [1]. In this Chapter, the use of the lectin monolithic capillary columns is extended to the selective isolation and separation of glycopeptides derived from the tryptic digest of glycoproteins.

In this Chapter, three lectins, including lentil lectin also known as *Lens culinaris* agglutinin (LCA), *Triticum vulgare*, also known as wheat germ agglutinin (WGA) and *Ricinus communis* agglutinin-I (RCA) were immobilized on monoliths based on

poly(glycidyl methacrylate-*co*-ethylene dimethacrylate) following recently reported protocols [1-3]. LCA and WGA are known as members of the lectin family with specificity to the core portion of *N*-linked sugar chains, i.e., *N*-glycans, while RCA belongs to the family of lectins which specifically interacts with the non-reducing terminal moieties of outer chain of glycans.

As discussed in Chapter III, WGA has strong affinity for *N,N'*-diacetylchitobiose, the tetrasaccharide  $\text{GlcNAc}\beta\text{1-4Man}\beta\text{1-4GlcNAc}\beta\text{1-4GlcNAc}$  and bisected hybrid-type glycans [4, 5], see Fig. 1 in Chapter III. Also glycoconjugates with clustered sialic acid residues have strong affinity to immobilized WGA [6]. In fact, the binding of WGA to glycopeptides has been shown to decrease after treatment with neuraminidase [7], an exoglycosidase that removes sialic acids from the non-reducing terminus of glycans [8]. Oligosaccharides with poly-*N*-acetylglucosamine chains have weak affinity and are retarded by the WGA column (i.e., elute with the binding mobile phase) [4]. The specificity of a given lectin is often expressed in terms of the best monosaccharide inhibitor, i.e., hapten sugar. The hapten sugar for WGA is *N*-acetyl-D-glucosamine (GlcNAc) [4, 5, 9].

*Lens culinaris* agglutinin (LCA) on the other hand recognizes sequences containing  $\alpha$ -linked mannose residues of *N*-glycans, but *N*-acetylglucosamine residues at the reducing terminus should be in pyranose form and substitution of its C-6 hydroxyl group with fucose is required [4, 10, 11]. In addition to biantennary *N*-glycans, C-2, C-2,6 branched triantennary sugar chains with fucosylated cores bind to LCA (see Fig. 1, Chapter III) [12]. Presence of bisecting GlcNAc does not alter the affinity of an

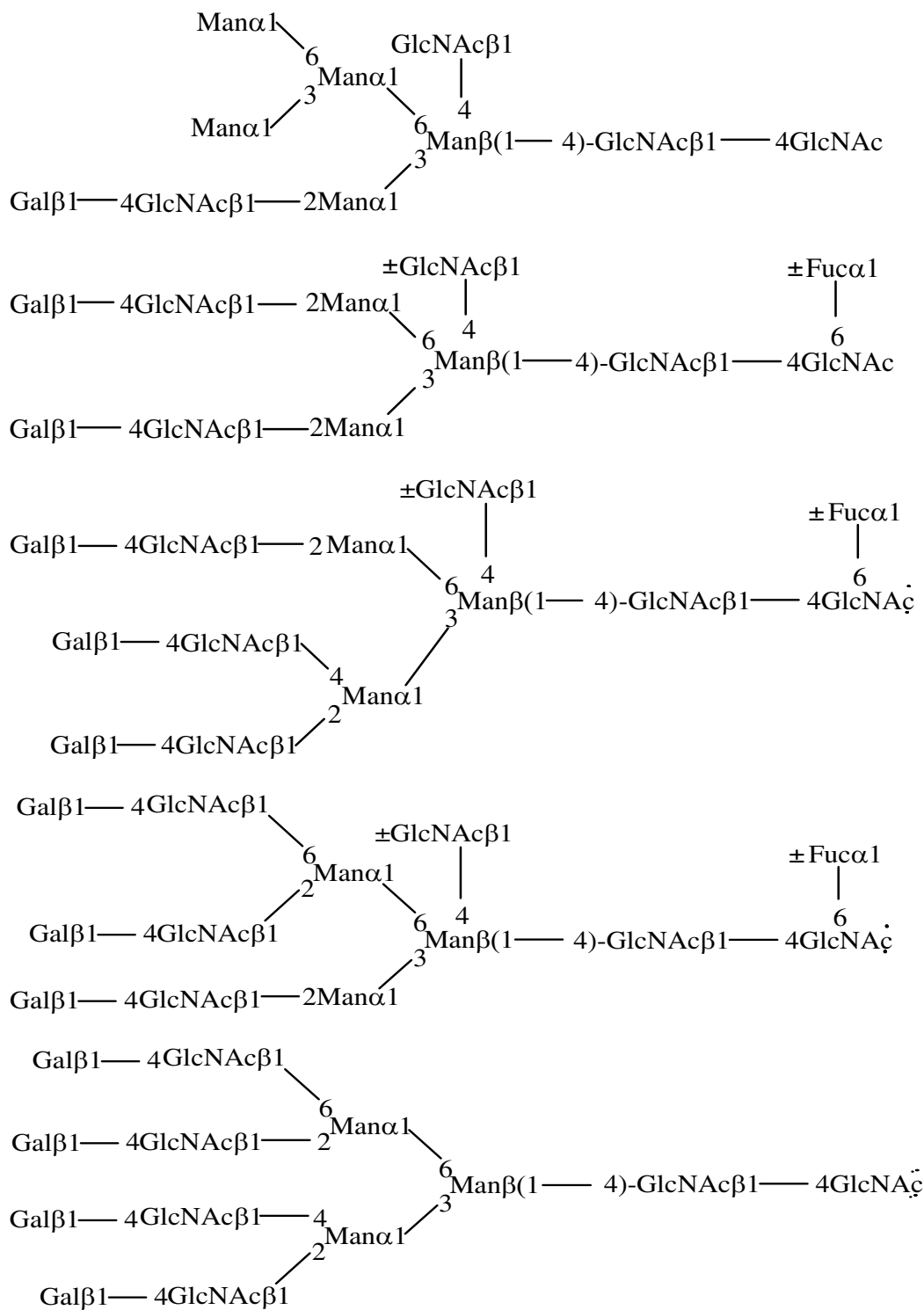


**Figure 1.** Structures exhibiting strong binding and requiring 0.1 M galactose for elution.

Specificity of RCA towards N-glycans. R = H or sugar residues; ± = present or not.



oligosaccharide [4]. By recognizing additional sugars as part of the receptor structure, LCA has a narrower specificity than WGA. For example, an  $\alpha$ -linked fucose residue attached to the *N*-acetylchitobiose portion of the core oligosaccharide markedly enhances affinity. The hapten monosaccharide for LCA is the methyl- $\alpha$ -D-mannopyranoside (Me- $\alpha$ -D-Man).

RCA interacts with oligosaccharides and glycoproteins by recognizing the  $\beta$ -galactosyl residues of *N*-glycans. The Gal $\beta$ 1 $\rightarrow$ 4GlcNAc group strongly binds to immobilized RCA, and is eluted with 10 mM lactose in Tris buffer [4]. Oligosaccharides with Gal $\beta$ 1 $\rightarrow$ 3GlcNAc or Gal $\beta$ 1 $\rightarrow$ 6 residues at their non-reducing termini are only retarded by the column. Thus, RCA interacts strongly with bisected hybrid type *N*-glycans, bisected as well as non bisected complex type *N*-glycans of the biantennary, triantennary and tetraantennary types (see Fig. 1). The hapten monosaccharide for RCA is the  $\beta$ -D-galactose (Gal).

The affinity of a given glycopeptide to a specific lectin is decided primarily by the nature of its sugar chains. Among the three lectins (i.e., LCA, RCA and WGA) studied here, RCA has a much broader selectivity than WGA and LCA towards *N*-glycans, while LCA selectivity is restricted to fucosylated complex type glycans.

## Experimental

### Instrumentation

The instrumentation used was the same as in Chapter IV.

## Reagents and Materials

Pentaerythritol diacrylate monostearate (PEDAS), ethylene glycol dimethacrylate (EDMA), glycidyl methacrylate (GMA), 2,2'-azobisisobutyronitrile (AIBN), 3-(trimethoxysilyl) propylmethacrylate, 1-dodecanol and diethylenetriamine (DETA) were from Aldrich (Milwaukee, WI, USA). Cyclohexanol and ACN (HPLC grade) were from Fisher Scientific (Fair Lawn, NJ, USA). WGA, LCA and RCA were obtained from Vector Laboratories (Burlingame, CA, USA). Human  $\alpha_1$ -acid glycoprotein (AGP), human transferrin, ovalbumin (egg albumin), human serum immunoglobulin G (IgG), GlcNAc, Me- $\alpha$ -D-Man, Gal, iodoacetamide and 2-mercaptoethanol were obtained from Sigma (St. Louis, MO, USA). Sodium phosphate monobasic was purchased from Mallinckrodt (Hazelwood, MO, USA). Sequencing grade-modified trypsin was obtained from Promega (Madison, WI, USA). Fused-silica capillaries with an internal diameter of 100  $\mu\text{m}$  and an outer diameter of 360  $\mu\text{m}$  were from Polymicro Technology (Phoenix, AZ, USA).

## Column Pretreatment

The inner wall of the fused-silica capillary was treated with 1.0 M sodium hydroxide for 30 min, flushed with 0.1 M hydrochloric acid for 30 min, and then rinsed with water for 30 min. The capillary inner wall was then allowed to react with 50% (v/v) solution of 3-(trimethoxysilyl)propylmethacrylate in acetone for 12 h to vinylize the inner wall of the capillary and lastly the capillary was rinsed thoroughly with methanol then water and dried under a stream of nitrogen.

### In situ Polymerization

In situ Polymerization for GMA Monolith. This was the same as in Chapter III

In situ Polymerization for PEDAS Monolith. This was same as in Chapters II and IV

### Immobilization of Lectins

The GMA monolith was first rinsed with water and then filled with 0.2 M H<sub>2</sub>SO<sub>4</sub> and heated at 80 °C for 3 h to hydrolyze the epoxy groups. The column was then rinsed with water followed by a freshly prepared solution of 0.1 M sodium periodate for 1 h to oxidize the ethylene glycol on the surface of the column to an aldehyde. Lectin was then immobilized to the monolithic column by pumping a solution of LCA at 4.0 mg/mL in 0.1 M sodium acetate buffer pH 6.4 containing 1 mM of CaCl<sub>2</sub>, MgCl<sub>2</sub>, MnCl<sub>2</sub>, 0.1 M Me- $\alpha$ -D-Man and 50 mM sodium cyanoborohydride through the column overnight at room temperature. WGA and RCA were immobilized using the same procedure at 5.0 mg/mL in 0.1 M sodium acetate buffer, pH 6.4, containing only 0.1 M GlcNAc and Gal, respectively, and 50 mM sodium cyanoborohydride. The resulting columns were then rinsed for 3 h at room temperature with a solution of 0.4 M Tris/HCl, pH 7.2 containing 50 mM sodium cyanoborohydride to react Tris with any unreacted aldehyde group. The column was then rinsed with water and cut to the desired length.

### Sample Preparation

The preparation of the samples of glycopeptides/peptides was done by tryptic digestion of AGP, IgG, ovalbumin and transferrin after reduction and alkylation following the Promega protocol [14]. Five milligrams of a given protein was dissolved in 100 mM  $\text{NH}_4\text{HCO}_3$  pH 8 and denatured using 6 M urea for 1 h at 37 °C. The denatured protein was further reacted with 50 mM mercaptoethanol for 1 h at 56 °C. Cysteinylyl residues in protein were subsequently alkylated with 100 mM iodoacetamide for 1 h at 37 °C. The solution was diluted with 100 mM  $\text{NH}_4\text{CO}_3$  (pH8) and 1 mM  $\text{CaCl}_2$  until the urea concentration was below 1.0 M. Lastly, 1  $\mu\text{g}/\mu\text{L}$  of modified trypsin was added and kept at 37 °C for overnight to complete the digestion of protein. Finally, 0.1% TFA was added to the digestion and sonicated in a water bath (RT) for 20 min to increase extraction and stop reaction.

### Serial Use of Lectin Column and C17 Column for Selective Capturing of Glycopeptides and Their Subsequent Separation by RP-CEC

The various lectin columns were first equilibrated with the loading (or binding) mobile phase for 30-45 min, after which the protein digests were loaded onto the column using a manually operated syringe pump. The peptides that had no affinity for the lectin (i.e., were not captured by the lectin column) were flushed out using the binding mobile phase. Meanwhile, the C17 column was equilibrated first with the running mobile phase for CEC for 30-45 min, then with the eluting mobile phase for the given lectin. The lectin column with the captured glycopeptides was then attached butt-to-butt to the C17 column (which was in the cartridge) and the eluting mobile phase for the given lectin was used to

load or transfer the captured glycopeptides onto the C17 in an offline format using the manually operated syringe pump. The lectin and the C17 monolithic columns were then disconnected and the RP-CEC run was done as described in the figure captions.

## Results and Discussion

### Single Lectin Columns

The tryptic digest of glycoproteins yields a mixture of peptides and glycopeptides where the glycopeptides can be numerous and exist in a large concentration range due to the known heterogeneity of glycoproteins, which leads to multiple glycoforms in a wide concentration range too. Therefore, an effective glycopeptide analysis by lectin affinity chromatography calls for prolonged injection time of the tryptic digest to allow the low abundance glycopeptides with affinity to the given immobilized lectin to concentrate on the lectin column with the aim of facilitating their subsequent detection.

The effectiveness of lectin monolithic capillary columns in on-line pre-concentration of dilute glycoprotein and glycan samples has been shown in recent investigations from our laboratory but not yet for glycopeptides [1-3]. In this regard, a dilute solution of human serum IgG tryptic digest that contains both glycopeptide and peptide fragments was injected into the LCA-monolith for 30 min using pressure driven flow (nano-LC). Thereafter, the column was first washed with the binding mobile phase to elute the unretained peptides and glycopeptide fragments. Following, the capillary column was eluted with the eluting mobile phase containing 0.2 M Me- $\alpha$ -D-Man as the

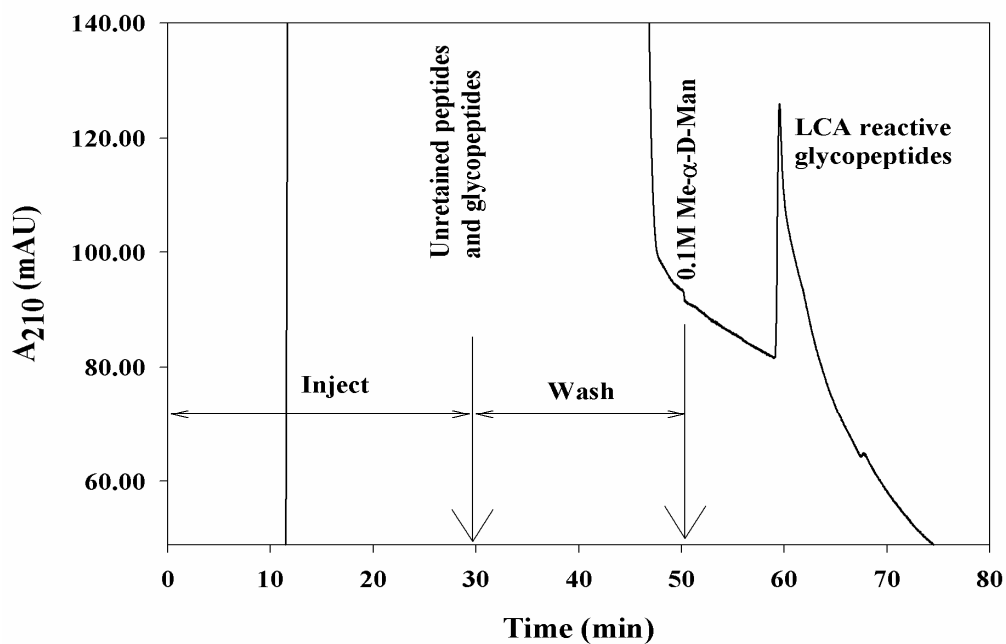


**Figure 2.** Chromatogram of IgG glycopeptides and peptides, using an LCA monolithic column, with 25 cm effective length, 33.5 cm total length x 100  $\mu\text{m}$  I.D. Binding mobile phase: 10 mM DETA, pH 6, containing 100 mM NaCl, 1 mM  $\text{CaCl}_2$ ,  $\text{MnCl}_2$  and  $\text{MgCl}_2$ ; washing mobile phase: 2.5 mM DETA, pH 6, introduced at 30 min as indicated by the arrow and eluting mobile phase: 0.2 M Me- $\alpha$ -D-Man in washing mobile phase. Pressure 10 bar and sample injection 30 min.

sugar hapten. As shown in Fig. 2, the LCA-reactive glycopeptides were eluted as a single peak. Human IgG is a glycoprotein, which is composed of two types of polypeptide chains, or major subclasses, IgG-1 and IgG-2 [15]. Each of the chains contains an Asn-linked carbohydrate chain at Asn-297. Their tryptic peptide sequences containing N-glycosylation sites are EEQYNSTYR for IgG-1 and EEQFNSTFR for IgG-2. As shown in Table 1, at least six glycopeptides can interact very strongly with immobilized LCA

due to the presence of the fucose residue at the core structure linked to GlcNAc at the reducing end.

**Table 1.** Structures of known N-glycans derived from human IgG at different degree of sialylation [15-18, 27]. *Sia* = sialic acid.

Structure	Glycosylation site
<p>Diagram illustrating the structure of an N-glycan with a core fucose. The glycan consists of a central <math>\text{Man}\beta(1-4)\text{-GlcNAc}\beta(1-4)\text{GlcNAc}(\beta 1-\text{N})\text{Asn}</math> core, which is linked to a <math>\text{GlcNAc}\beta(1-2)\text{Man}\alpha(1)</math> branch. A <math>\text{Fuc}\alpha(1)</math> residue is attached to the <math>\text{GlcNAc}\beta(1-4)</math> linkage. The glycan is attached to Asn-297.</p>	Asn-297
<p>Diagram illustrating the structure of an N-glycan with a core fucose and a galactose residue. The glycan consists of a central <math>\text{Man}\beta(1-4)\text{-GlcNAc}\beta(1-4)\text{GlcNAc}(\beta 1-\text{N})\text{Asn}</math> core, which is linked to a <math>\text{GlcNAc}\beta(1-2)\text{Man}\alpha(1)</math> branch. A <math>\text{Fuc}\alpha(1)</math> residue is attached to the <math>\text{GlcNAc}\beta(1-4)</math> linkage. A <math>\text{Gal}\beta(1-4)\text{GlcNAc}\beta(1-2)\text{Man}\alpha(1)</math> branch is attached to the central Manose. The glycan is attached to Asn-297.</p>	Asn-297
<p>Diagram illustrating the structure of an N-glycan with a core fucose and a galactose residue. The glycan consists of a central <math>\text{Man}\beta(1-4)\text{-GlcNAc}\beta(1-4)\text{GlcNAc}(\beta 1-\text{N})\text{Asn}</math> core, which is linked to a <math>\text{GlcNAc}\beta(1-2)\text{Man}\alpha(1)</math> branch. A <math>\text{Fuc}\alpha(1)</math> residue is attached to the <math>\text{GlcNAc}\beta(1-4)</math> linkage. A <math>\text{Gal}\beta(1-4)\text{GlcNAc}\beta(1-2)\text{Man}\alpha(1)</math> branch is attached to the central Manose. The glycan is attached to Asn-297.</p>	Asn-297
<p>Diagram illustrating the structure of an N-glycan with a core fucose and a galactose residue. The glycan consists of a central <math>\text{Man}\beta(1-4)\text{-GlcNAc}\beta(1-4)\text{GlcNAc}(\beta 1-\text{N})\text{Asn}</math> core, which is linked to a <math>\text{GlcNAc}\beta(1-2)\text{Man}\alpha(1)</math> branch. A <math>\text{Fuc}\alpha(1)</math> residue is attached to the <math>\text{GlcNAc}\beta(1-4)</math> linkage. A <math>\text{Gal}\beta(1-4)\text{GlcNAc}\beta(1-2)\text{Man}\alpha(1)</math> branch is attached to the central Manose. The glycan is attached to Asn-297.</p>	Asn-297
<p>Diagram illustrating the structure of an N-glycan with a core fucose and a galactose residue. The glycan consists of a central <math>\text{Man}\beta(1-4)\text{-GlcNAc}\beta(1-4)\text{GlcNAc}(\beta 1-\text{N})\text{Asn}</math> core, which is linked to a <math>\text{GlcNAc}\beta(1-2)\text{Man}\alpha(1)</math> branch. A <math>\text{Fuc}\alpha(1)</math> residue is attached to the <math>\text{GlcNAc}\beta(1-4)</math> linkage. A <math>\text{Gal}\beta(1-4)\text{GlcNAc}\beta(1-2)\text{Man}\alpha(1)</math> branch is attached to the central Manose. The glycan is attached to Asn-297.</p>	Asn-297
<p>Diagram illustrating the structure of an N-glycan with a core fucose and a galactose residue. The glycan consists of a central <math>\text{Man}\beta(1-4)\text{-GlcNAc}\beta(1-4)\text{GlcNAc}(\beta 1-\text{N})\text{Asn}</math> core, which is linked to a <math>\text{GlcNAc}\beta(1-2)\text{Man}\alpha(1)</math> branch. A <math>\text{Fuc}\alpha(1)</math> residue is attached to the <math>\text{GlcNAc}\beta(1-4)</math> linkage. A <math>\text{Gal}\beta(1-4)\text{GlcNAc}\beta(1-2)\text{Man}\alpha(1)</math> branch is attached to the central Manose. The glycan is attached to Asn-297.</p>	Asn-297

$\begin{array}{l} \text{Sia}\alpha 1\text{---}6\text{Gal}\beta 1\text{---}4\text{GlcNAc}\beta 1\text{---}2\text{Man}\alpha 1 \\ \phantom{\text{Sia}\alpha 1\text{---}6\text{Gal}\beta 1\text{---}4\text{GlcNAc}\beta 1\text{---}2\text{Man}\alpha 1} \phantom{ } \phantom{ } \phantom{ } \phantom{ } \phantom{ } \phantom{ } \phantom{ } \phantom{ } \\ \phantom{\text{Sia}\alpha 1\text{---}6\text{Gal}\beta 1\text{---}4\text{GlcNAc}\beta 1\text{---}2\text{Man}\alpha 1} \phantom{ } \phantom{ } \phantom{ } \phantom{ } \phantom{ } \phantom{ } \phantom{ } \phantom{ } \\ \text{Gal}\beta 1\text{---}4\text{GlcNAc}\beta 1\text{---}2\text{Man}\alpha 1 \end{array}$	$\begin{array}{l} \text{Fuca}1 \\   \\ 6 \\   \\ \text{Man}\beta(1\text{---}4)\text{---GlcNAc}\beta 1\text{---}4\text{GlcNAc}(\beta 1\text{---N})\text{Asn} \end{array}$	Asn-297
$\begin{array}{l} \text{Sia}\alpha 1\text{---}6\text{Gal}\beta 1\text{---}4\text{GlcNAc}\beta 1\text{---}2\text{Man}\alpha 1 \\ \phantom{\text{Sia}\alpha 1\text{---}6\text{Gal}\beta 1\text{---}4\text{GlcNAc}\beta 1\text{---}2\text{Man}\alpha 1} \phantom{ } \phantom{ } \phantom{ } \phantom{ } \phantom{ } \phantom{ } \phantom{ } \phantom{ } \\ \text{Gal}\beta 1\text{---}4\text{GlcNAc}\beta 1\text{---}2\text{Man}\alpha 1 \end{array}$	$\begin{array}{l} \text{GlcNAc}\beta 1 \\   \\ 4 \\   \\ \text{Man}\beta(1\text{---}4)\text{---GlcNAc}\beta 1\text{---}4\text{GlcNAc}(\beta 1\text{---N})\text{Asn} \end{array}$	Asn-297
$\begin{array}{l} \text{Sia}\alpha 1\text{---}6\text{Gal}\beta 1\text{---}4\text{GlcNAc}\beta 1\text{---}2\text{Man}\alpha 1 \\ \phantom{\text{Sia}\alpha 1\text{---}6\text{Gal}\beta 1\text{---}4\text{GlcNAc}\beta 1\text{---}2\text{Man}\alpha 1} \phantom{ } \phantom{ } \phantom{ } \phantom{ } \phantom{ } \phantom{ } \phantom{ } \phantom{ } \\ \text{Sia}\alpha 1\text{---}6\text{Gal}\beta 1\text{---}4\text{GlcNAc}\beta 1\text{---}2\text{Man}\alpha 1 \end{array}$	$\begin{array}{l} \text{Fuca}1 \\   \\ 6 \\   \\ \text{Man}\beta(1\text{---}4)\text{---GlcNAc}\beta 1\text{---}4\text{GlcNAc}(\beta 1\text{---N})\text{Asn} \end{array}$	Asn-297



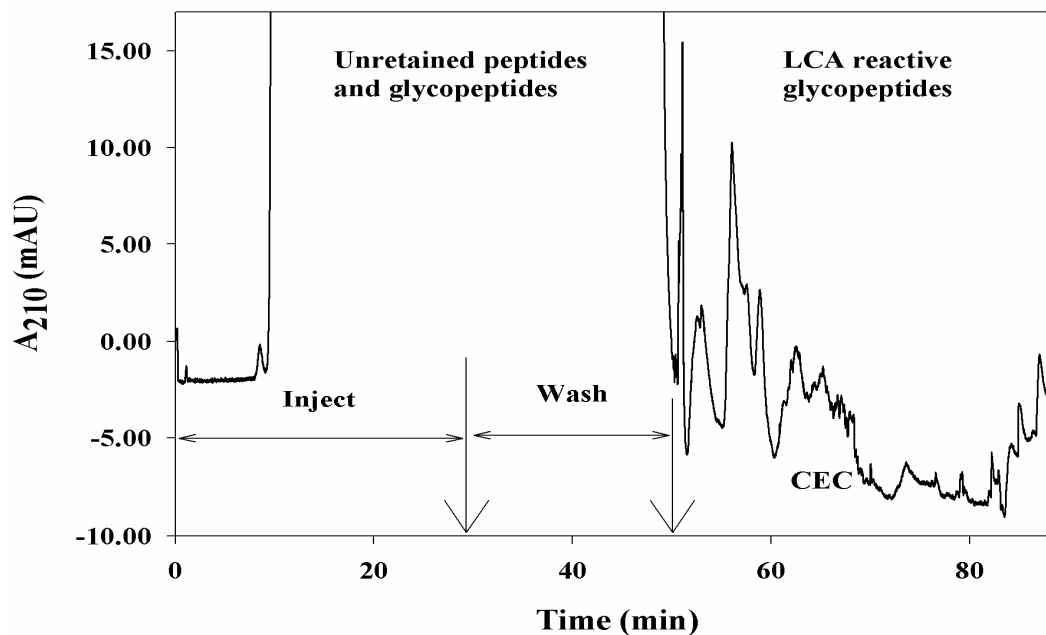


**Figure 3.** *Electrochromatogram of IgG glycopeptides and peptides obtained on and LCA monolithic column with 25 cm effective length, 33.5 cm total length x 100  $\mu$ m I.D. Binding mobile phase: 10 mM DETA, pH 6, containing 100 mM NaCl, 1 mM CaCl<sub>2</sub>, MnCl<sub>2</sub> and MgCl<sub>2</sub>; washing mobile phase: 2.5 mM DETA, pH 6 in binding mobile phase without the divalent cations, introduced at 30 min as indicated by the arrow and eluting mobile phase: 0.1M Me- $\alpha$ -D-Man in 2.5 mM phosphate buffer pH 3. Pressure 10 bar and sample injection 30 min. Voltage -20 kV.*

To demonstrate the usefulness of affinity CEC, the same tryptic digest of IgG was applied for 30 min to the LCA monolithic capillary column using pressure driven flow as above followed by a washing step for 20 min with a lower ionic strength mobile phase. The LCA reactive glycopeptides were eluted and separated by CEC using an eluting

mobile phase as shown in Fig. 3. As can be seen in Fig.3, unlike nano-LC, which gives only one peak, CEC yielded several well-separated peaks due to their differential electromigration caused by differences in charge-to-mass ratio of the glycopeptides. Structural studies of oligosaccharides of human IgG revealed that the carbohydrate chains of this glycoprotein are basically biantennary sugar chains [16, 17]. Thus, the presence or absence of two galactose, of the bisecting *N*-acetylglucosamine and of the fucose residues produce different carbohydrate chains as shown in Table 1 [18]. We believe these are the peaks that were observed in the CEC mode. The eluting mobile phase incorporated sodium monophosphate pH 3.0 to boost the EOF. As discussed in Chapter III, before running affinity CEC, a washing step by nano-LC is required in order to equilibrate the column with lower ionic strength mobile phase devoid of divalent metal cations. This washing step is done before CEC elution with the eluting mobile phase containing the sugar hapten in order to avoid high current and in turn Joule heating, which may result in the deactivation of the lectin column (i.e., loss of affinity). In the remainder of this chapter, prior to running affinity CEC, two nano-LC steps are carried out: an injection step with a high ionic strength mobile phase (the binding or loading mobile phase) followed by a second nano-LC step which involves the washing out of the high ionic strength mobile phase from the column.

Another interesting model glycoprotein for evaluating affinity CEC in the separation and isolation of glycopeptides is AGP. Figure 4 shows the affinity CEC of human AGP glycopeptides using the LCA monolithic capillary column. AGP has a high carbohydrate content (the highest in plasma proteins), very acidic pI due to the high sialylation of the glycans chains (12%) with a mass of 42 kDa. It has 183 amino acid

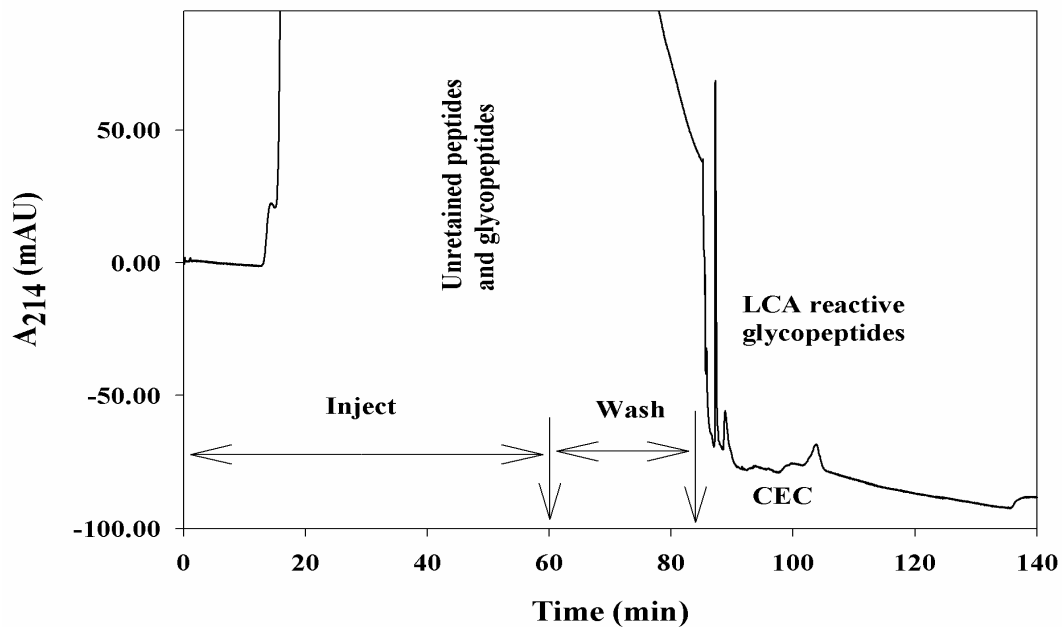


**Figure 4.** *Electrochromatogram of AGP glycopeptides and peptides obtained on and LCA monolithic column with 25 cm effective length, 33.5 cm total length x 100  $\mu\text{m}$  I.D. Binding mobile phase: 10 mM DETA, pH 6, containing 100 mM NaCl, 1 mM  $\text{CaCl}_2$ ,  $\text{MnCl}_2$  and  $\text{MgCl}_2$ ; washing mobile phase: 2.5 mM DETA, pH 6 in binding mobile phase without the divalent cations, introduced at 60 min as indicated by the arrow and eluting mobile phase: 0.1M Me- $\alpha$ -D-Man in 2.5 mM phosphate buffer pH 3. Pressure 10 bar and sample injection 60 min. Voltage -20 kV.*

residues and five glycosylation sites at Asn-15, Asn-38, Asn-54, Asn-75 and Asn-85 in the *N*-terminal as shown in Table 2 [19-21]. The glycans structures have been extensively studied and it has been shown that an individual polypeptide carries several different types of glycans structure with considerable heterogeneity at the same

**Table 2.** Structures of known *N*-glycans derived from human AGP at varying degree of sialylation [19, 20]. *Sia* = sialic acid.

Structure	Glycosylation site
<p><i>Sia</i><math>\alpha</math></p>	Asn-15, 38 or 54
<p><i>Sia</i><math>\alpha</math></p>	Asn-15, 38, 54, 75 or 85
<p><i>Sia</i><math>\alpha</math></p>	Asn-15, 54 or 85
<p><i>Sia</i><math>\alpha</math></p>	Asn-38, 75 or 85
<p><i>Sia</i><math>\alpha</math></p>	Asn-54, 75 or 85

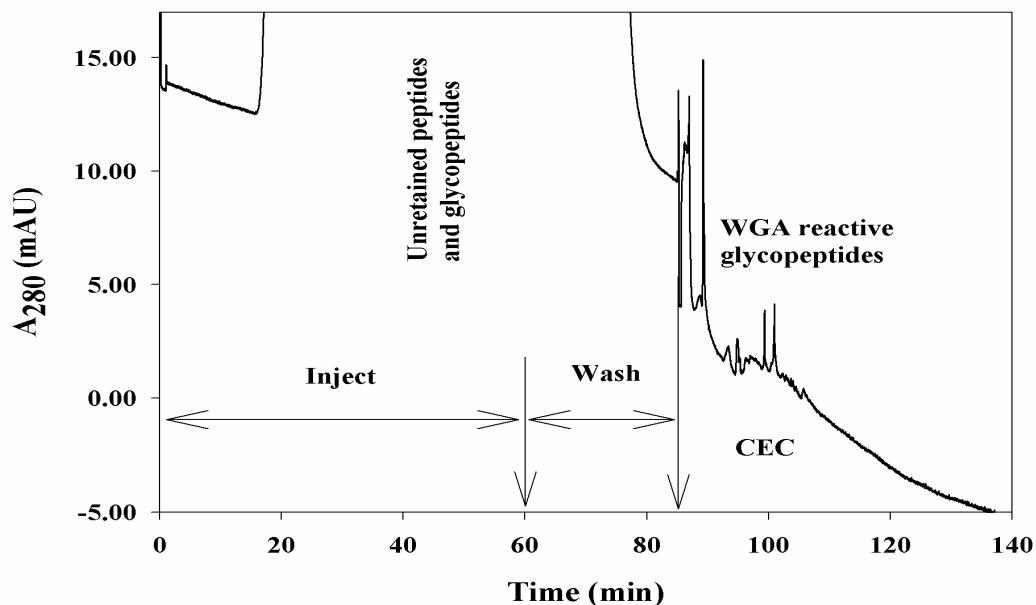


**Figure 5.** *Electrochromatogram of AGP glycopeptides and peptides obtained on and WGA monolithic column with 25 cm effective length, 33.5 cm total length x 100  $\mu$ m I.D. Binding mobile phase: 10 mM DETA, pH 6, containing 100 mM NaCl, 1 mM CaCl<sub>2</sub>, MnCl<sub>2</sub> and MgCl<sub>2</sub>; washing mobile phase: 2.5 mM DETA, pH 6 in binding mobile phase without the divalent cations, introduced at 60 min as indicated by the arrow and eluting mobile phase: 0.1M Me- $\alpha$ -D-Man in 2.5 mM phosphate buffer pH 3. Pressure 10 bar and sample injection 60 min. Voltage -20 kV.*

glycosylation site. Similar to the IgG tryptic digest, the AGP tryptic digest was injected for 60 min, followed by washing the column with the low ionic strength mobile phase for 20 min. As can be seen in Fig. 4, the CEC mode brought about the separation of the LCA

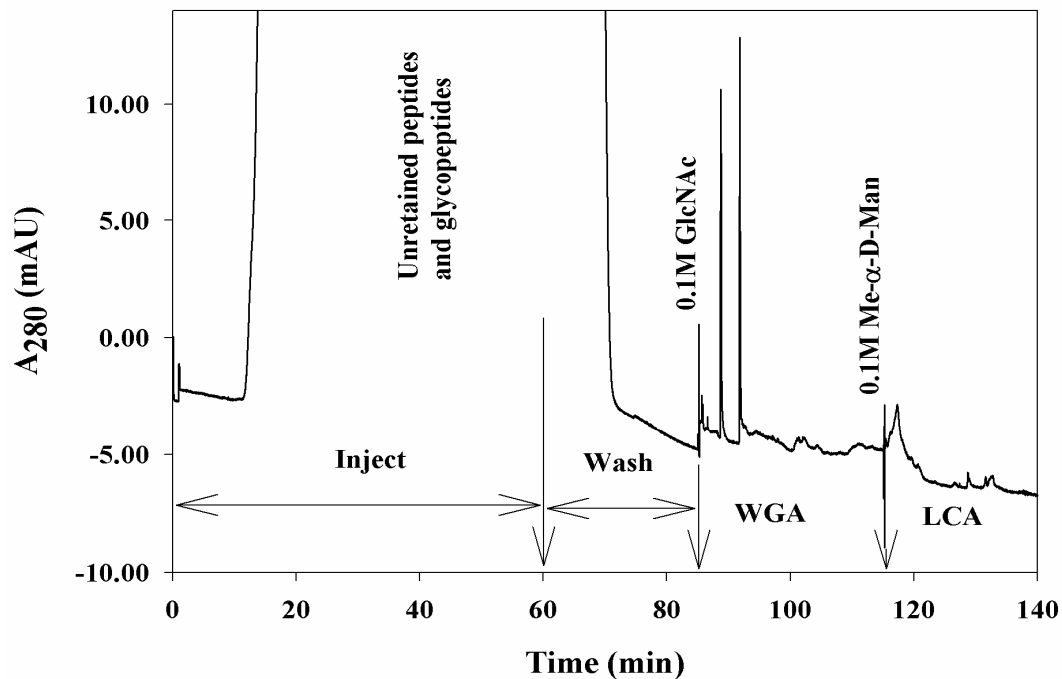
reactive glycopeptides. These reactive glycopeptide fragments are believed to carry the fucosylated glycans in their outer branches, see Table 2.

Fig. 5 shows the affinity CEC of human AGP glycopeptides using the WGA monolithic capillary column. The AGP tryptic digest was injected for 60 min, followed by washing for 20 min and then elution with a mobile phase containing the hapten sugar. As can be seen in Fig. 5, the various WGA-reactive glycopeptides were separated into different peaks. These glycopeptides are believed to correspond to those sialylated complex glycans, see Table 2.

### Tandem Lectin Columns

As shown in the above section each lectin column concentrates and separates its reactive glycopeptides. Since each lectin has its own hapten monosaccharide that can be used independently to cause the elution and separation of the captured glycopeptides, it becomes logical to couple two or more lectin columns in series (i.e., tandem lectin columns) to increase the peak capacity of lectin affinity nano-LC or CEC.

The principle of tandem lectin columns has already been shown in Chapter III in the isolation of several glycoproteins in a single run [1]. In this Chapter, the principle of tandem lectin columns is exploited and demonstrated in the isolation and separation of various glycopeptides by affinity CEC. Figure 6 shows the AGP tryptic digest injected into two lectin columns, WGA and LCA monolithic capillary columns coupled in series in the order WGA → LCA. The reactive glycopeptides yielded separate peaks for each column.



**Figure 6.** *Electrochromatogram of AGP glycopeptides and peptides obtained on and WGA→LCA monolithic column with 25 cm effective length, 33.5 cm total length x 100 μm I.D. WGA monolith occupies the first segment (12.5 cm) and is connected butt to butt using a zero dead volume Teflon tubing to LCA monolith next segment also 12.5 cm. Binding mobile phase: 10 mM DETA, pH 6, containing 100 mM NaCl, 1 mM CaCl<sub>2</sub>, MnCl<sub>2</sub> and MgCl<sub>2</sub>; washing mobile phase: 2.5 mM DETA, pH 6 in binding mobile phase without the divalent cations, introduced at 60min as indicated by the arrow and eluting mobile phase: 0.1M Me-α-D-Man and 0.1M GlcNAc in 2.5 mM phosphate buffer pH 3. Pressure 10 bar and sample injection 60 min. Voltage -20 kV.*

As discussed above and in Chapter III, affinity nano-LC yields one peak for each capillary column regardless of the number of glycopeptides in the mixture [1]. Affinity

nano-LC using tandem lectin columns could produce more peaks than the number of coupled lectin columns provided that one of the lectin columns can capture some of the glycopeptides that are also captured by other lectin columns that are coupled in series. A typical and representative example is shown in Fig. 7. In this example three lectins columns were coupled in series in the order RCA → WGA → LCA. RCA is reactive with some of the glycopeptides that also react with WGA and LCA. By eluting the tandem columns with a mobile phase containing GlcNAc the glycopeptide(s) that was reactive with the WGA column but not reactive with the RCA column or the LCA column, will be swept out thus producing one single peak. Next, eluting the coupled columns with a mobile phase containing Me- $\alpha$ -D-Man elutes those glycopeptides that were reactive with the LCA column but not with the WGA and RCA column, which explains the single peak observed (see Fig. 7). Thereafter, the tandem columns were eluted with a mobile phase containing Gal, which elutes the glycopeptides that are reactive with the RCA column. Repeating the elution with mobile phases containing GlcNAc and Me- $\alpha$ -D-Man yielded one peak for each elution step. This signifies that the glycopeptides that were captured by RCA are also reactive with the LCA and WGA columns. This example produces five different peaks for three coupled lectin columns.

#### Serial Selective Capturing of Glycopeptides by Immobilized Lectins and Their Subsequent Separation by RP-CEC

In this section, the use of serial lectin affinity nano-LC and RP-CEC for the selective capturing and separation of glycopeptides is demonstrated using the tryptic digests of three glycoproteins namely AGP, transferrin and ovalbumin. Three lectin



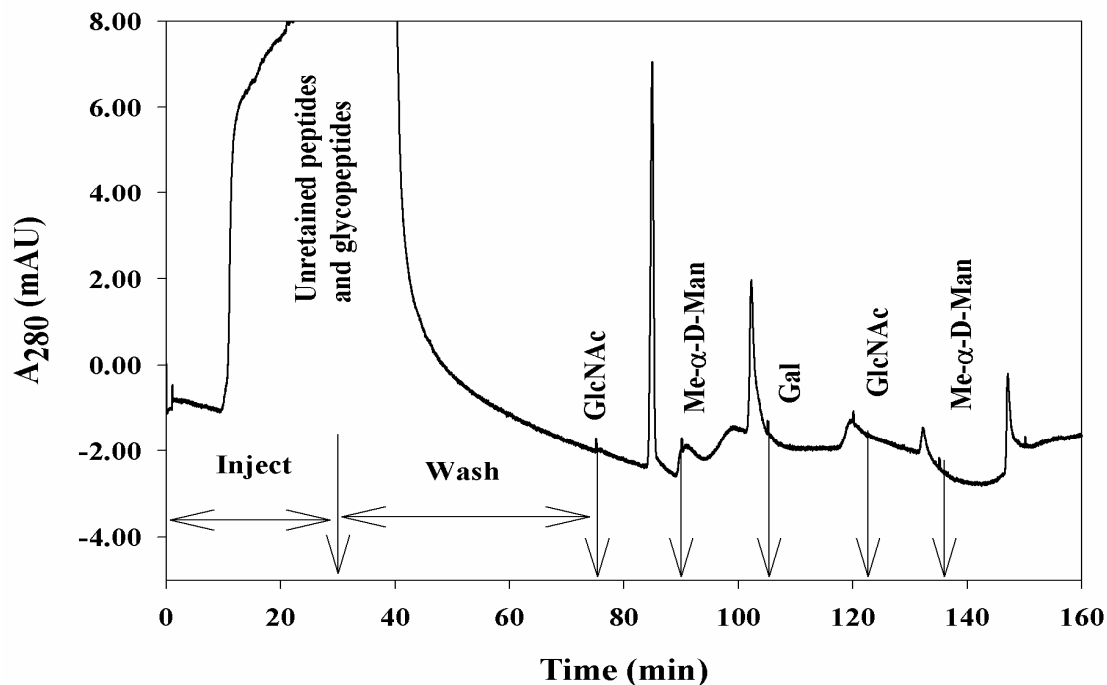


**Figure 7.** Chromatogram of AGP glycopeptides and peptides obtained on and RCA→WGA→LCA monolithic column with 25 cm effective length, 33.5 cm total length x 100 μm I.D. RCA monolith occupies the first segment (8.3 cm) and is connected butt to butt using a zero dead volume Teflon tubing to WGA monolith next segment also 8.3 cm and lastly to LCA monolith also 8.3 cm. Binding mobile phase: 10 mM DETA, pH 6, containing 100 mM NaCl, 1 mM CaCl<sub>2</sub>, MnCl<sub>2</sub> and MgCl<sub>2</sub>; washing mobile phase: 2.5 mM DETA, pH 6 in binding mobile phase without the divalent cations, introduced at 30 min as indicated by the arrow and eluting mobile phase: 0.2M Me-α-D-Man, 0.2M GlcNAc and 0.2M Gal in 2.5 mM phosphate buffer pH 3. Pressure 12 bar and sample injection 30 min.

columns, including WGA, LCA and RCA were used serially with RP-CE using a C17 monolithic column. In each case involving the use of a given lectin column for the capture of the corresponding reactive glycopeptides, the tryptic digest of a given glycoprotein was injected on the lectin column under investigation using a manually operated syringe pump followed by washing unretained peptides and glycopeptides from the lectin column. Thereafter, the lectin column was connected to the C17 monolithic column. The lectin column was then eluted with the manually operated syringe pump using the proper eluting mobile phase containing the hapten sugar of lectin. For more details about the serial lectin affinity nano-LC and RP-CEC, see Experimental.

Figure 8a, b and c show the RP-CEC of the glycopeptides of ovalbumin that are reactive with RCA, LCA and WGA, respectively. Ovalbumin with a mass of 43 kDa consists of 385 amino acid residues. It has a single glycosylation site at Asn-292 with a second potential glycosylation site at Asn-311. The N-glycans of ovalbumin shown in Table 3 [16, 21, 22] can be grouped into the high mannose type and the hybrid type, and the latter can be further divided into two categories based on the presence or absence of galactose residue at the reducing termini.[23, 24] On the basis of the reactivity of the three lectins, RCA and WGA, with their affinity to bisected hybrid *N*-glycans, are the candidate lectins to capture the glycopeptides containing these structures. Unexpectedly, the immobilized LCA shows reactivity as manifested by one major peak and two minor ones shown in Fig. 8b.

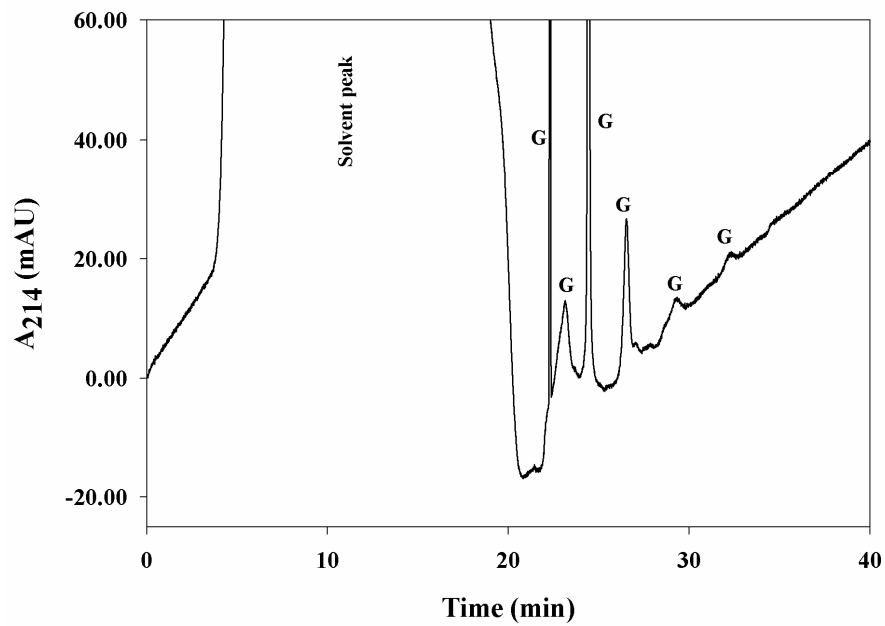
Figure 9a, b and c show the RP-CEC glycopeptide mapping of transferrin tryptic digest that are reactive with RCA, WGA and LCA, respectively. Transferrin is a glycoprotein containing 679 amino acid residues with a mass of 80 kDa. The *N*-

**Table 3.** Structures of known *N*-glycans derived from ovalbumin [28].

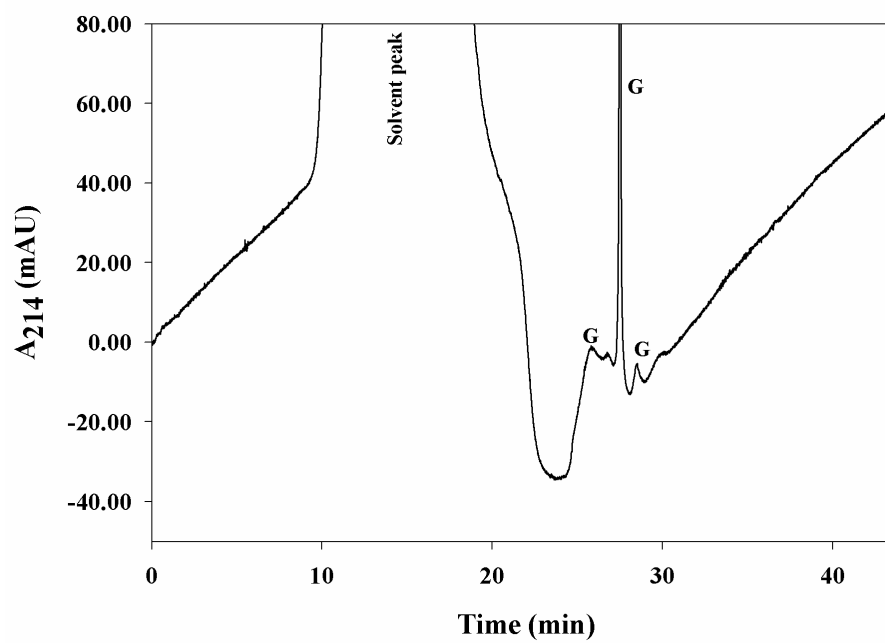
Structure	Glycosylation site
<p>Man<math>\alpha</math>1-6          Man<math>\alpha</math>1-3          Man<math>\alpha</math>1-6          Man<math>\alpha</math>1-3          Man<math>\beta</math>(1-4)-GlcNAc<math>\beta</math>1-4GlcNAc(<math>\beta</math>1-N)Asn</p>	Asn-292
<p>Man<math>\alpha</math>1-6          Man<math>\alpha</math>1-3          Man<math>\alpha</math>1-6          Man<math>\alpha</math>1-2          Man<math>\alpha</math>1-3          Man<math>\beta</math>(1-4)-GlcNAc<math>\beta</math>1-4GlcNAc(<math>\beta</math>1-N)Asn</p>	Asn-292
<p>Man<math>\alpha</math>1-6          Man<math>\alpha</math>1-3          Man<math>\alpha</math>1-6          Man<math>\alpha</math>1-2          Man<math>\alpha</math>1-6          Man<math>\beta</math>(1-4)-GlcNAc<math>\beta</math>1-4GlcNAc(<math>\beta</math>1-N)Asn</p>	Asn-292
<p>Man<math>\alpha</math>1-6          Man<math>\alpha</math>1-3          Man<math>\alpha</math>1-6          GlcNAc<math>\beta</math>1-4          Man<math>\beta</math>(1-4)-GlcNAc<math>\beta</math>1-4GlcNAc(<math>\beta</math>1-N)Asn</p>	Asn-292
<p>Man<math>\alpha</math>1-6          Man<math>\alpha</math>1-3          Man<math>\alpha</math>1-6          GlcNAc<math>\beta</math>1-4          Man<math>\alpha</math>1-2          Man<math>\beta</math>(1-4)-GlcNAc<math>\beta</math>1-4GlcNAc(<math>\beta</math>1-N)Asn</p>	Asn-292
<p>Man<math>\alpha</math>1-6          Man<math>\alpha</math>1-3          Man<math>\alpha</math>1-6          GlcNAc<math>\beta</math>1-4          Man<math>\alpha</math>1-2          Man<math>\alpha</math>1-6          Man<math>\beta</math>(1-4)-GlcNAc<math>\beta</math>1-4GlcNAc(<math>\beta</math>1-N)Asn</p>	Asn-292
<p>Man<math>\alpha</math>1-6          Man<math>\alpha</math>1-3          Man<math>\alpha</math>1-6          GlcNAc<math>\beta</math>1-4          Man<math>\alpha</math>1-2          Man<math>\alpha</math>1-3          Man<math>\alpha</math>1-6          Man<math>\alpha</math>1-6          Man<math>\beta</math>(1-4)-GlcNAc<math>\beta</math>1-4GlcNAc(<math>\beta</math>1-N)Asn</p>	Asn-292

<p>Manα1 6 3 Manα1 Manα1 GlcNAcβ1—4 Manα1 GlcNAcβ1—2 Manβ(1—4)-GlcNAcβ1—4GlcNAc(β1—N)Asn</p>	Asn-292
<p>Manα1 6 3 Manα1 Manα1 GlcNAcβ1—4 Manβ(1—4)-GlcNAcβ1—4GlcNAc(β1—N)Asn Galβ1—4GlcNAcβ1—4 Manα1 GlcNAcβ1—2</p>	Asn-292

(a)



(b)



(c)

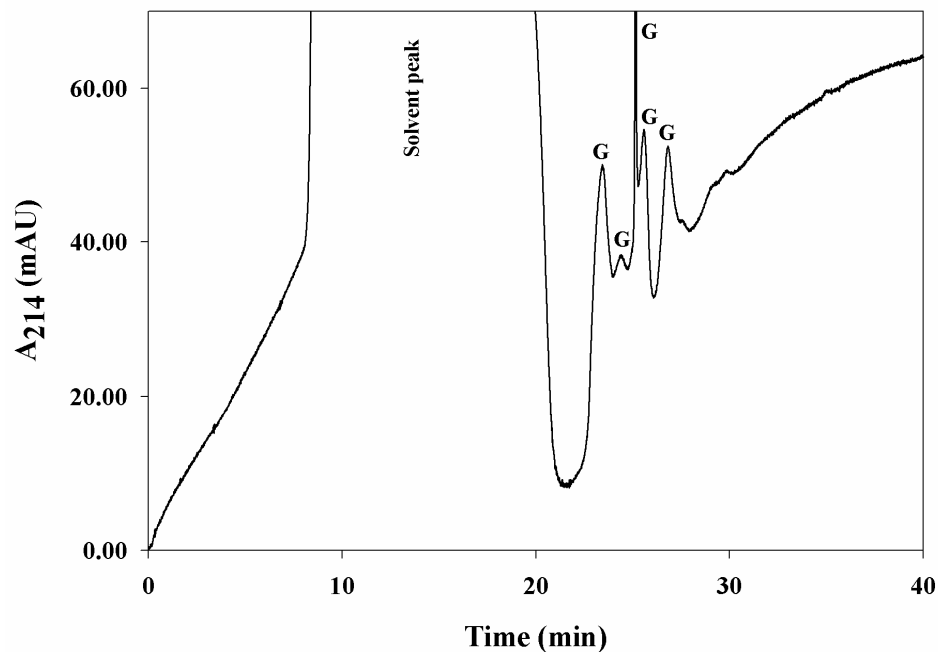
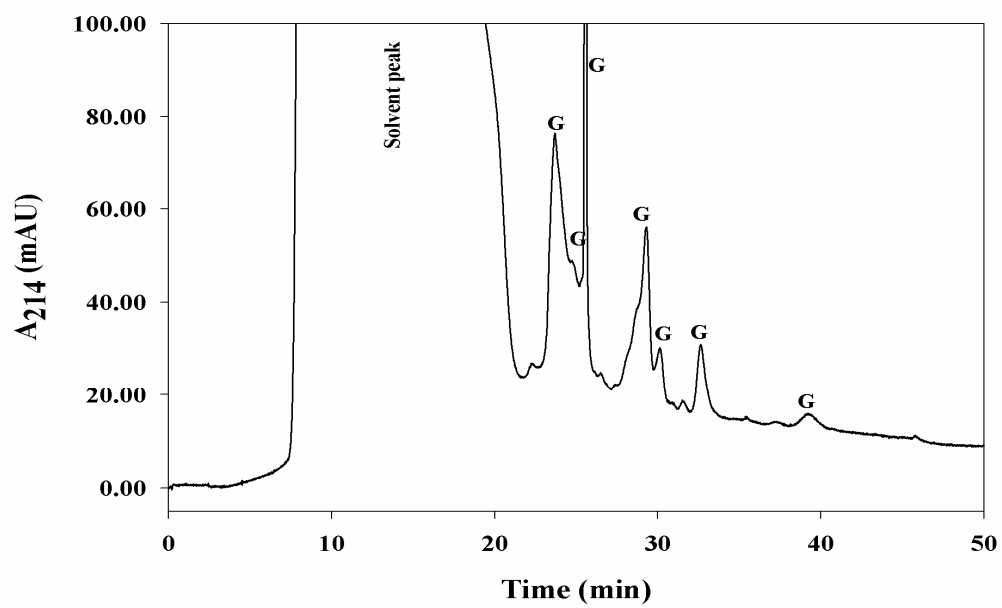


**Figure 8.** Different glycopeptides of ovalbumin on different lectin columns. (a) RCA reactive (b) LCA reactive and (c) WGA reactive. Hydroorganic mobile phase, 30% v/v ACN, 100 mM sodium phosphate, pH 7; capillary column, 50 cm effective length, 57 cm total length x 100  $\mu$ m ID; voltage, 10 kV. G, stands for glycopeptide.

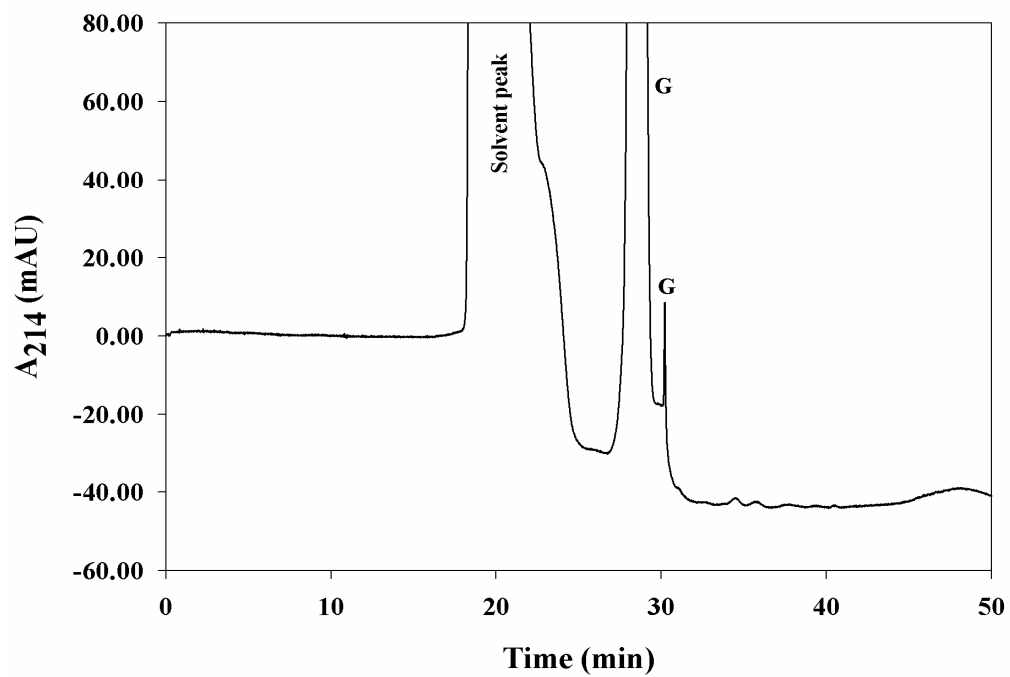
glycosylation occurs at Asn-413 and Asn-611 with varying glycan structures as shown in Table 4 [25]. It is observed that the two glycosylation sites may be occupied either by di-, tri- or tetraantennary glycans of the *N*-acetylglucosamine type or complex type [26]. All these glycans (i.e., including the di-, tri and tetraantennary glycans) show reactivity with RCA and the di-antennary with WGA. This may explain the larger number of peaks observed in Fig. 9a than in Fig. 9b, (i.e., those captured by the immobilized RCA rather



(a)



(b)





(c)

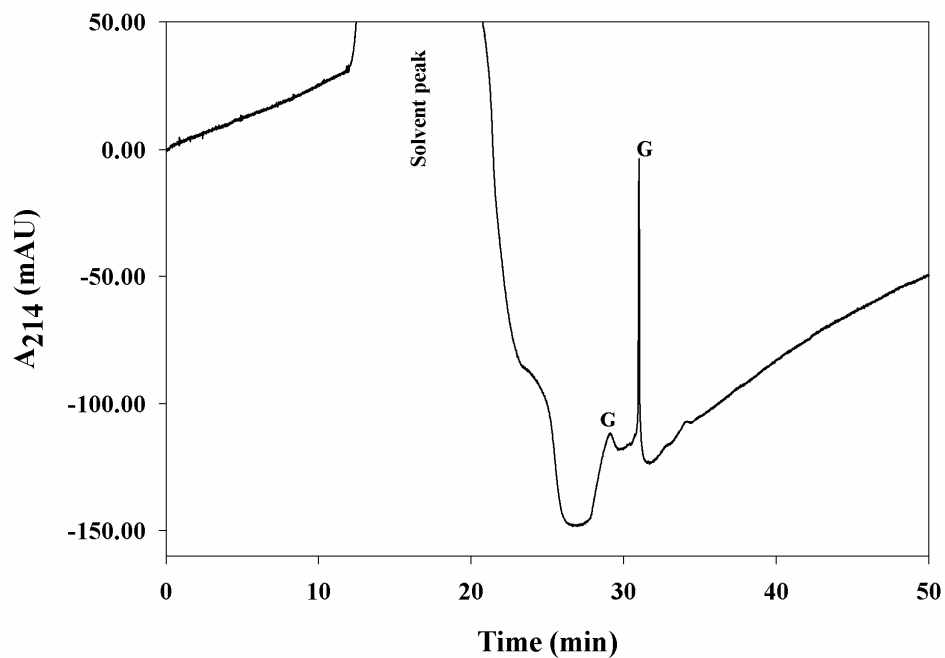
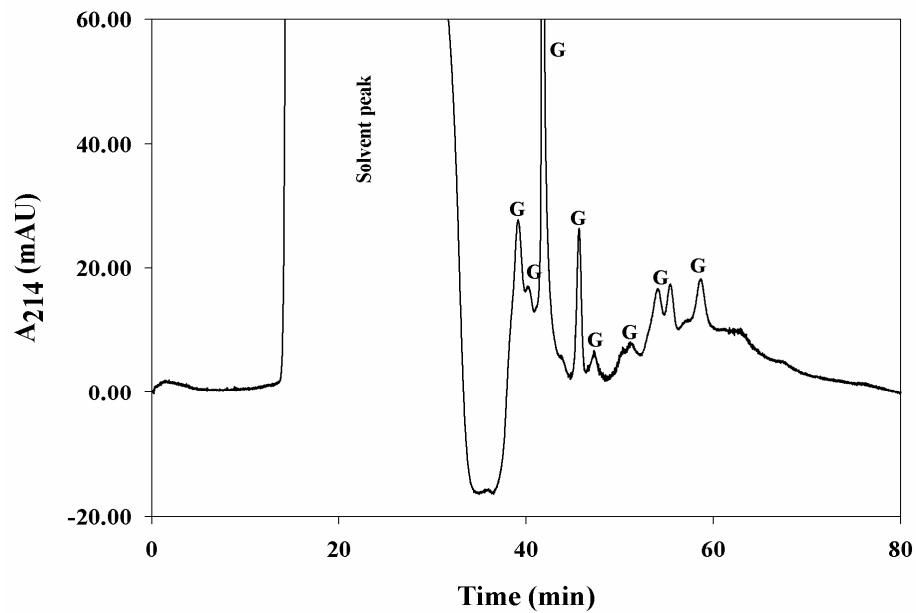


**Figure 9.** Different glycopeptides of transferrin on different lectin columns. (a) RCA reactive (b) LCA reactive and (c) WGA reactive. Conditions, same as in Fig. 8. G, stands for glycopeptide.

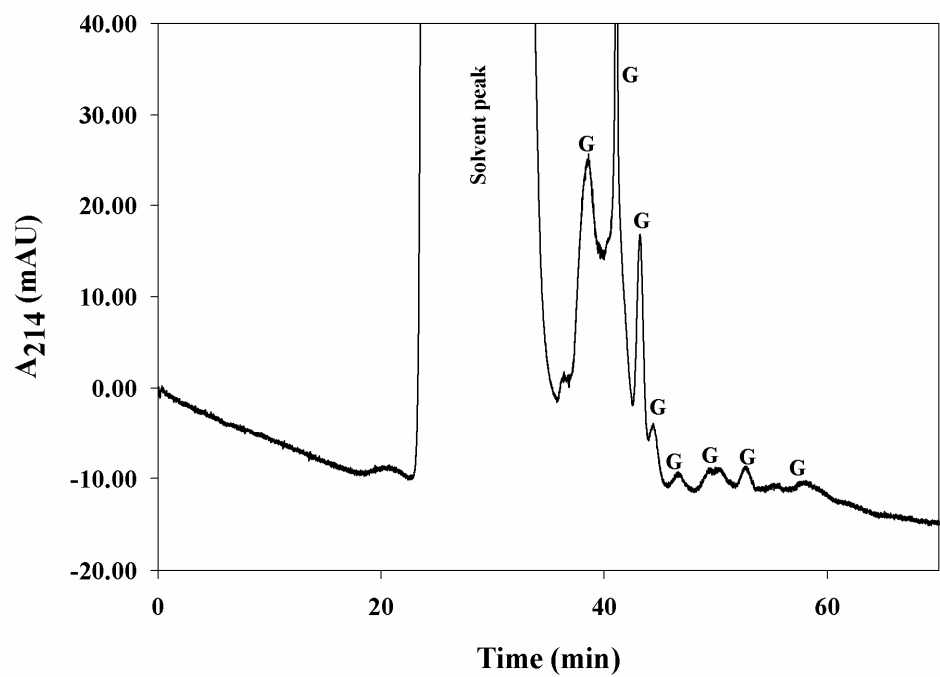
than by the immobilized WGA). Despite the absence of *N*-glycans with affinity toward the immobilized LCA column, one single peak is obtained by RP-CEC, Fig. 9c.

The *N*-glycan fragments of AGP are shown in Table 2. All of these glycans should be reactive with RCA, a fact that explains the multiple peaks observed in Fig. 10a. The di-antennary complex type *N*-glycans should be reactive with WGA while the fucosylated tri- and tetraantennary complex type *N*-glycans show reactivity toward LCA.

(a)



(b)



(c)

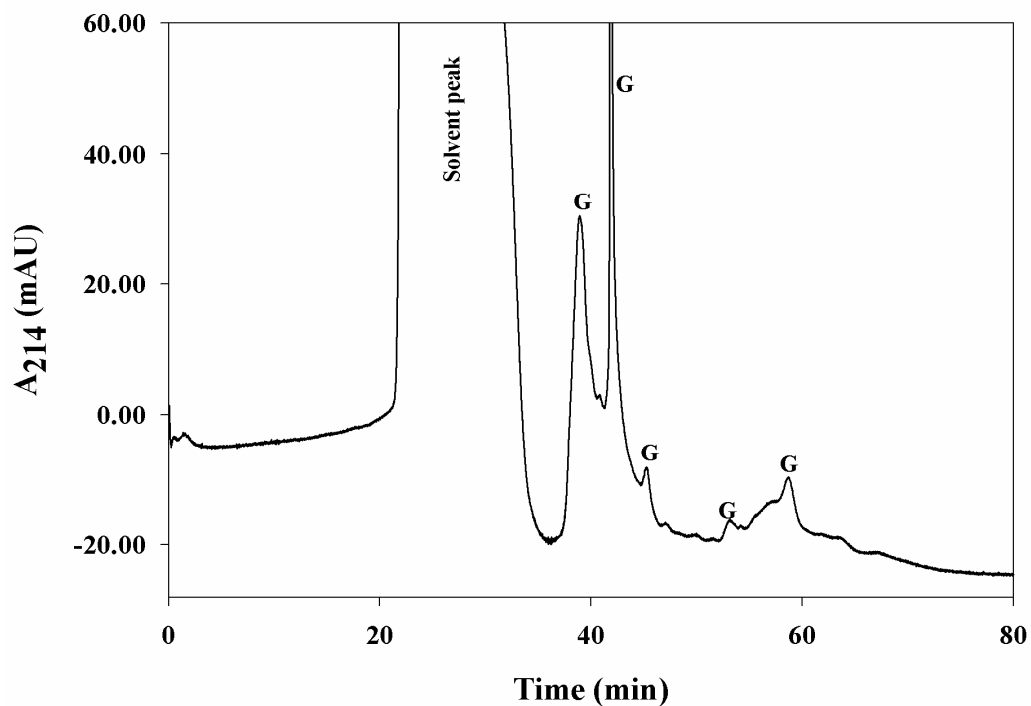


**Figure 10.** *Different glycopeptides of AGP on different lectin columns. (a) RCA reactive (b) LCA reactive and (c) WGA reactive. Conditions, same as in Fig. 8. G, stands for glycopeptide.*

Thus, fewer glycopeptides should be captured by the LCA and WGA as shown in Fig. 10b and Fig. 10c, respectively.

## Conclusions

This study examined the isolation and separation of glycopeptides by lectin affinity CEC and affinity nano-LC. While lectin affinity nano-LC yields one single peak for the captured glycopeptides by eluting the lectin column with the hapten sugar, lectin affinity CEC offers the possibility of separating the different captured glycopeptides upon elution, as the glycopeptides will migrate differentially in the electric field by virtue of differences in charge-to-mass ratios. Since each lectin column has its own hapten sugar, tandem lectin capillary columns are a powerful format to capture and separate several glycopeptides with varying affinity to different lectin columns. Also, serial lectin affinity nano-LC and reversed-phase CEC are useful formats for the selective capture and concentration of glycopeptides and their subsequent separations by RP-CEC based on differences in the polarity of the glycopeptides and their charge-to-mass ratios. These novel separation schemes have been demonstrated and exploited for the first time for the separation of glycopeptides derived from complex tryptic digest of glycoproteins.

## References

- (1) Okanda, F. M., El Rassi, Z., *Electrophoresis*, **2006**, 27, 1020-1030.
- (2) Bedair, M., El Rassi, Z., *J. Chromatogr. A*, **2004**, 1044, 177-186.
- (3) Bedair, M., El Rassi, Z., *J. Chromatogr. A*, **2005**, 1079, 236-45.
- (4) Kobata, A., Yamashita, K., *Fractionation of oligosaccharides by serial affinity chromatography with use of immobilized lectin columns*, in *Glycobiology A Practical Approach*, Fukuda, M. and Kobata, A. (Eds), **1993**, IRL Press: Oxford. pp. 103-125.
- (5) Debray, H., Montreuil, J., *Specificity of lectins toward oligosaccharidic sequences belonging to N- and O-glycosylproteins*, in *Affinity Electrophoresis: Principles and Application*, Breborowicz, J. and Mackiewicz, A., (Eds), **1991**, CRC Press: Boca Raton. p. 23-57.
- (6) Bhavanandan, V. P., Umemoto, J., Banks, J. R., Davidson, E. A., *Biochemistry*, **1977**, 16, 4426-4437.
- (7) Osawa, T., Tsuji, T., *Ann. Rev. Biochem.*, **1987**, 56, 21-42.
- (8) Prime, S., Merry, T., *Exoglycosidase sequencing of N-linked glycans by the reagent array analysis method*, in *Glycoanalysis Protocols*, E.F. Hounsell, Editor. **1998**, Humana Press Inc.: Totowa. p. 53-69.
- (9) Montreuil, J., *Glycoproteins*, in *Carbohydrate analysis. A practical approach*, F. Chaplin and J. Kennedy, Editors. **1986**, IRL Press. p. 143-204.
- (10) Kornfeld, K., Reitman, M. L., Kornfeld, R., *J. Biol. Chem.*, **1981**, 256, 6633-6640.

- (11) Debray, H., Decout, D., Strecker, G., Spik, G., Montreuil, J., *Eur. J. Biochem.*, **1981**, *117*, 41-55.
- (12) Tsuji, T., Irimura, T., Osawa, T., *J. Biol. Chem.*, **1981**, *256*, 10497-10502.
- (13) Okanda, F., El Rassi, Z., *Electrophoresis*, **2005**, *26*, 1988-1995.
- (14) www.promega.com, *www.promega.com*. **2006**.
- (15) Takegawa, Y., Deguchi, K., Keira, T., Ito, H., Nakagawa, H., Nishimura, S., *J. Chromatogr. A*, **2006**, *1113*, 177-181.
- (16) Charlwood, J., Birrell, H., Bouvier, E., Langridge, J., Camilleri, P., *Anal. Chem.*, **2000**, *72*, 1469-1474.
- (17) Endo, T., Furukawa, K., *Rheumatoid arthritis and Serum IgG*, in *Glycoproteins and Disease*, J. Montreuil et al., Editor. **1996**, Elsevier: Toronto. p. 277-289.
- (18) Grimm, R., Birrell, H., Ross, G., Charlwood, J., Camilleri, P., *Anal. Chem.*, **1998**, *70*, 3840-3844.
- (19) Treuheit, M., Costello, C., Halsall, H., *Biochem. J.*, **1992**, *283*, 105-12.
- (20) Dage, J. L., Ackermann, B. L., Halsall, H. B., *Glycobiology*, **1998**, *8*, 755-760.
- (21) Nakajima, K., Oda, Y., Kinoshita, M., Kakehi, K., *J. Proteome Res.*, **2003**, *2*, 81-88.
- (22) An, H., Peavy, T., Hedrick, J., Lebrilla, C., *Anal. Chem.*, **2003**, *75*, 5628-5637.
- (23) Uegaki, K., Taga, A., Akada, Y., Suzuki, S., Honda, S., *Anal. Biochem.*, **2002**, *309*, 269-278.
- (24) Yet, M., Chin, C., Wold, F., *J. Biol. Chem.*, **1988**, *263*, 111-7.
- (25) MacGillivray, R., Mendez, E., Shewale, J., Sinha, S., Lineback-Zins, J., Brew, K., *J. Biol. Chem.*, **1983**, *258*, 3543-53.

- (26) Montreuil, J., Spik, G., Mazurier, J., *Transferrin superfamily*, in *Glycoproteins II*, Montreuil, J., (Ed). **1997**, Elsevier. pp. 203-242.
- (27) Takegawa, Y., Deguchi, K., Nakagawa, H., Nishimura, S., *Anal. Chem.*, **2005**, *77*, 6062-8.
- (28) Honda, S. M., A., Suzuki, S., Kakehi, K., *Anal. Biochem.*, **1990**, *191*, 228-34.

## VITA

Fred Martin Okanda

Candidate for the Degree of

Doctor of Philosophy

Thesis: NON-POLAR AND AFFINITY MONOLITHIC STATIONARY PHASES FOR BIOPOLYMER SEPARATIONS BY CAPILLARY ELECTROCHROMATOGRAPHY AND NANO-LIQUID CHROMATOGRAPHY

Major Field: Chemistry

Biographical:

Personal Data: Born in Nairobi, Kenya, on November 16, 1975, the son of Michael Okanda and Clarice Okanda.

Education: Graduated from Kanga High School, Rongo, Kenya in December 1992; received Bachelor of Science degree in Chemistry from Moi University, Eldoret, Kenya in December 1999. Completed the requirements for the Doctor of Philosophy degree with a major in Chemistry at Oklahoma State University, Stillwater, Oklahoma in December 2006.

Experience: Worked at the International Centre of Insect Physiology and Ecology (I.C.I.P.E.), Nairobi, Kenya, December 1999 to December 2001; employed by Oklahoma State University, Chemistry Department, as a teaching assistant, January 2002 to present.

Professional Memberships: American Chemical Society, California Separation Science Society and Phi Lambda Upsilon (honorary chemical society).